Role of IL-6 Transsignaling in acute CCl_4-induced liver damage

Dissertation
zur Erlangung des Doktorgrades
der Mathematisch-Naturwissenschaftlichen Fakultät
der Christian-Albrechts-Universität
zu Kiel

vorgelegt von
Jessica Gewiese

Kiel 2010

Referent: Prof. Dr. Rose-John
Korreferent: Prof. Dr. Schulz
Tag der mündlichen Prüfung: 14.06.2010
Zum Druck genehmigt: 14.06.2010
Der Dekan

1 Introduction

1.1 Interleukin 6

The pleiotropic cytokine Interleukin 6 (IL-6) was originally identified as an antigen-independent B-cell differentiation factor that activates B-cells to produce immunoglobulins (1, 2). Meanwhile it is known that IL-6 is involved in a wide range of biological activities in immune regulation and it is secreted by various lymphoid cell types, such as T-cells, B-cells, macrophages and monocytes (3). Apart from lymphoid cells, IL-6 is produced also by various types of nonlymphoid cells, such as fibroblasts, keratinocytes, endothelial cells and several tumor cells (3).

Altered levels of IL-6 have been found in a variety of diseases including multiple myeloma, Crohn's disease, mesangial glomerulonephritis, osteoporosis, cardiac ischemia, cachexia and rheumatoid arthritis (4).

IL-6 has been described to have pro- as well as anti-inflammatory properties (5, 6). In fact, it promotes inflammation through the expansion and activation of T-cells, differentiation of B-cells and the induction of acute-phase response by hepatocytes (6). Furthermore IL-6 is produced in large amounts by endothelial cells in response to proinflammatory signals including TNF-α (7) and hypoxia (8).

Due to its high ability to activate an inflammatory response, IL-6 expression is strictly regulated and the protein is hardly expressed under steady state conditions. It is commonly produced at local tissue sites and is released in case of tissue damage, which could be infection, injury and endotoxaemia. IL-6 can also become chronically elevated, resulting in a number of serious diseases.

In the liver, IL-6 acts as a major regulator of the hepatic acute phase response by stimulating hepatocytes to produce C-reactive protein, fibrinogen and serum amyloid A (9). Furthermore IL-6 induces differentiation of cytotoxic T-cells by enhancing the production of IL-2 and IL-2 receptor (10) and differentiation of macrophages (11). Additionally, circulating IL-6 together with tumor necrosis factor α (TNF-α) and interleukin-1 (IL-1) cause fever and induce leukocytosis which is valuable for pathogen elimination (12).

Homozygous IL-6 knockout (IL-$6^{-/-}$) mice develop normally but show a compromised acute phase response after tissue damage or infection, which becomes evident in the lacking ability to control bacterial infections like infection with *Listeria monocytogenes* and an impaired T-cell dependent antibody response (13). Additionally, IL-$6^{-/-}$ mice

are completely protected from chronic inflammatory diseases such as collagen-induced arthritis (14) and are resistant to experimental autoimmune encephalomyelitis (EAE), an animal model for multiple sclerosis (15).
In conclusion, the phenotype of the IL-6$^{-/-}$ mice emphasizes that IL-6 is an eminent cytokine involved in regulation of host response after infection and plays an important role in controlling immune regulation.

1.2 Classical IL-6 signaling

The IL-6-type family of cytokines acts via receptor complexes that contain at least one subunit of the signal transducing glycoprotein 130 (gp130). The family comprises Interleukin-6 (IL-6), Interleukin-11 (IL-11), viral IL-6, IL-27, IL-31, neuropoietin (NP), leukaemia inhibitory factor (LIF), oncostatin M (OSM), ciliary neurotrophic factor (CNTF), cardiotropin-1 (CT-1) and cardiotrophin-like cytokine (CLC) (16, 17).
Each member of the IL-6 type family of cytokines is characterized by a certain pattern of receptor recruitment.
IL-6, IL-11 and CNTF first bind to their corresponding nontransducing α -receptor, which subsequently leads to the recruitment and dimerization of the signaling subunits gp130 and LIFR (18). IL-6 and IL-11 signal via a homodimer of two gp130 subunits (Fig. 1). CNTF recruits one gp130 subunit and one LIF receptor (LIFR) subunit. LIF, CT-1, IL-27, IL-31, viral-IL-6 and OSM can directly interact with their signaling receptor subunits without requiring an α-receptor subunit (19). The cytokine CLC can only bind to the signal transducing subunits gp130 and LIFR in the presence of the additional soluble cytokine receptor soluble CNTFR (20).

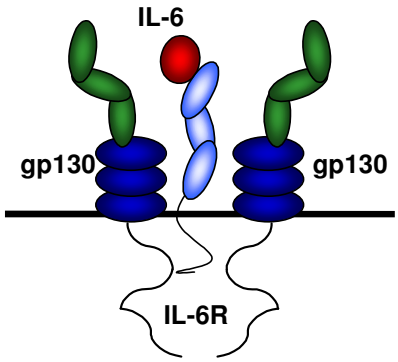

Figure 1: Classical IL-6 Signaling. IL-6 first binds to its specific nontransducing α –receptor (IL-6 Receptor), which subsequently leads to the recruitment and dimerization of two signaling subunits gp130.

Dimerization of the signal transducing subunits gp130 leads to activation by phosphorylation of the Janus kinases (JAK) (21) (Fig. 2).
Activated JAK kinases phosphorylate tyrosine residues at the cytoplasmatic domain of gp130. This leads to the recruitment of SH2 domain proteins like SHP-2 and STAT proteins. There are six tyrosine residues in gp130 and phosphorylation of the four distal tyrosines leads to recruitment and activation of the signal transducer and activator of transcription (STAT) proteins (22).

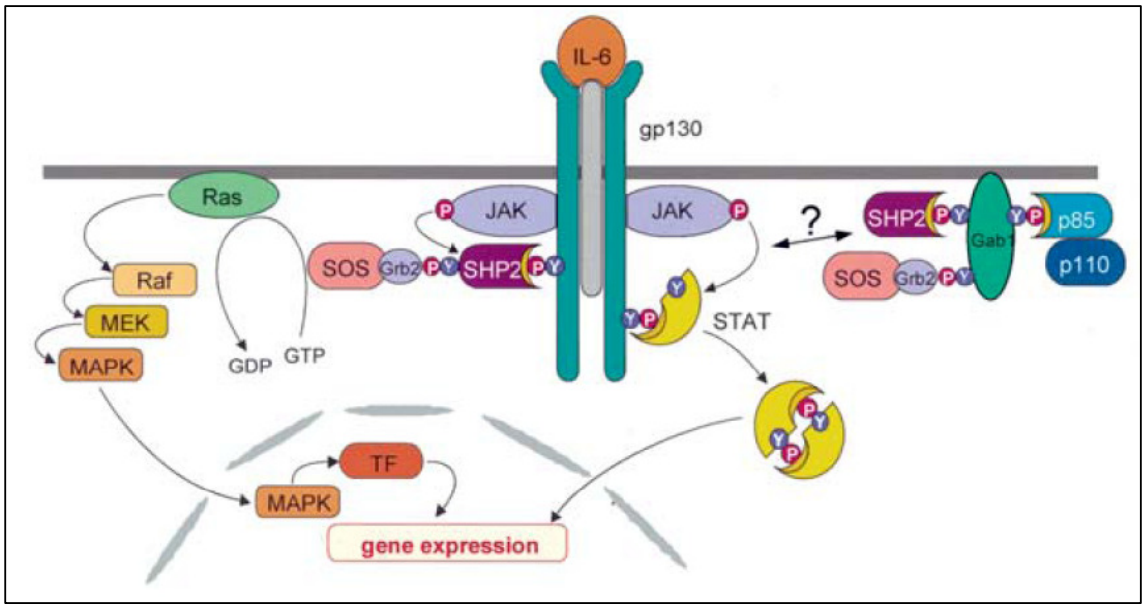

Figure 2: IL-6 activates the JAK/STAT pathway and the MAPK cascade. Representation of the two major pathways activated by IL-6-type cytokines. TF, transcription factor (16).

IL-6 binding leads to an activation of STAT3 and STAT1 (23, 24). Directly after tyrosine phosphorylation, STATs form homo- and heterodimers and translocate to the nucleus. Subsequently, transcription of target genes is activated, including those involved in inflammation, acute phase response (e.g. C-reactive protein (25) and Lipopolysaccharide (26)) and proliferation (like c-Fos (27) and Jun B (28)).

PIAS3 (Protein inhibitor of activated STAT3) blocks the DNA binding activity of STAT3 and inhibits STAT3-mediated gene activation. Although STAT1 is also phosphorylated in response to IL-6, PIAS3 do not interact with STAT1 or affect its DNA-binding or transcriptional activity. Therefore is PIAS3 a specfic inhibitor of STAT3 signaling pathways (29).

A second way to down-regulate the STAT pathway is the negative feedback inhibitor SOCS (suppressor of cytokine signalling). The transcription of the SOCS proteins is induced by STAT3. SOCS proteins bind to the SHP2 (SH2-domain-containing tyrosine phosphatase)- binding site Tyr^{759} of gp130 and reduces the MAPK (Ras mitogen-activated protein kinase) cascade (30, 31). SOCS1 and SOCS3 are functionally most related and potently inhibit IL-6-type signaling. Both have been shown to act on the JAKs, and thereby inhibit the phosphorylation of gp130, STATs and the JAKs themselves (31, 32).

Dimerization of IL-6-type cytokine receptors does not only lead to activation of the JAK/STAT-signalling pathway, but also to the induction of the MAPK cascade. The binding of SHP2 to Tyr^{759} of gp130 was identified to be crucial for the activation of MAPK cascade (33). SHP2 is rapidly recruited to tyrosine-phosphorylated gp130 and becomes also phosphorylated in a JAK1-dependent manner. Subsequently, tyrosine-phosphorylated SHP2 interacts with Grb2 and two C-terminal tyrosine residues within SHP2 and this interacts with the Grb2–SOS complex. Finally, recruitment of SOS to the receptor complex at the membrane allows Ras activation, which in turn leads to the activation of the Ras–Raf–MAPK cascade (16).

1.3 IL-6 Transsignaling

As described before, IL-6 first binds to its specific nontransducing α –receptor, the IL-6 Receptor (IL-6R), which subsequently leads to the recruitment and homodimerization of two signaling subunits gp130 and to gene activation via signaltransduction of the Jak/STAT pathway.

While gp130 is expressed on all cell types, expression of the IL-6 Receptor (IL-6R) is restricted to hepatocytes and some leukocyte sub-populations including monocytes, neutrophils and some T-cells ($CD4^+$, $CD8^+$, $CD4^+CD25^-$ and $CD25^{high}$ regulatory T-cells (34)) and B-cells subtypes (6, 19).

Cells lacking the IL-6R are not able to respond to IL-6 through the classical IL-6 pathway. However, a naturally occuring soluble form of the IL-6R, which is generated either by limited proteolysis of the membrane-bound IL-6R (35) or by translation from an alternatively spliced mRNA (36), can bind to IL-6. Thereby, the soluble IL-6R binds IL-6 with the same affinity as membrane-bound IL-6R and the complex of IL-6 and sIL-6R can stimulate cells lacking membrane-bound IL-6R, but expressing gp130

(Fig. 3). This alternative IL-6 signaling pathway has been named Transsignaling (37-39).

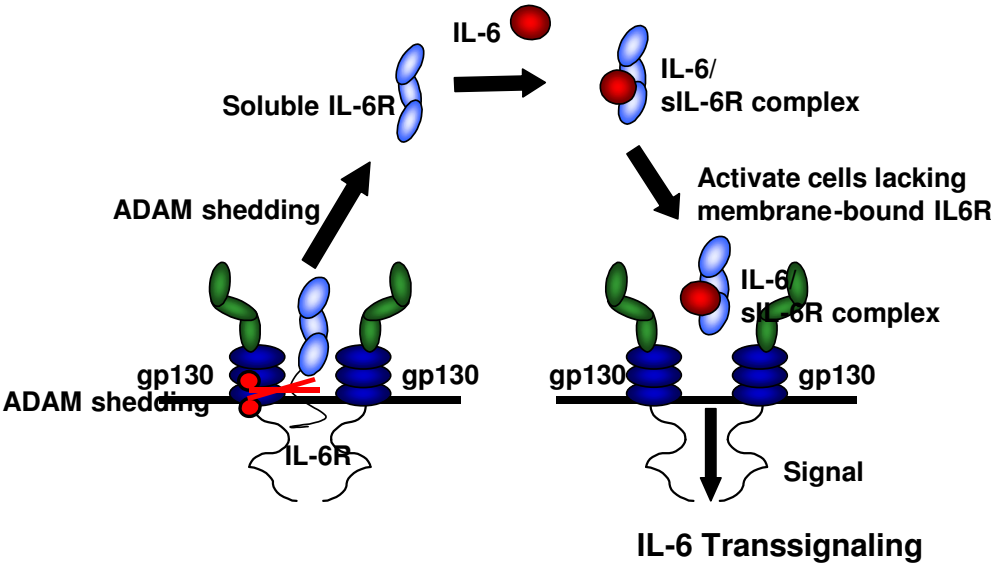

Figure 3: IL-6 Transsignaling. Soluble IL-6R, which is generated either by limited proteolysis of the membrane-bound IL-6R or by translation from an alternatively spliced mRNA binds IL-6 with the same affinity as membrane-bound IL-6R. The complex of IL-6 and sIL-6R can stimulate cells lacking membrane-bound IL-6R.

Shedding of the IL-6 receptor can be initiated by different stimuli such as phorbol ester (35), C-reactive- protein (40), pore-forming toxins (41), cholesterol depletion (42) and apoptosis (43). While constitutive shedding of the IL-6R is mediated by ADAM10 (A disintegrin and metalloproteinase 10), induced cleavage is arranged by the metalloprotease TACE (ADAM17) (42).

In healthy humans, the naturally occuring soluble form of the IL-6R is found in the blood at concentrations of about 50-80 ng/ml (44). sIL-6R levels increase in some inflammatory diseases such as peritonitis (45) and rheumatoid arthritis (46) by a factor of 2.

IL-6 Transsignaling has been shown to be relevant in a variety of physiological and pathophysiological processes, including T-cell-and lymphocyte-trafficking and-infiltration (12, 47, 48), osteoclast formation (49), smooth muscle cell activation (50), Crohn`s disease and colon cancer (51-53).

In conclusion, the IL-6/sIL-6R complex has, due to the ubiquitous expression of gp130, the potential to stimulate all cells of the body.

1.4 Agonists and Antagonists of IL-6 Transsignaling

Soluble cytokine receptors can either act as antagonists competing with the membrane bound receptors for their cognate ligands or they can act as agonists.

Most of the soluble cytokine receptors, e.g. IL-1R (54), TNF-R (55) and IL-4R (56) function as antagonists by competing against their membrane-bound correspondents.

The soluble IL-6R is an agonistic soluble cytokine receptor that binds its ligand IL-6 with comparable affinity as the membrane bound IL-6R. Cells that only express gp130 but no IL-6R cannot be stimulated by IL-6, unless a soluble form of the IL-6R is present (57).

To mimic IL-6 Transsignaling a designer cytokine, Hyper-IL-6, has been constructed. Hyper-IL-6 is a fusion protein consisting of IL-6 and the soluble IL-6R, which are connected via a flexible peptide linker. Thereby the association of the ligand/receptor complex is achieved (58).

Hyper-IL-6 is 100 to 1000 times more potent to induce biological reactions than the two separate proteins IL-6 and sIL-6R. IL-6 alone binds with an affinity of 10^{-9}M to the IL-6R, whereas IL-6/ IL-6R complex binds the gp130 protein with an affinity of 10^{-11}M (58, 59).

Moreover, the accelerating effect of Hyper-IL-6 has been described in liver damage and regeneration (60, 61).

In addition to the soluble IL-6R exists a soluble form of gp130 protein (sgp130). Levels of sgp130 (100-400 ng/ml) have been detected in human blood. This sgp130 can bind to the IL-6/sIL-6R complex, but not to IL-6 alone and thereby inhibits signaling via membrane bound gp130 (62). It has been concluded that sgp130 functions as the natural inhibitor of IL-6 Transsignaling but not of classical IL-6 signaling (Fig. 4) (63).

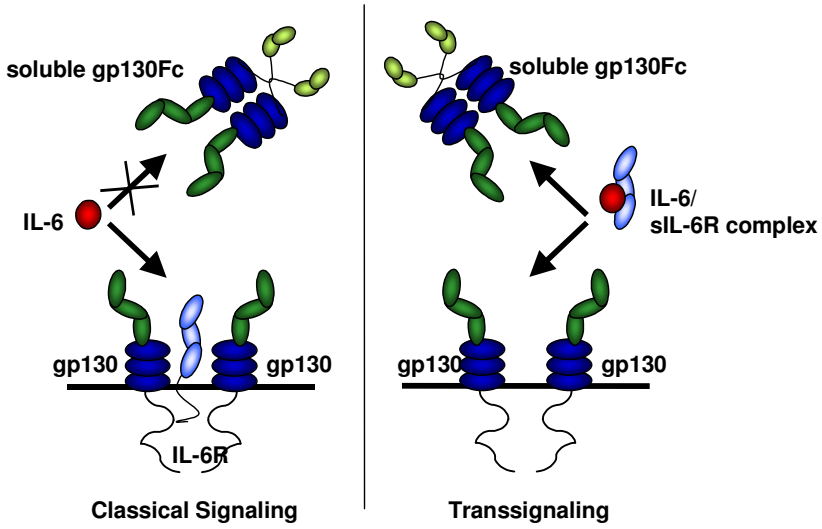

Figure 4: Soluble gp130 mediated inhibition of IL-6 Transsignaling. sgp130 is binding the IL-6/sIL-6R complex and thereby inhibiting signaling via membrane bound gp130. As a consequence sgp130 function as the natural inhibitor of IL-6 Transsignaling but not of classical IL-6 signaling.

A variant of sgp130, called sgp130Fc, was designed by fusing the complete extracellular region of murine gp130 with the Fc-part of a human IgG1-antibody. It has been shown that dimerized sgp130Fc is able to inhibit IL-6/sIL-6R-mediated Transsignaling with a 10-fold higher activity than monomeric sgp130 (63). This sgp130Fc designer molecule can be used as a molecular tool to distinguish between classic IL-6 and IL-6 Transsignaling.
It has been shown that sgp130Fc can abrogate inflammation in a transgenic mouse model, in which IL-6 Transsignaling is blocked (64).

1.5 Structure of the liver

With 2% of total body weight is the liver one of the largest organs of humans with crucial function in synthesis, storage, metabolization and detoxification. The liver is the primary organ for detoxification of toxins, drugs or other pollutants.
It is divided into a larger right and a smaller left lobe (Fig. 5). On the caudal side of the liver are the major afferent vessels (hepatic artery, portal vein) and the common bile. On the cranial side the liver veins end into the vena cava inferior (63, 64).

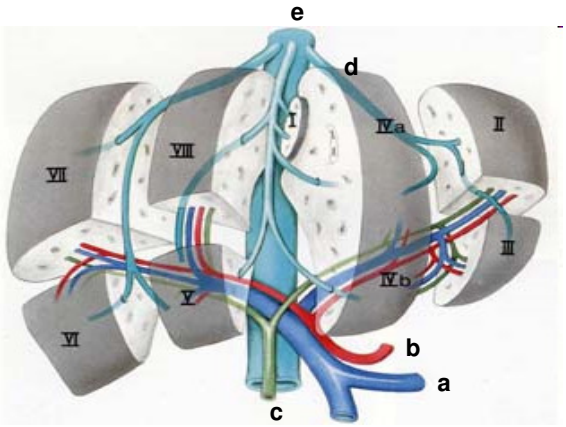

Figure 5 : Human liver division into eight segments (I-VIII). The larger right lobe (segments V-VIII) and the smaller left liver lobe (segments I-IV). a: portal vein (blue), b: hepatic artery (red), c: bile duct (green), d: liver vein (fine, light blue), e: vena cava inferior (thick, light blue) (65).

The portal vein collects blood from the unpaired abdominal organs and leads it to the liver. The blood of the portal vein contains sparse oxygen (venous), and is after a meal rich in nutrients (from the digestive organs) or in degradation products (e.g. bilirubin). This hepatic portal vein (*vena portae*) merges with the hepatic artery (oxygen-rich) into the liver.

The liver lobes are divided into smaller lobes with a maximal size of 1-2 mm. This smaller lobes appeare in cross sections as hexagonal arrangements and consist mainly of hepatocytes. In the corners of these hexagonal hepatocytes are located the periportal fields with the Glisson`s triangle (Fig. 6). The Glisson`s triangles consist of one branch of a hepatic artery (*Arteria interlobularis)*, one branch of a portal vein (*Vena interlobularis)* and one branch of a bile duct (*Ductus biliferus*). One branch of a hepatic artery and one branch of a portal vein are mixed and circulate to direction of the central vein. The central vein finally transports the blood into the vena cava inferior. Bile is derived from the bilecapillaries (Fig. 7).

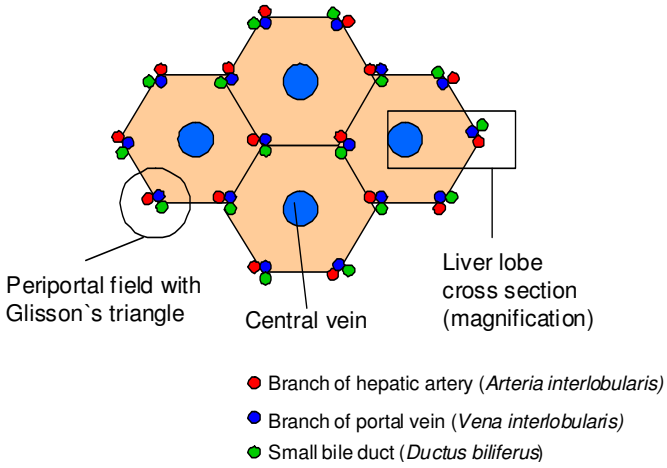

Figure 6: Schematic cross section of a small liver lobe. In the corners of the hexagonal hepatocytes are located the periportal fields with the Glisson`s triangle. Red: hepatic artery, blue: portal vein, green: bile duct.

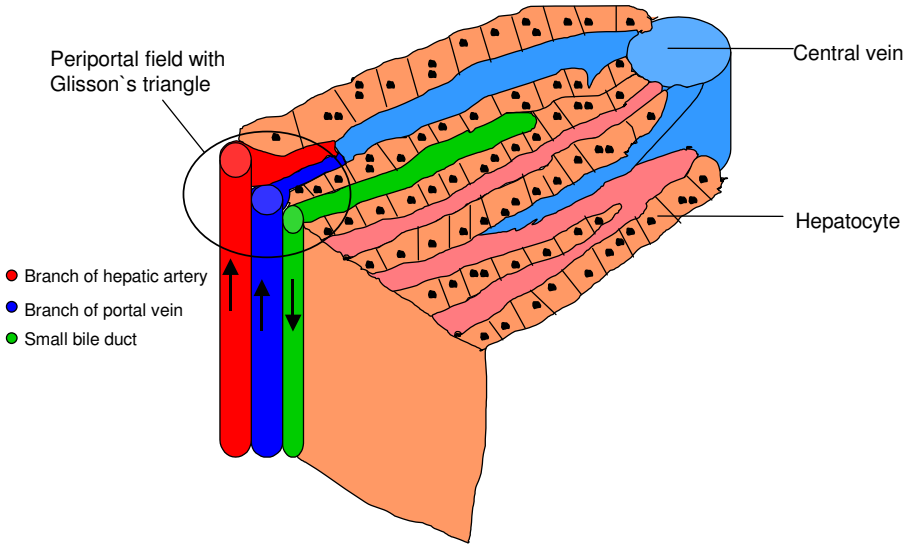

Figure 7: Schematic magnified cross section of a small liver lobe. Magnified square of figure 6 showing a periportal field in detail. One branch of a hepatic artery and one branch of a portal vein are mixed and flow to direction of the central vein. The central vein transports the blood into the vena cava inferior. Bile is derived from the bilecapillaries.

The capillaries of the liver (the hepatic sinusoids) are located between the hepatocytes.This sinusoids are lined with windowed endothelial cells and contain the specific macrophages of the liver, the Kupffer cells (Fig. 8). The sinusoids transport the blood of the portal vein together with the blood of the hepatic artery through the hepatic lobules towards the lobule center, where the blood is received by a central vein (*vena centralis*). The space between the endothelial cells of the sinusoids and the hepatocytes is called the space of disse. In this space of disse the proper

detoxification takes place and further more the *Ito* cells (stellate cells) are arranged (Fig. 8).

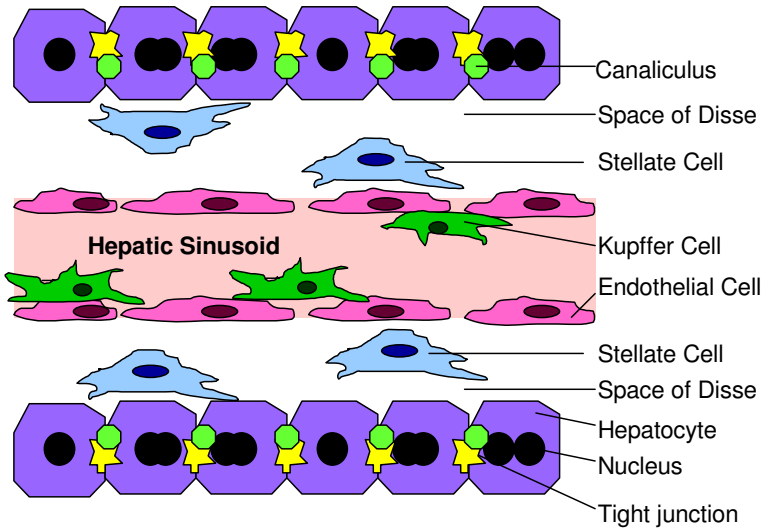

Figure 8: Structure of hepatic sinusoids and hepatocytes. The hepatic sinusoids are lined with windowed endothelial cells (pink) and contain the liver specific macrophages, the Kupffer cells (green). The space between the endothelial cells of the sinusoids and the hepatocytes is called the space of disse. The stellate cells (blue) are arranged in the space of disse. The hepatocytes (violet) are connected among each other with bilechannels (canaliculus) and tight junctions.

1.6 Function of the liver

Besides its function of detoxification, the liver has a wide range of functions including protein synthesis (e.g. coagulation factors), storage and metabolism (e.g. glycogen storage and synthesis, decomposition of red blood cells, plasma protein synthesis, lipid metabolism, bile and hormone production).

In the following two examples relevant for discussion are worked out in more detail:

Glycogen synthase is a glycosyltransferase enzyme that catalyses the reaction of 1,4-α-D-glucose to glycogen. Two isozymes of glycogen synthase are present in humans:

Glycogen synthase 1 is expressed in muscle and other tissue, whereas expression of glycogen synthase 2 is restricted to hepatocytes.

Liver glycogen serves as a storage pool to maintain the blood glucose level during fasting, whereas muscle glycogen functions as a stock to provide energy during activity.

Phosphorylation of glycogen synthase decreases its activity, whereas dephosphorylation converts the enzyme in the fully active form (65).

Different protein kinases, especially the cAMP dependent Proteinkinase A (PKA) and the Glycogen synthase kinase 3 (GSK-3) phosphorylate serine and threonine residues of the glycogen synthase and this results in an inhibition of glycogen synthase.
GSK-3 can be inhibited by Akt phosphorylation, which is part of the insulin signal transduction pathway. In consequence, phosphorylated GSK-3 (P-GSK-3) displays the inactive form of GSK-3 (66).

Cytochrome P450 (CYP450) is a very large and diverse group of enzymes, consisting of 18 families and 43 subfamilies. Most of CYP450 enzymes are expressed in the liver. CYPs are the major enzymes involved in drug metabolism and bioactivation (e.g. monooxygenase reaction), accounting for approximately 75% of the total metabolism (67). Furthermore CYPs play important roles in steroid hormone synthesis (e.g. estrogen and testosterone), cholesterol synthesis and vitamin D metabolism.

The liver is the first organ exposed to toxins from the gastrointestinal tract, for this reason, the liver holds the ability to regenerate and proliferate after damage or injury.

1.7 The role of IL-6 signaling in liver regeneration

To discriminate between the biologic function of human IL-6 (hIL-6) alone and that of the hIL-6/hsIL-6R complex, Peters et al. generated double-transgenic mice coexpressing hIL-6 and hsIL- 6R (hIL-6/ hsIL-6R mice). The hIL-6/ hsIL-6R mice were compared with hsIL-6R and hIL-6 single transgenic mice and nontransgenic littermates. In hIL-6/ hsIL-6R double transgenic mice were observed hepatocellular hyperplasia frequently surrounded by peliosis and necrosis, significant acceleration and aggravation of plasmacytoma formation, and excessive activation of extramedullary hematopoiesis in spleen and liver followed by a subsequent increase of all cellular components in the peripheral blood (68). IL-6 classic and Transsignaling seem to play a major role in liver proliferation.
Excessive alcohol intake, drug overdose (e.g. paracetamol, tetracycline), fatty liver disease (FLD) and viral hepatitis can lead to potent liver damage. The liver has the unique capacity to regenerate after damage and injury. Only in the case of massive hepatic damage it leads to organ failure. Anyhow, liver failure is still a serious medical

problem and enhancing the potential of liver regeneration could be an effective and promising aim.
Inhibition of hepatocellular apoptosis and necrosis and therewith enhancement of the endogenous potential for liver regeneration could be the basis for the prospective treatment of liver injury and organ failure.
The important role of circulating proinflammatory cytokines like IL-1-beta, TNF-alpha and IL-6 has already been demonstrated (69). The role of IL-6 during liver regeneration has been extensively investigated and has established a critical role for IL-6 in mediating pro-mitotic and pro-survival activities within the regenerative process (70).

The easiest stimulus for liver regeneration is the removal of liver tissue (hepatectomy). Thereafter the residual tissue is growing until the original mass is achieved.
In liver research the model of two-thirds partial hepatectomy in rats was first pioneered by Higgins and Anderson (71) in 1931. In this model, two-thirds of the liver are surgically removed and the remaining liver enlarges in a hyperplastic response by replication of all residual hepatocytes of the liver. Once the liver has regained its original mass (5-7 days), proliferation stops (72).
Adult hepatocytes are quiescent cells and rarely undergo cell division. They maintain the ability to proliferate in response to cell damage or loss of function (72), by undergoing one or two rounds of cell division and then return to their quiescent stage. Hepatocytes are resting in the G_0 phase of the cell cycle. Gene activation (priming) is required for hepatocytes to enter into the G_1 phase (Fig. 9). In early G_1 phase, the cells fully respond to growth factors (e.g. HGF, TGFα) and then can progress through the cell cycle, overcome the G_1 restriction point and undergo DNA replication. Tumor necrosis factor-α (TNF-α) and IL-6 where found in different studies (70, 73) to act as priming factors, inducing activation of NFκB and STAT3.

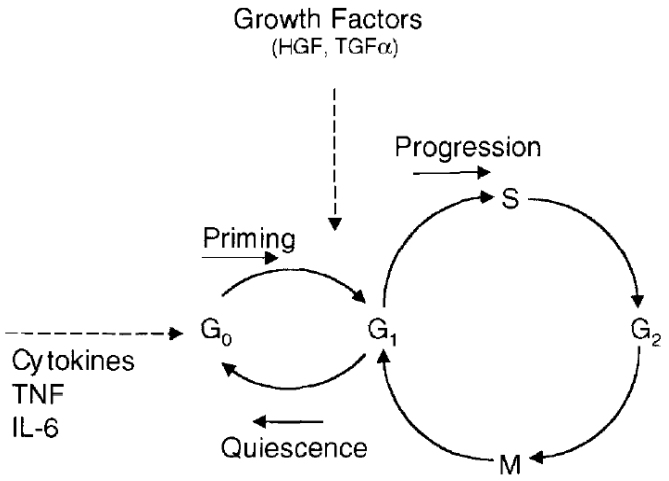

Figure 9: Multistep model of liver regeneration. Liver regeneration is divided into two phases, priming and cell cycle progression. Priming is a reversible process initiated by cytokines as well as nutritional and hormonal signals. Priming sensitizes the cells to growth factors but is ineffective in their absence. Growth factors are required for cells to move beyond a restriction point in G1. Expression of cyclin D1 signals the point in G1/S at which cells can progress to DNA replication independently of growth factors (74).

IL-6 expression dramatically increases shortly following partial hepatectomy (75) and has been shown to mediate promitotic, pro-survival and anti-apoptotic responses to hepatocytes within the regenerative process (70, 76, 77).
After partial hepatectomy were observed in IL-6 deficient mice a delayed hepatocyte mitotic response, as well as increased liver necrosis and mortality (70). In contrast to that finding, different groups published data concerning gp130 deficient mice, in which they observed only marginal effects on cell cycle and DNA synthesis after partial hepatectomy. This is leading to the notion that gp130-dependent signaling has no direct influence on cell cycle progression after partial hepatectomy but is relevant to activate protective pathways during hepatocyte proliferation (77).
Because IL-6 plays a key role in acute-phase response which is taking place during liver injury, IL-6 can be identified as crucial factor during liver injury and regeneration.

Treatment of mice with Hyper-IL-6 after partial hepatectomy resulted in an accelerated liver regeneration, which might be due to an observed decreased apoptosis and necrosis. These data indicate an important role of IL-6 Transsignaling during liver regeneration. The mechanism by which Hyper-IL-6 affects these regenerative process is still unknown (61, 78).

1.8 CCl_4 induced liver damage

There are various other animal models of liver damage simulating different human pathological conditions.

Acute liver failure can be simulated by intraperitoneal D-galactosamine (D-Gal) treatment. D-Gal is an intracellular uridine depleting drug that blocks transcription and thereby causes acute liver damage (79).

Concanavalin A (ConA) was used to study inflammatory liver disease. T-cell mediated hepatitis in mice can be induced by intravenous injection of the T-cell mitogenic plant lectin ConA (80).

CCl_4 can be used to mimic drug induced hepatoxicity. Paracetamol (acetaminophen) and ethanol are common liver damaging substances that are metabolized by a cytochrome P450 dependent monooxygenase to reactive metabolites (81).

CCl_4 is an organic compound, which was formerly widely used as refrigerant and as a cleaning agent. CCl_4 is a hepatotoxin that, depending on the dosage, induces acute liver failure or chronic liver damage leading to fibrosis (82).

CCl_4 needs to be metabolized to induce liver damage. This metabolic activation is performed mainly by the enzyme Cyp450 2E1 in the endoplasmatic reticulum of hepatocytes. Through this reaction, the reactive $CCl_3^{\bullet}$ and $CCL_3O_2^{\bullet}$ radicals are formed which can covalently bind to proteins, lipids and nucleic acids and thus induce liver damage and initiate lipid peroxidation (82, 83) (Fig. 10).

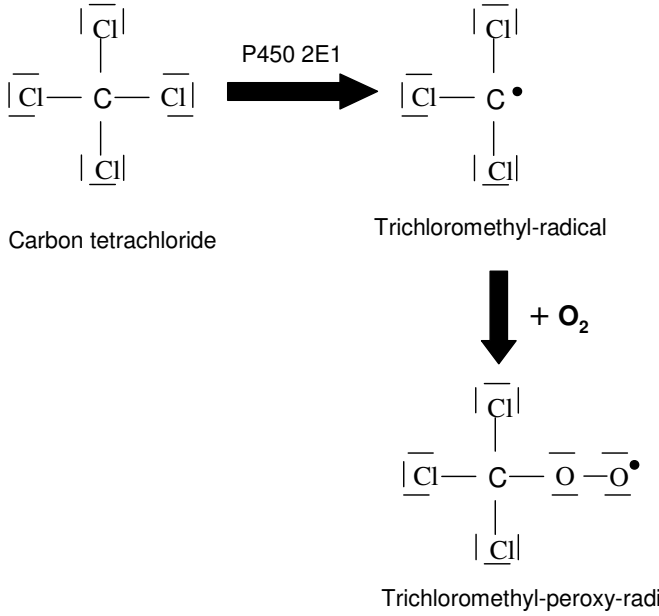

Figure 10: Carbon tetrachloride (CCl_4) and its metabolites. CCl_4 is metabolized by cytochrome P450 2E1 into trichloromethyl-radical ($CCl_3^{\bullet}$) and trichloromethyl-peroxy-radical ($CCL_3O_2^{\bullet}$).

Lipid peroxidation in cell membranes occurs via reactive oxygen species (ROS), such as superoxide radical ($O_2^{\bullet}$) and hydroxyl radical (OH^-), and can cause destruction of cell components and cell death (84).

Recently, it has been shown that CCl_4 not only causes primary liver necrosis, but also hepatocyte apoptosis (85).

Inflammatory processes are involved in the development of CCl_4-induced hepatotoxicity, in which Kupffer cells (the resident macrophages of the liver) secrete cytokines such as tumor necrosis factor-α (TNF-α), IL-1, IL-6 and IL-10 (86-91). In liver regeneration after CCl_4 injury, TNF-α is important for hepatocyte proliferation, acting as a mitogen. CCl_4-induced liver necrosis can be significantly ameliorated by treatment with anti-TNFα antibodies (88).

In acute CCl_4-induced liver damage, IL-$6^{-/-}$ mice reacted more sensitive to CCl_4 than wild type mice. Serum alanine aminotransferase (ALT) and aspartate aminotransferase (AST) levels were higher in IL-$6^{-/-}$ mice as compared to WT mice and these livers showed less liver cell proliferation and more apoptosis. These effects could be reversed by previous IL-6 treatment (92). Katz et al demonstrated that IL-$6^{-/-}$ mice died in a dose-dependent manner 24–48 h after i.p. injections of CCl_4, whereas WT mice were still viable. WT mice survived higher CCl_4 dosages than IL-$6^{-/-}$ animals. Histological studies showed more necrotic areas in IL-6 knockout mice. Although IL-6 injections failed to compensate this effect in IL-6 knockout animals, injecting Hyper-IL-6 dose dependently increased survival rates (93).

In contrast, chronical CCl_4 treatment of IL-6 knockout mice showed reduced liver damage scores, lower aminotransferase levels and diminished apoptosis (94).

2 Aim of this study

Interleukin-6 is known to play an important role in mediating pro-mitotic and pro-survival activities within the regenerative liver process.

The aim of the present study is to investigate the impact of IL-6 Transsignaling on liver damage and regeneration in a CCl_4-based mouse model of acute drug-induced liver damage. In further experiments, only the effect of a total IL-6 blockade by using IL-$6^{-/-}$ mice or IL-6 neutralizing antibody, as well as artificially induced IL-6 Transsignaling by Hyper-IL-6 have been analyzed. By blocking endogenous IL-6 Transsignaling via sgp130 we demonstrate for the first time the importance of the sIL-6R in response to chemically induced liver damage.

Therefore C57/Bl6 mice were treated 18 h before CCl_4-injection with soluble gp130Fc to block, or with Hyper-IL-6 to accelerate IL-6 Transsignaling.

Subsequently parameters of liver damage and regeneration, e.g. alanine aminotransferase (ALT), aspartate aminotransferase (AST) serum parameter, IL-6 production, and induction of acute phase response were measured.

3 Material and Methods

3.1 Material

3.1.1 Chemicals

All chemicals used were from ROTH, SIGMA or MERCK, unless otherwise stated. If it is not mentioned otherwise, deionized water (Millipore) was used as solvent.
All molecular weight markers, DNA polymerases (Taq, Pfu, DreamTaq) and Reverse Transcriptase were obtained from MBI Fermentas (St. Leon-Rot, Germany).
Oligonucleotides were ordered from Metabion (München, Germany).

3.1.2 Animals

Male C57Bl/6N were purchased from Charles River (Sulzfeld, Germany) and were maintained at a 12-hour light-dark cycle under standard conditions and provided with food and water *ad libitum*. For all experiments 4 – 6 mice per group were used.
Transgenic homozygous sgp130 mice were generated and backcrossed to C57Bl/6N to generation 7 (64). Mice were bred at a 12-hour light-dark cycle under standard conditions and provided with food and water *ad libitum*. For blood flow cytometrie analysis 4 – 6 mice per group were used.
sgp130Fc is expressed under the transcriptional control of the PEPCK promoter, which is mainly active in liver and kidney. Since the liver exhibits a high synthetic capacity, transgenic proteins driven by the PEPCK promoter have been shown to be secreted at high amounts into blood.

3.1.3 Animal food

The standard feed was obtained from SSNIFF Spezialdiäten GmbH (Soest, Germany).
Standard :

crude protein 19 %
crude fat 3.30 %
crude fibre 4.90 %
crude ash 6.70 %

Additives: Vitamin A: 15,000 IE/kg; Vitamin D3: 1,000 IE/kg; Vitamin E: 100 mg/kg; Cu: 5 mg/kg

3.1.4 Solutions and Buffers

Immuno Blotting

Blocking buffer *(Immuno blot)*	5 %	milk powder or BSA in TBS-T
Transfer buffer *(Immuno blot)*	25 mM	Tris-HCl, pH 8.3
	192 mM	glycine
	20 % (v/v)	methanol
Lysis buffer *(Tissue lysis)*	150 mM	NaCl
	2 mM	EDTA
	50 mM	Tris-HCl, pH 7.4
	1 % (w/v)	Triton X-100
	1 % (w/v)	NP-40
	1 mM	Na_3VO_4
	1 mM	NaF
	1 x	protease inhibitors
Protease-inhibitors	COMPLETE™ pills, Roche (Mannheim, Germany) Resuspending 1 pill in 50 ml Lysis buffer	
Running gel 10 % (15 %) *(protein gels)*	7.74 ml (4.5 ml)	deionized water
	5.1 ml (5.1 ml)	1.5 M Tris, pH 8.8
	0.2 ml (0.2 ml)	10 %SDS
	6.6 ml (9.9 ml)	30 % Acrylamide-Bis
	0.2 ml (0.2 ml)	10 % APS
	0.02 ml (0.02 ml)	TEMED
Stacking gel (4 %) *(protein gels)*	3.72 ml	deionized water
	0.625 ml	0.5 M Tris-HCl, pH 6.8
	0.05 ml	10 % SDS
	0.67 ml	30 % Acrylamid-Bis
	25 µl	10 % APS

	7 µl	TEMED
SDS running buffer	25 mM	Tris-HCl, pH 8.3
(protein gels)	192 mM	glycine
	0.1 % (w/v)	SDS
Coomassie staining	40 % (v/v)	ethanol
(protein gels)	10 % (v/v)	acetic acid
	0.1 % (w/v)	coomassie R250
Destaining solution	10 % (v/v)	acetic acid
(protein gels)	40 % (v/v)	methanol
Sample-buffer (5x)	10 % (w/v)	SDS
(protein gels)	5 % (w/v)	β-mercaptoethanol
	50 % (w/v)	glycerol
	0.13 % (w/v)	bromphenol blue
	300 mM	Tris-HCl, pH 6.8
Sample-buffer (2x)	4 % (w/v)	SDS
(protein gels)	20 % (w/v)	glycerol
	5 % (v/v)	β-mercaptoethanol
	0.13 % (w/v)	bromphenol blue
	125 mM	Tris-HCl, pH 6.8
Stripping solution	0.5 M	NaCl
(Immuno blot)	0.5 M	acetic acid
Tris buffered saline	10 mM	Tris-HCl, pH 8.0
(TBS	150 mM	NaCl
Immuno blot)		
TBS-T	1 % (v/v)	Tween-20 in TBS
(Immuno blot)		

DNA Methods

TBE (0.5x)	44.5 mM	boric-acid
(agarose-gels)	10 mM	EDTA, pH 8.0
	44.5 mM	Tris-HCl
DNA-sample buffer (5x)	20 % (w/v)	glycerol in TBE buffer
(DNA-gels)	0.025 % (w/v)	bromphenol blue

ELISA

Phosphate buffered saline	150 mM	NaCl
(PBS)	8 mM	Na_2HPO_4, pH 7.4
	1.7 mM	NaH_2PO_4, pH 7.4
Washing buffer *(PBS-T)*	0.05 % (v/v)	Tween-20 in PBS
Blocking buffer *(ELISA)*	1-5%	BSA in PBS-T
Streptavidin solution *(Strep-HRP, Roche)*	1:5,000	PBS-T
Stopping solution *(ELISA)*	1.8 M	H_2O_2

FACS

Blocking solution	0.5 µl	mouse or rat serum
	0.5 µl	Fc-Receptor Block (BD Biosciences)
	ad 10 µl	EDTA buffer
EDTA buffer	2 mM	EDTA in PBS sterile filtrated

TBARS

Thiobarbituric acid *(TBA)*	67 mg	in 1ml DMSO + 9 ml H_2O 0.67 % (w/v)
1,1,3,3-tetramethoxy propane *(TMP)*	4.167 µl	in 1ml EtOH + 49 ml H_2O (500 µM)
Trichloroacetic acid	10 % (w/v)	in H_2O ice cold

Microsomal preparation

Microsome buffer	10 mM	KH_2PO_4
	0.25 M	Sucrose
	1 mM	EDTA
	0.1 % (w/v)	BSA
	1 mM	DTT
	pH 7.4	

3.1.5 Primary Antibodies

Immuno Blotting

anti-β-actin	rabbit polyclonal antibody which detects endogenous levels of human ß-actin (45 kDa), which showes species cross-reactivity with mouse (Cell signaling, Boston, USA). IB: dilution 1:1,000 (5 % BSA in TBS-T)
anti-Phospho-STAT3	rabbit monoclonal antibody which detects endogenous levels of rabbit STAT3 only when phosphoryated at tyrosine 705 (79, 86 kDa), which showes species cross-reactivity with mouse (Cell signaling, Boston, USA). IB: dilution 1:2,000 (5 % BSA in TBS-T)

anti-STAT3	mouse monoclonal antibody which detects endogenous levels of total mouse STAT3 protein (79, 86 kDa) (Cell Signaling). IB: dilution 1:1,000 (5 % milk powder in TBS-T)
anti-P450 2E1	rabbit polyclonal antibody which detects full length native rat cytochrome P450 2E1 (50-55 kDa), which showes species cross-reactivity with mouse. For usage in microsomal preparations, because of cellular localization in endoplasmatic reticulum membrane (abcam, Cambridge, UK). IB: dilution 1:5,000 (5 % milk powder in TBS-T)
anti-GSK-3ß	mouse monoclonal antibody which detects endogenous levels of total mouse GSK-3ß protein (46 kDa) (BD Biosciences, Heidelberg, Germany). IB: dilution 1:1,000 (3 % BSA in TBS-T)
anti-Phospho-GSK-3ß	mouse monoclonal antibody which detects endogenous levels of total mouse GSK-3ß (46 kDa) only when phosphorylated at tyrosine 216 (BD Biosciences, Heidelberg, Germany). IB: dilution 1:1,000 (3 % BSA in TBS-T)
anti-caspase-8	mouse monoclonal antibody which detects endogenous levels of mouse full length caspase-8 (57 kDa), the cleaved intermediate p43/p41 and the caspase-8 active fragment p18 (Cell signaling). IB: dilution 1:1,000 (5 % BSA in TBS-T)

Animal treatment

anti-Ly6G/Ly6C	rat monoclonal antibody which reacts with a common mouse epitope on Ly-6G and Ly-6C, previously known as the myeloid differentiation antigen Gr-1. The antibody

	recognizes granulocytes (neutrophils and eosinophils) and monocytes (BD Biosciences). Treatment: 100 µg/ mouse i.p.
anti-IL-6	Rat monoclonal antibody (MP5-20F3) reacts with mouse interleukin-6 (IL-6). The MP5-20F3 antibody is a neutralizing antibody (InVivo BioTech Services, Henningsdorf, Germany). Treatment: 200 µg/mouse i.p.

FACS

Fc-Block	Mouse Fc Block CD 16/32 mAB (BD Biosciences)
anti-Ly-6G/Ly-6C	FITC Rat anti-mouse Ly-6G and Ly-6C (clone RB6-8C5) (BD Biosciences) reacts with a common epitope on Ly-6G and Ly-6C (Gr-1). FACS: dilution 1:400
anti-CD11b	PE Rat anti-mouse CD11b (Clone M1/70) (BD Biosciences) reacts with the 170 kDa α-chain of Mac-1 (CD11b/CD18, αß2 integrin), also known as complement receptor 3 (CR3), which mediated adhesion to C3bi and ICAM-1 (CD54). Mac-1 is expressed on granulocytes, macrophages, myeloid-derived dendritic cells, natural killer cells, and B-1 cells. FACS: dilution 1:33
anti-F4/80	APC Rat anti-mouse F4/80 antibody (clone BM8) (eBioscience, San Diego, USA) reacts with mouse F4/80 antigen, an approximately 125 kDa transmembrane protein. The F4/80 antigen is expressed by a majority of mature macrophages. Other cell types such as Langerhans and Kupffer cells have been reported to express this antigen too.

FACS: dilution 1:100

anti-CD3 — APC Hamster anti-mouse CD3 antibody (clone 145-2C11) (BD Biosciences) reacts with the 25 kDa ε chain of the T-cell receptor-associated CD3 complex.
FACS: dilution 1:400

Immunohistochemistry

anti-neutrophil — rat monoclonal antibody which detects a polymorphic 40 kDa antigen expressed by mouse polymorphonuclear neutrophil cells, but absent on resident tissue macrophages (AbDserotec, Düsseldorf, Germany).
IHC: dilution 1:2,000

anti-BrdU — mouse monoclonal antibody which detects 5-bromo-2-deoxyuridine (Vector Laboratories, CA).
IHC: dilution 1:50

3.1.6 Secondary Antibodies

All horseradish-coupled secondary antibodies were purchased from Amersham Bioscience (Buckinghamshire, United Kingdom) and used in a dilution of 1:5,000.

3.1.7 Recombinant cytokines

human IL-6 — kindly provided by Steffi Schnell and Annett Kaßner (Biochemical Department, University of Kiel); was prepared and purified as described in (95).

Hyper-IL-6 — The fusion protein of the human IL-6 and the human IL-6R, Hyper-IL-6 ; kindly provided by Steffi Schnell and Annett Kaßner (Biochemical Department, University of Kiel), was prepared and purified as described in (58).

sgp130-Fc	kindly provided by Steffi Schnell and Annett Kaßner (Biochemical Department, University of Kiel); was prepared and purified as described in (63).

3.2 Molecular biology methods

3.2.1 DNA Gelelectrophoresis

DNA fragments were separated by horizontal electrophoresis cambers (BioRad) using agarose gels. Agarose gels were prepared by heating 1-2 % (w/v) agarose (Biozym) in 0.5 x TBE buffer, depending on the size of the DNA fragments, and the gels were supplemented with 0.05 % ethidium bromide. The samples were mixed with an appropriate amount of 6 x DNA sample buffer and loaded on the agarose gel. The gels were run at constant voltage (100 V) and finally documented using the Gel Doc 2000 UV-light documentation system (BioRad).

3.2.2 RNA Isolation

Total RNA from liver tissue was isolated using the NucleoSpin RNA II Kit (Macherey-Nagel) according to the manufacturer`s instructions. RNA concentration was determined by UV-spectrophotometry using the NanoDrop ND-1000 (peqLab Biotechnologie GmbH). 2 µg of isolated total RNA was used as template for the RT-PCR reaction, as further described in 3.2.4.

3.2.3 Polymerase chain reaction (PCR)

A ß-actin DNA fragment was PCR-amplified using an Eppendorf PCR-cycler in a total volume of 20 µl. The enzyme DreamTaq-polymerase as well as the appropriate buffers were obtained from MBI Fermentas. The following reaction mixture was used:

PCR-buffer (10x)	2.5 µl
Nucleotides (dNTPs)	10 mM each
Forward-primer	10 pmol (appendix)
Reverse-primer	10 pmol (appendix)
DreamTaq-polymerase	1 U
ddH_2O	add 20 µl
Template	2 ng

The PCR was performed using the following thermal cycling :

95°C	3 min		initial denaturation step
57°C	50 sec	1 x	primer annealing
72°C	50 sec		elongation
95°C	40 sec		denaturation
57°C	50 sec	33 x	primer annealing
72°C	50 sec		elongation
72°C	2 min	1 x	final elongation step

3.2.4 Reverse transcription PCR (RT-PCR)

RT-PCR is a PCR amplification of a product from the reverse transcription (RT) reaction, whereby a template mRNA is translated into a single-stranded cDNA. RevertAid M-MuLV Reverse Transcriptase from Fermentas was applied according to the manufacturer`s instructions. The reactions were performed using oligo (dT) primer annealing the 3' poly(A) mRNA tail. The PCR settings were described above. The following reaction mixture was used:

RNA	2 µg
Oligo (dT)	0.5 µg
ddH_2O	add 11.5 µl

The mixture was heated at 70°C for 5 min and then cooled on ice. The following components were subsequently added:

Reaction buffer (5x)	4 µl
dNTPs	20 mM each
RevertAid M-MuLV RT	1 µl
ddH_2O	add 20 µl

The reaction mix was incubated for 1 hour at 42°C. Afterwards the Reverse Transcriptase was heat inactivated at 70°C for 10 min. The mixture was filled add 100 µl with ddH_2O. 1 µl of the resulting cDNA was used directly for the subsequent PCR.

3.2.5 Quantitative polymerase chain reaction (Real Time PCR)

After RNA extraction and processing, TaqMan-based “gene expression assays” for β2-microglobulin (Mm00437762_m1), SAA1 (Mm00656927_g1), SAA3 (Mm00441203_m1), GSK-3ß (Mm00444911_m1) and Haptoglobin (Mm00516884_m1) were performed. All primers were bought at Applied biosystems (ABI, Foster City, CA). Reactions were performed on an ABI-Prism/7000 Sequence Detection System (ABI). Primers for ß2-microglobulin are binding around exon 1-2 boundary, for SAA1 around exon 3 - 4 boundary, for SAA3 around exon 2-3 boundary, for GSK-3ß around exon 8-9 boundary and for haptoglobin around exon 4 - 5 boundary. All data were analyzed in duplicates. mRNA Expression levels were normalized to ß2-microglobulin expression. The expression level of solvent treated C57Bl/6 mice was set to 1. All other values are given as fold control of expression in solvent control animals.

3.2.6 Protein preparation and concentration (BCA)

Protein extracts were prepared from tissue samples (~100 mg) by homogenization in 500 µl cell lysis buffer. The protein concentration was determined using the BCA kit according to the manufacturer`s instructions (Pierce). The extinction was determined at 568 nm in a microtiter plate reader (Tecan, Maennedorf, Switzerland).

3.2.7 SDS-polyacrylamide gel electrophoresis

Separation of proteins was performed with a discontinuous SDS-polyacrylamide gel electrophoresis (SDS-PAGE) using the Mini-Protean III system (BioRad).

After complete polymerization of the gel, the chamber was assembled as described by the manufactures protocol. Up to 30 µl sample were loaded in the pockets and the gel was run at constant voltage (120 V) until entry into stacking gel, when voltage was rised to 180 V for the remainder. The gel run was stopped when the bromphenol blue line reached the end of the gel. Gels were then either stained with coomassie or transferred to PVDF membrane and immuno blotting was performed.

3.2.8 Immuno Blot analysis

Proteins were transferred from the SDS-gel on a PVDF membrane (GE Healthcare, Uppsala, Sweden) using a MINI TRANSBLOT-apparatus (BioRad Laboratories GmbH, Munich, Germany). The blotting sandwich was assembled as described in the

manufactures protocol. Proteins were transferred electrophoretically at 4°C in Blotting-buffer at constant voltage (90 V, 120 min).

After electrophoretic transfer, the membranes were removed from the sandwiches and placed with the protein-bound side up in a 50 ml falcon. Membranes were immediately incubated with 20 ml blocking buffer for 1 hour at RT. Afterwards, the primary antibody was added in the apropriate dilution overnight at 4°C. The primary antibody was removed by washing the membrane 3 times for 10 min with TBS-T. The corresponding secondary antibody was applied for 1 hour at RT in TBS-T/ 4% milk powder in dark. Afterwards the membrane was washed again 3 times for 10 min with TBS-T and developed using the ECL-Plus Western blotting Detection System (GE Healthcare). The signals were visualized by X-ray film (GE Healthcare) in darkroom or with the chemiluminescence kamara system LAS-1000 (Fujifilm, USA) for defined time periods.

3.2.9 TBARS quantification

Thiobarbituric acid reactive substances (TBARS) were used as an index of of lipid peroxidation and oxidative stress. Thiobarbituric acid (TBA) forms under high temperatures adducts with the lipid peroxidation product malondialdehyde (MDA), which can be measured at 532 nm. 1 mg liver tissue homogenate (100 µl) was mixed with 200 µl ice cold 10% (w/v) trichloroacetic acid to precipitate proteins. After incubation (15 min on ice) and centrifugation (2,200 x g, 15 min, 4°C) 200 µl of the supernatant was mixed with an equal volume TBA (Merck, Darmstadt, Germany) and incubated for 10 min at 100°C. After cooling, the formed TBA-MDA-adduct was measured colorimetrically at 532 nm in triplicates using TMP (1,1,3,3-tetramethoxypropane, Sigma-Aldrich, Steinheim, Germany) as standard (Tecan Reader, Maennedorf, Switzerland).

3.2.10 Enzyme-linked immunosorbent Assay (ELISA)

To determine the concentration of different antigens the “sandwich” ELISA method was used. First, the capture antibody was coated to a microtitre plate (Greiner Microlon, Solingen, Germany). After blocking, antigen was added and allowed to complex with the bound antibody. Unbound products were removed by extensive washing, and a biotinylated detection antibody was added. Finally subsequent addition of streptavidin-horseradish peroxidase (Roche, Mannheim, Germany) and

peroxidase substrate (Roche, Mannheim, Germany) led to a calorimetric reaction which allowed the quantitation by measuring the amount of bound detection antibody. To determine the absolute amount of antigen in the samples a purified antigen standard was used. The following general protocol was used:

50 µl of coating antibody-solution was added to each well and incubated at RT over night; the wells were washed three times with 300 µl PBS-T; 200 µl of blocking buffer was added to saturate the remaining protein binding sites on the microtiter plate for 1 hour at room temperature; the wells were washed three times with 300 µl PBS-T. The samples (mostly plasma or liver homogenate) were diluted in PBS supplemented with 1 % BSA and 50 µl of diluted sample or purified antigen standard were added to each well for 2 hours at RT.

Thereafter the wells were washed three times with PBS-T and 50 µl of detection antidody solution was added to each well and incubated at RT for 2 hours. The wells were washed three times with PBS-T and 100 µl of streptavidin-horseradish peroxidase solution (1:5,000 in PBS supplemented with 1 % BSA) was added and incubated for 45 min at RT. The wells were again washed three times with PBS-T and 75 µl of the peroxidase substrate BM blue POD (Roche) was added for approximately 20 min and the reaction was stopped by addition of 75 µl stopping solution. The optical densities at 450 nm were measured on an ELISA plate reader (SLT Rainbow; Tecan, Maennedorf, Switzerland).

The human gp130 ELISA kit, the murine IL-6R ELISA kit, as well as the murine IL-6 ELISA kit were purchased from R&D systems and were used according to the manufactures protocol.

3.2.11 Statistical analysis

Data are expressed as mean values ± SD; 4-6 mice were used per experimental group. Statistical analysis was performed by using a Student's unpaired *t* test (GraphPad InStat version 3.0, GraphPad Software, San Diego California USA). A p-value below 0.05 was considered statistically significant (* $P < 0.05$; ** $P < 0.01$; *** $P < 0.001$).

3.3 Animal Methods

3.3.1 CCl_4 induced liver damage

Male C57Bl/6N mice were kept at a 12-hour light-dark cycle under standard conditions and provided with food and water *ad libitum*. For all experiments 4 – 6 mice per group were used. Liver damage was induced by a single intraperitoneal injection of CCl_4 (Sigma, Deisenhofen, Germany) dissolved in rape oil immediately before treatment and applied as one dose of 3 ml/kg body weight. All experiments were performed according to the German guidelines for animal care and protection (V 31272241.121-3 (41-3/06)).

3.3.2 Blockade of IL-6 Transsignaling with sgp130Fc

Mice were treated i.p. with 250 µg sgp130Fc 18 h prior to CCl_4 treatment. sgp130Fc levels were measured via Enzyme-linked immunoabsorbent assays in the serum of the mice as described (Rabe and others 2008) using a human gp130 Elisa Kit (DuoSet human gp130 ELISA Kit, R&D Systems, Wiesbaden, Germany) according to the manufacturers' instructions. Serum was diluted 1:2,000 in 1% BSA/PBS and measured in duplicates. Recombinant gp130 was used as standard.

3.3.3 Enhancement of IL-6 Transsignaling with Hyper-IL-6

10-12 weeks old male C57/Bl6 mice were treated with 4 µg Hyper-IL-6 i.p. 18 hours prior to CCl_4 treatment.

3.3.4 Neutrophil depletion

As described previously (64), neutrophils were depleted using a purified rat anti-mouseLy6G/Ly6C monoclonal antibody (mAb) (BD Bioscience, Heidelberg, Germany). Mice were injected with 100 µg mAb i.p. 18 h prior to CCl_4. Depletion was controlled with stainings of neutrophils on paraffin tissue sections as described below.

3.3.5 Blockade of IL-6 Signaling

Circulating IL-6 was depleted by using a purified monoclonal anti-IL-6 Antibody. Mice were injected with 200 µg antibody i.p. 18 hours prior to CCl_4. Mice were sacrificed at different timepoints after CCl_4 treatment and liver and blood samples were taken. To control for depletion, IL-6 ELISA on serum samples was used as described above.

3.3.6 Plasma/ Serum preparation of whole mouse blood

Whole mouse blood was collected either by tail bleeding or cardiac puncture. Tubes for taking blood (Sarstedt, Nümbrecht, Germany) were coated with Lithium-Heparin to prevent clotting. Plasma was obtained by centrifugation (5 min, 10,000 rpm, 4°C) and stored at –20°C.

Serum was obtained by collecting whole mouse blood in not-coated tubes and led it coagulate for 1-2 hours at 4°C. Afterwards serum was obtained by centrifugation (5 min, 10,000 rpm, 4°C) and stored at –20°C.

3.3.7 Serum parameter

Serum alanine aminotransferase (ALT), serum aspartate aminotransferase (AST), potassium and uric acid were determined in diluted blood serum using a Reflotron analyzer (Roche Diagnostics, Basel, Switzerland) and Reflotron test strips. Blood glucose levels were measured using a OneTouch Ultra device (LifeScan, Neckargemünd, Germany). Mouse whole blood was used for analysis.

3.3.8 Flow cytometry analysis of mouse blood

To analyze the number of neutrophils in mouse blood flow cytometry analysis was performed.

For this, 20 µl blood was collected from mouse tail, immediately transferred into 100 µl FACS EDTA buffer to prevent clotting and inverted briefly. For each staining 100 µl of blood/ EDTA buffer mixture was tranferred into a well of a 96-well-plate. One additional sample was necessary for each individual staining antibody and one for a negative staining control.

The samples were blocked with 10 µl FACS blocking solution and icubated 5 min on ice. Afterwards staining mastermix was prepared:

FITC Ly6G: 0.25 µl/ sample
PE CD11b: 3 µl/ sample
APC F480: 1 µl/sample

For individual stainings FITC Ly6G 0.25 µl, PE CD11b 3 µl and APC CD3 0.25 µl were used.

All stainings were incubated for 30 min in the dark at 4°C. Thereafter 96-well-plate was centrifuged at 1,500 rpm for 5 min at 4°C, supernatant was discarded and pellet was immediately resuspend in 100 µl 1 x FACS Lysing solution (BD Biosciences). Samples were incubated for 10 min in the dark at RT and centrifuged again (1,500 rpm, 5 min, 4°C). Supernatant was discarded and pellet was again resuspend in 100 µl 1 x FACS Lysing solution (BD Biosciences) and incubated for 5 min (in the dark, RT). After centrifugation (1,500 rpm, 5 min, 4°C) supernatant was discarded, pellet was resuspend in 200 µl PBS and immediately transferred into FACS-tubes (Sarstedt) for analyzing in flow cytometry (FACS-Canto; Becton Dickinson, Heidelberg, Germany).

3.3.9 BrdU Labeling

BrdU (5-bromo-2-deoxyuridine) is a synthetic nucleoside that is an analogue of thymidine and provides a simple technique for labeling and identifying proliferating cells. BrdU can be incorporated into the newly synthesized DNA of replicating cells (during the S-phase of the cell cycle), substituting for thymidine during DNA replication. Antibodies specific for BrdU can then be used to detect the incorporated chemical, thus indicating cells that were actively replicating.
Two hours prior to sacrificing, mice were injected with 10 µl/µg body weight BrdU. Positive cells were visualized immunhistochemically and representative pictures were given.

3.3.10 Histological and immunohistochemical analysis

Liver samples were handled as indicated below:

4 % Formaldehyde	over night, 4°C
H_2O	5 hours
70 % EtOH	over night, RT
96 % EtOH I	30 min
96 % EtOH II	60 min
100 % EtOH I	60 min
100 % EtOH II	30 min
Xylol I	90 min
Xylol II	90 min

Paraffin I	30 min
Paraffin II	over night
Paraffin III	60 min

HE staining

Tissue sections were shortly incubated in Gill3 Hematoxylin (Thermo Scientific, Cheshire, UK), differentiated in 0.5% acetic acid, rinsed in tap water and counterstained with Giemsa's azur eosin methylene blue solution (Merck, Darmstadt, Germany). Necrotic areas were quantified using ImageJ-Software. Necrotic areas were calculated from 30 random highpowered fields of three mice and given in percent of total area**.**

DAPI staining

Tissue sections were stained with DAPI (4',6-Diamidino-2-phenylindole dihydrochloride) (Sigma, Deisenhofen, Germany) at 0.1 µg/ml PBS.

Periodic Acidic Schiff (PAS) staining

Glycogen was stained within the liver with PAS stainings as described previously (Drucker et al.). Shortly, tissue sections were incubated in 0.8 % periodic acid (Sigma, Deisenhofen, Germany) followed by an incubation in Schiff´s reagent (Sigma, Deisenhofen, Germany). Sections were counterstained with Shandon Gill3 Hematoxylin (Thermo Scientific, Cheshire, UK).

Neutrophil staining

Staining for neutrophils was carried out using a monoclonal rat anti-mouse Neutrophil Antibody (AbDserotec, Düsseldorf, Germany) diluted in sample diluent (Dako, Glostrup, Denmark). After incubation with biotinylated polyclonal rabbit anti-rat antibody (Dako, Glostrup, Denmark) and EnVision-HRP (Dako, Glostrup, Denmark) the signal was developed with AEC Substrate (Dako, Glostrup, Denmark). Samples were counterstained with Shandon Gill3 Hematoxylin (Thermo Scientific, Cheshire, UK).

5-bromo-2-deoxyuridine (BrdU) staining

Staining for BrdU was carried out using a mouse monoclonal BrdU Antibody (Vector Laboratories, CA) diluted in sample diluent (Dako, Glostrup, Denmark). After incubation with labeled polymer-HRP-anti-mouse antibody (Dako envision, Glostrup, Denmark), the signal was developed with AEC Substrate (Dako, Glostrup, Denmark). Samples were counterstained with Shandon Gill3 Hematoxylin (Thermo Scientific, Cheshire, UK).

Tunel staining

Staining for Apoptosis was carried out using a Peroxidase in Situ Apoptosis Detection Kit (Chemicon International, Billerica, USA). The signal was developed with DAB Substrate (3,3' Diaminobenzidine, Dako, Glostrup, Denmark) and samples were counterstained with methylgreen (Serva, Heidelberg, Germany).

3.3.11 Preparation of Microsomes

Mice livers were homogenized in 10 mM KH_2PO_4, pH 7.4, containing 0.25 M sucrose, 1 mM EDTA, 0.1% (w/v) BSA and 1 mM DTT at 4°C. The homogenate was centrifuged at 750 x *g* for 15 min and the supernatant was again centrifuged until the pellet remained pale (normally 3-5 centifugation steps). The pellet was discarded. Subsequently the supernatant was centrifuged at 10,300 x g for 20 min. The pellet was discarded and the supernatant was centrifuged at 137,000 x g for 70 min. The supernatant was discarded and the pellet was resuspended in buffer and centrifuged again at 137,000 x g for 70 min. The final pellet was resuspended in buffer and stored at –80°C. Samples were taken for measuring protein concentration using the BCA Kit (Pierce, Rockford, IL). Equal amounts of protein were analyzed with immuno blotting analysis using a polyclonal CYP2E1 Ab (Abcam, Cambridge, UK) as described above.

3.4 Primers and Markers

DNA-Ladder

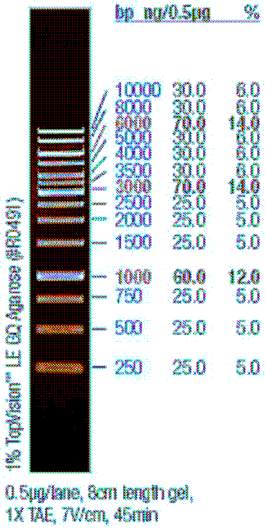

Figure 3.4.1: 1 kb DNA-Ladder from Fermentas.

Protein-Ladder

A **B**

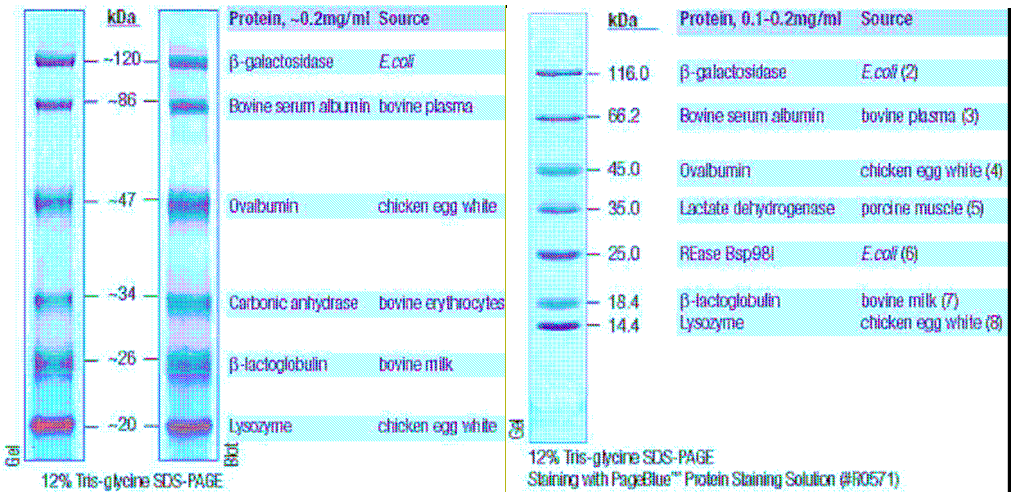

Figure 3.4.2: Protein Molecular Markers (Fermentas). (A) Prestained Protein Molecular Marker (20-120 kDa) from Fermentas. (B) Protein Molecular Weight Marker (14,4-116 kDa) for Coomassie- or silverstaining from Fermentas.

4 Results

4.1 Identifying the critical dosis of CCl_4 by using different concentrations

Acute liver damage was induced with a single injection of CCl_4. Liver damage was quantified by measuring serum alanine aminotransferase (ALT), aspartate transferase (AST) levels, blood glucose levels, as well as histological evaluation via HE-stainings.

ALT catalyzes the transfer of an amino group from alanine to a-ketoglutarate. Usually ALT is detectable in high concentration within hepatocytes. In case of hepatic damage, ALT is found in the sera.

AST catalyzes the conversion of aspartate and alpha-ketoglutarate to oxaloacetate and glutamate, and vice-versa. Serum levels are raised in acute liver damage. As it is also present in red blood cells, cardiac muscle, skeletal muscle, kidney and brain tissue, elevated serum levels might be as well due to damage to those tissue.

In the first instance, a CCl_4 concentration to study effects of IL-6 Transsignaling on CCl_4 induced liver damage should be determined.

In the beginning, C57Bl/6N mice were treated with 3 ml/kg body weight CCl_4 to induce an acute liver damage. Blood samples were taken direct, 24 and 48 hours after CCl_4 injection. ELISA for soluble IL-6Receptor (sIL-6R) was carried out and revealed significant elevated sIL-6R levels in the sera of CCl_4 treated mice when compared to mock treated mice ($P< 0.005$) (Fig. 4.1.1). To investigate the effect of IL-6 Transsignaling to CCl_4 induced liver damage, IL-6 Transsignaling should be modulated by either blocking via sgp130Fc or accelerating via Hyper-IL-6.

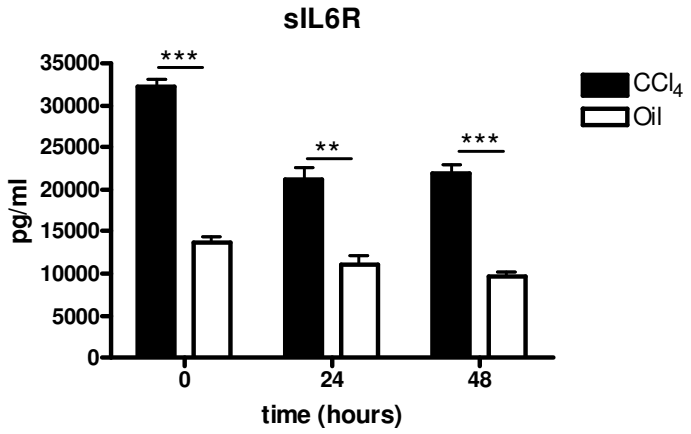

Figure 4.1.1: Soluble IL-6R levels after CCl_4 injection. C57Bl/6N mice were treated with 3 ml/kg body weight CCl_4. sIL-6R ELISA in mouse sera was performed at the indicated timepoints. A significant increase of sIL-6R was detected after CCl_4 injection. Unpaired student`s t test: ** P< 0.005; ***P< 0.0001.

10-12 weeks old male C57/Bl6N were injected intraperitoneally (i.p.) with 1, 3 and 8 ml CCl_4 per kg body weight dissolved in rape-oil. Mice were treated with 250 µg sgp130Fc i.p. to block IL-6 Transsignaling, 4 µg Hyper-IL-6 i.p. to accelerate IL-6 Transsignaling, or mock treatment 18 hours prior to CCl_4 intoxication.

In mice treated with 1 ml CCl_4/ kg body weight were obtained 48 hours after CCl_4 induced liver damage elevated ALT and AST serum levels. Animals pretreated with sgp130Fc developed slightly increased ALT and AST levels when compared to CCl_4 only or Hyper-IL-6 pretreated mice (Fig. 4.1.2A).

In mice treated with 3 ml CCl_4/ kg body weight were obtained higher ALT and AST serum levels, which were significantly increased in mice with blocked IL-6 Transsignaling via sgp130Fc (Fig. 4.1.2B).

In mice treated with 8 ml CCl_4/ kg body weight were observed no differences between CCl_4 only, sgp130Fc pretreated or Hyper-IL-6 pretreated groups (Fig. 4.1.2C).

48 hours after intoxication blood glucose levels were slightly reduced in all CCl_4 treated mice (100-150 mg/dl) in comparison to mock treated mice (200 mg/dl) with no differences between the pretreated groups (Fig. 4.1.3). Modulating IL-6 signaling however had no effect on glucose levels.

HE stainings of liver sections revealed increased damage around central veins of mice treated with CCl_4. When the CCl_4 dosage was elevated, also the extent of liver damage increased (Fig. 4.1.4).

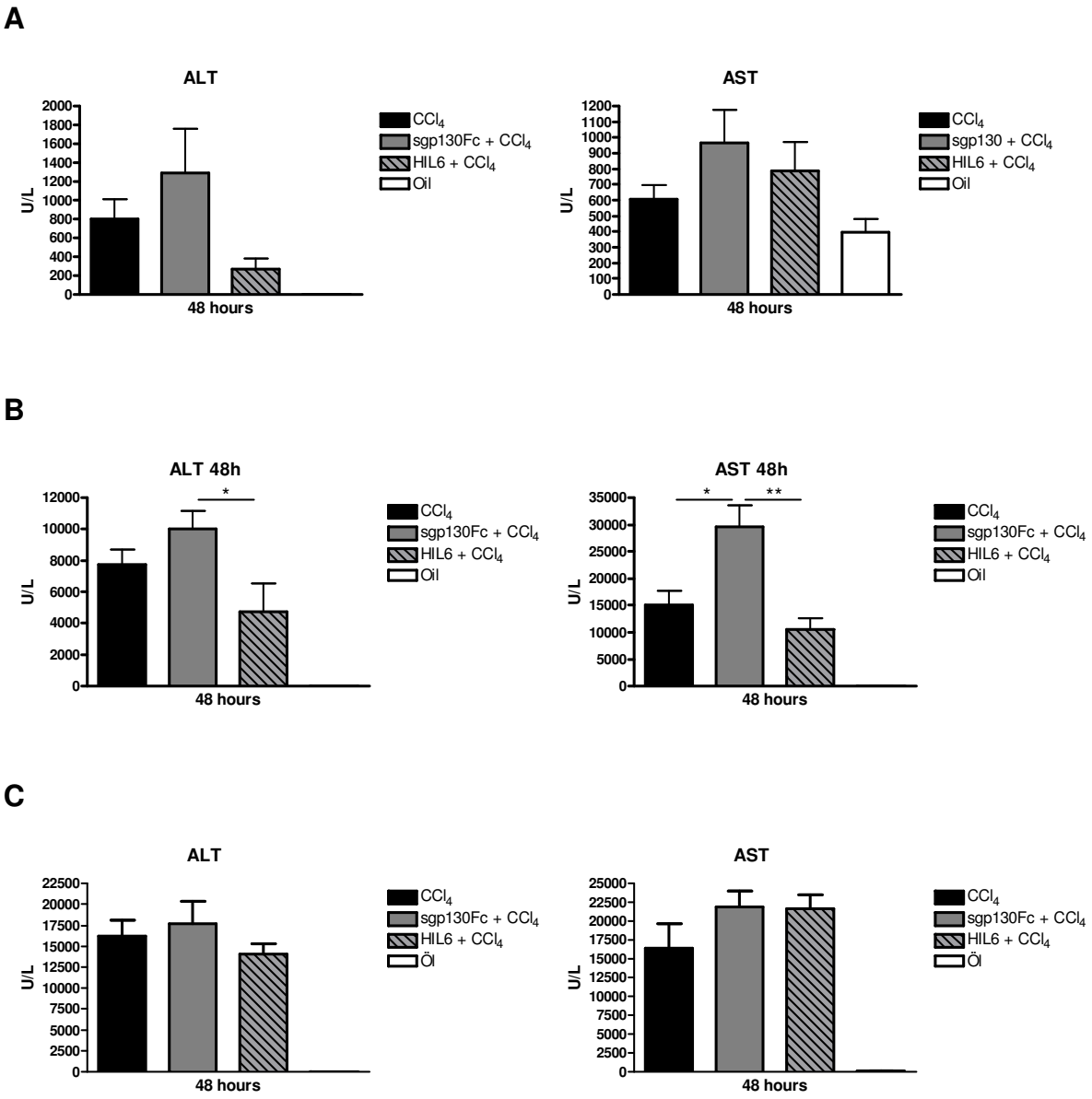

Figure 4.1.2: Measurement of ALT and AST serum levels. C57Bl/6N mice were treated with 1 (A), 3 (B) and 8 (C) ml/kg body weight CCl_4 after previous injection of sgp130Fc, Hyper-IL-6 or mock treatment. ALT and AST serum levels were measured 48 hours after setting the liver damage. Unpaired student`s t test: * $P< 0.05$; ** $P< 0.005$.

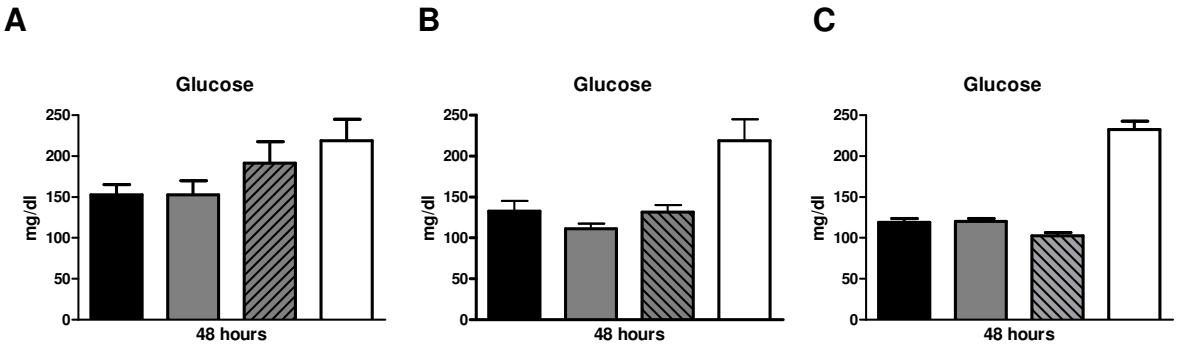

Figure 4.1.3: Measurement of blood glucose levels. C57Bl/6N mice were treated with 1 (A), 3 (B) and 8 (C) ml/kg body weight CCl_4 after previous injection of PBS (black bars), sgp130Fc (grey bars), Hyper-IL-6 (striped bars) or mock treatment (white bars). Glucose levels from whole blood revealed a slight reduction in all CCl_4 treated groups with no differences between the groups.

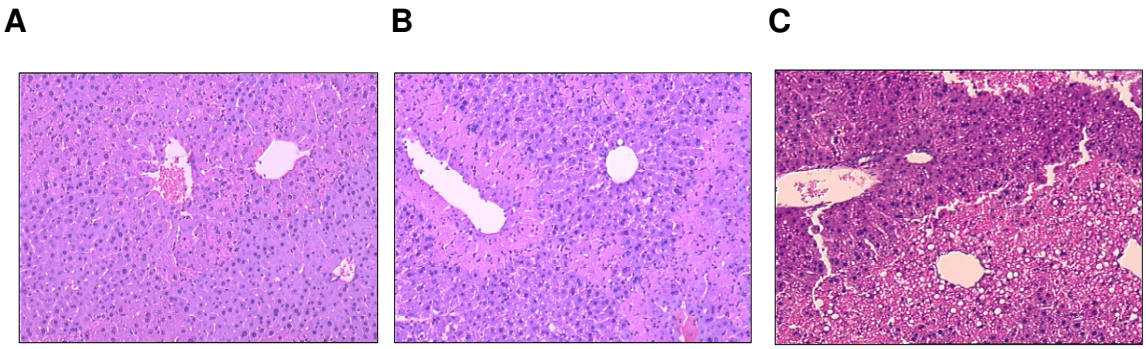

Figure 4.1.4: HE staining of a CCl_4 intoxicated liver. Hematoxylin /Eosin stainings of liver sections 48 hours after CCl_4 treatment in 20 fold magnification. C57/Bl6N mice were treated with 1 (A), 3 (B) and 8 (C) ml/kg body weight CCl_4 i.p. Livers showed increasing damage around central veins with increasing CCl_4 dosage.

4.2 Blockade of IL-6 Transsignaling via sgp130Fc

To specifically block IL-6 Transsignaling, mice were injected with 250 µg sgp130Fc i.p. 18 hours before CCl_4 treatment. Serum levels at the time of sacrificing showed that sgp130Fc levels were around 55 pg/ml 6 hours after CCl_4 treatment, and decreased slowly within the course of experiment to around 35 pg/ml (Fig 4.2.1).

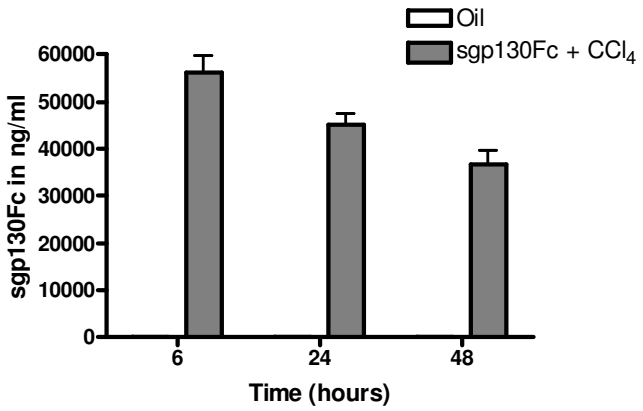

Figure 4.2.1: Serum sgp130Fc levels. C57Bl/6 mice were injected with 250 µg /mouse i.p. 18 hours before CCl_4 intoxication. Serum sgp130Fc levels were measured via ELISA at the indicated time points. The protein was relatively stable and showed a slight reduction within the duration of the experiment.

4.3 Quantification of CCl_4-induced liver damage

In all following experiments 10-12 weeks old male C57/Bl6N mice were injected intraperitoneally with 3 ml CCl_4 per kg body weight dissolved in rape-oil. Mice were pretreated with PBS i.p., 250 µg sgp130Fc i.p., 4 µg Hyper-IL-6 i.p., or mock treatment 18 hours prior to CCl_4 intoxication.

Mice were sacrificed at different time points between 6 and 48 hours post injection. For analyzing the acute phase response, mice were sacrificed 0, 2, 4 and 6 hours after CCl_4 intoxication.

4.3.1 ALT and AST serum levels

ALT and AST values were elevated after CCl_4 treatment at all time points in comparison to mock treated control animals.

6 hours after CCl_4 intoxication ALT levels reached values around 1,000 U/L with no significant differences between the CCl_4 treated groups. Serum levels of mock treated mice achieved ALT serum levels of 400 U/L.

AST serum levels of CCl_4 treated mice were elevated to around 1,700 U/L, while IL-6 Transsignaling blocked mice showed slightly increased values of about 2,500 U/L. Activating of IL-6 Transsignaling showed a little decrease in AST levels 6 hours after CCl_4 treatment to values around 1,000 U/L. Control animals revealed AST values of around 500 U/L.

24 hours after the intoxication ALT and AST values were strongly elvated in all groups compared to control animals.

CCl_4 treatment led to ALT levels of about 4,000 U/L. When IL-6 Transsignaling was blocked, ALT levels increased significantly to 12,000 U/L ($P< 0.0001$). When IL-6 Transsignaling was activated by Hyper-IL-6, ALT levels reached values around 5,000 U/L, which was a significant reduction compared to sgp130Fc pretreated mice ($P< 0.0001$), but had no obvious protective effect compared to only CCl_4 treated mice.

The same tendencies were observed in AST measurements. AST levels were clearly elevated over solvent controls in all groups. AST levels of CCl_4 treated animals reached values about 10,000U/l. When IL-6 Transsignaling was blocked, AST levels increased significantly to about 27,000 U/L ($P< 0.05$). Activating IL-6 Transsignaling by Hyper-IL-6 led to AST levels of about 15,000 U/L, which was a significant reduction compared to blocked IL-6 Transsignaling ($P< 0.05$). As observed in ALT levels, there was no protective effect of Hyper-IL-6 treatment notable.

48 hours post-injection of CCl_4, serum transferase levels continued to increase. Hyper-IL-6 pretreatment led to decreased ALT and AST levels, whereas sgp130Fc treatment led to significantly increased levels (Fig. 4.3.1).

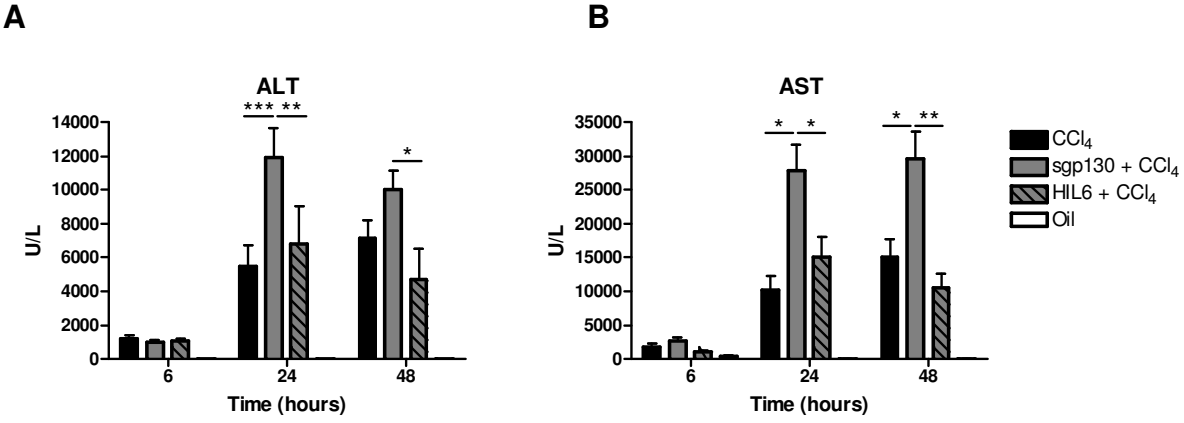

Figure 4.3.1: Measurement of ALT and AST serum levels. C57Bl/6N mice were treated with CCl_4 after previous injection of PBS, sgp130Fc, Hyper-IL-6 or mock treatment. ALT (A) and AST (B) serum levels were measured at the indicated time points. Serum levels were significantly elvated when mice were pretreated with sgp130 24 and 48 hours after the damage. Unpaired student`s t test: * $P< 0.05$; ** $P< 0.005$; ***$P< 0.0001$.

4.3.2 Blood glucose levels

CCl_4 injection led to a decrease in blood glucose levels after 24 to 48 hours (100-120 mg/dl) compared to mock treated control mice (220-250 mg/dl). There was no significant difference detectable between the different treated mouse groups (Fig. 4.3.2).

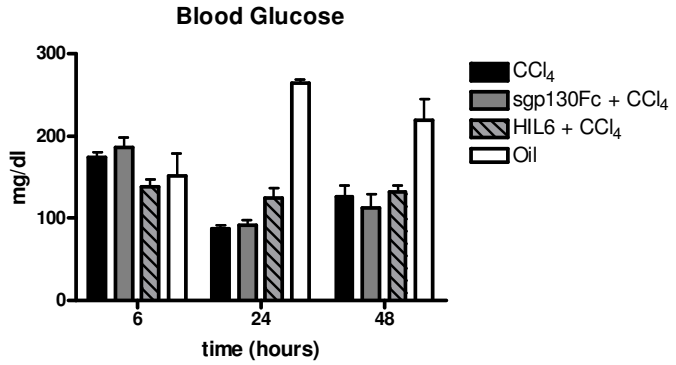

Figure 4.3.2: Blood glucose levels after CCl_4 intoxication. Blood glucose levels were measured at the indicated time points. In comparison to mock control animals, blood glucose levels were lower but showed no differences between the different pre-treatment groups.

4.3.3 HE and DAPI stainings

Livers of mice 48 hours after CCl_4 treatment were first fixed in formaldehyde, dehydrated in alcohol and afterwards embedded in paraffin. Hematoxylin/Eosin stainings were performed to give an overview about the architecture and the extent of damaged regions and intact areals. Histological examination of the overall liver damage 48 h after CCl_4 administration showed smaller necrotic areas in CCl_4 treated mice compared to sgp130Fc pretreated mice (Fig. 4.3.3 a, b, c, d). Quantification of liver damage 48 h after CCl_4-induced liver damage indicated that only 33.2% of the liver was necrotic in CCl_4 treated mice compared to 58,6% in sgp130Fc pretreated mice (Fig. 4.3.4 B). No significant difference was seen in the number of apoptotic nuclei as measured by TUNEL staining (Fig. 4.3.3 e, f). Using DAPI staining, we noted less intact nuclei and extended necrotic areas in sgp130Fc pretreated animals (g, h). The reduction of DAPI positive hepatocytes is shown in Fig. 4.3.4 A.

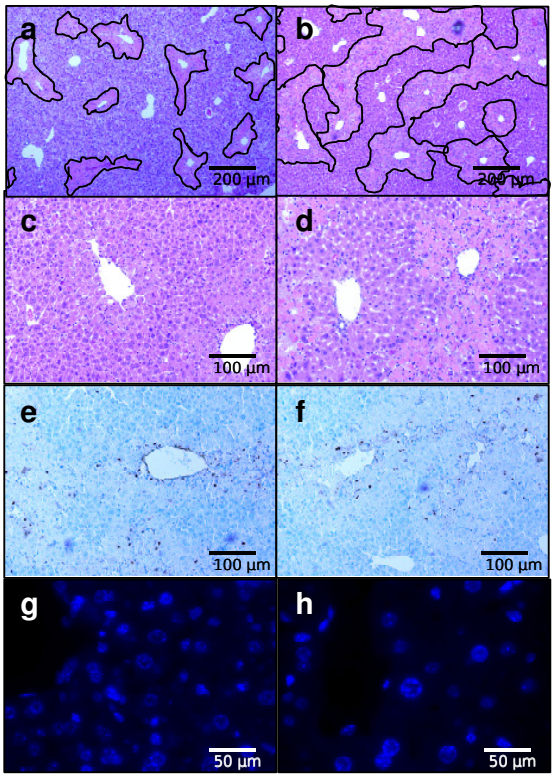

Figure 4.3.3: Histological evaluations of liver sections 48 hours after CCl_4 injection. (a) Hematoxylin Eosin stainings (10 fold magnification) of CCl_4 only and (b) of sgp130Fc pretreated mice, (c) Hematoxylin Eosin stainings (20 fold magnification) of CCl_4 only and (d) of sgp130Fc pretreated mice, (e) Tunel stainings (20 fold magnification) of CCl_4 only and (f) of sgp130Fc pretreated mice, (g) DAPI stainings (40 fold magnification) of CCl_4 only and (h) of sgp130Fc pretreated mice. Damage is more severe in sgp130 pretreated animals, but the occurrence of apoptotic events are comparable.

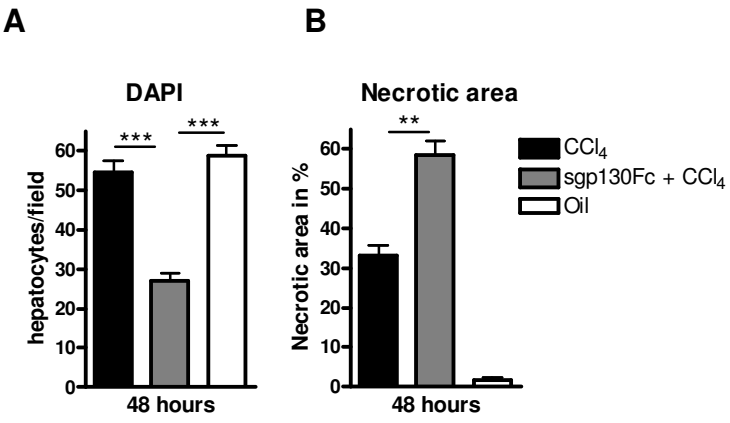

Figure 4.3.4: Quantification of liver damage. (A) Quantification of DAPI stainings show that more nuclei are intact in CCl_4 treated animals in comparison to sgp130Fc pretreated animals ($P< 0.0001$). (B) Quantification of HE stainings show more necrotic area in sgp130Fc pretreated mice ($P< 0.005$) when compared to CCl_4 treated mice.

4.3.4 Uric acid and potassium serum level

To further quantify cell damage, uric acid and potassium levels in blood serum were measured.

Uric acid plays a protective role in defending organs and tissues from oxidative damage by attenuating oxidation of plasma lipids, lipoproteins and unsaturated fatty acids. There has been identified a critical role for uric acid in antioxident defense and lipid peroxidation in human blood plasma (96-99).

48 hours after CCl_4 treatment, uric acid levels increased in blood serum. In sgp130Fc pretreated mice uric acid serum level reached values about 15 mg/dl, which was significantly higher when compared to CCl_4 only treated animals, where values reached around 7 mg/dl ($P< 0.05$). In Hyper-IL-6 pretreated mice uric acid levels only reached levels of around 3 mg/dl, which was significantly less than in sgp130Fc pretreated ($P< 0.005$) and in CCl_4 only treated mice ($P< 0.05$) (Fig. 4.3.5A).

Also potassium levels increased to higher values in sgp130Fc pre-treated animals. Values reached levels of around 20 mval/L, whereas Hyper-IL-6 pretreated and CCl_4 only treated mice reached values of about 14 mval/L (Fig. 4.3.5B).

This indicates that cell damage is higher when IL-6 Transsignaling is blocked. We conclude from this findings that there has to be components specifically activated under the blockade of IL-6 Transsignaling which are responsible for an enhanced damage, or that protective pathways are blocked in this model of acute CCl_4 intoxication.

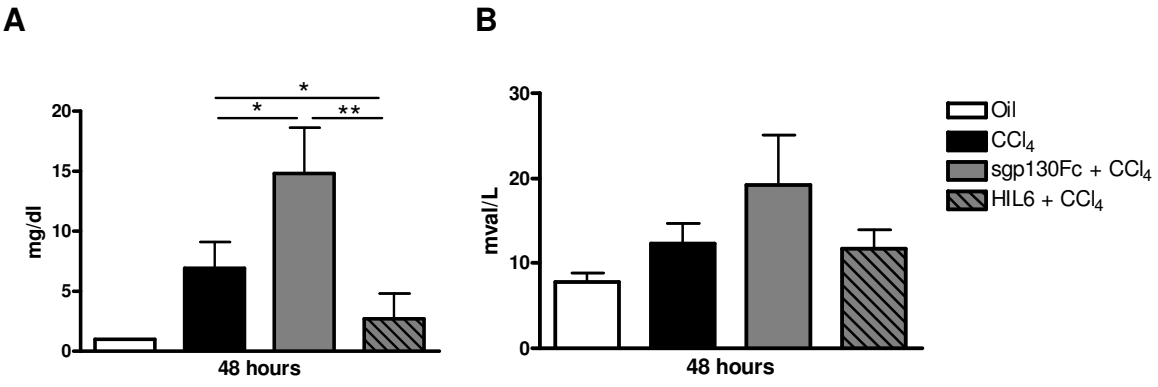

Figure 4.3.5: Uric acid and potassium serum levels. (A) Uric acid levels increased significantly 48 hours after CCl_4 treatment. The rise was significantly higher when IL-6 Transsignaling was blocked (sgp130Fc, grey bars). Enhancement of Transsignaling with a single, previous injection of Hyper-IL-6 led to significant lower uric acid levels. Unpaired student`s t test: * $P< 0.05$; ** $P< 0.005$. (B) Potassium levels increased slightly in sgp130Fc pretreated mice 48 hours after CCl_4 treatment.

4.4 Quantification of lipid peroxidation by measuring TBARS

Thiobarbituric acid reactive substances (TBARS) are an index of lipid peroxidation and oxidative stress and were measured in liver tissue homogenate 0 to 6 hours after CCl_4 treatment.

4 hours after CCl_4 induced liver damage, TBARS levels of sgp130Fc pretreated mice peaked at 7 µM, which was significantly higher than in CCl_4 only treated mice, where TBARS values reached only 4 µM ($P< 0.05$). In mock treated mice TBARS held at basic levels of 0.5 µM.

6 hours after CCl_4 treatment TBARS declined but stayed significantly higher in livers of mice with blocked IL-6 Transsignaling ($P< 0.05$) (Fig. 4.4.1).

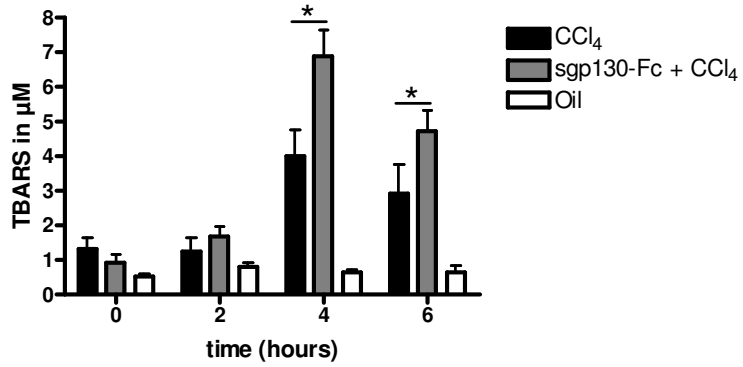

Figure 4.4.1: Evaluation of oxidative stress by TBARS quantifications. C57Bl/6N mice were treated with CCl_4 after previous injection of sgp130Fc or mock treatment. TBARS were measured in total protein lysates at the indicated time points after the intoxication. Values increased significantly in sgp130Fc pretreated mice 4 and 6 hours after CCl_4 treatment (*$P< 0.05$).

4.5 Expression levels of P450 2E1 (Cyp2E1)

The mechanism of oxidative liver damage after CCl_4 treatment depends on biotransformation of CCl_4 into the free radicals $CCl_3^{\bullet}$ and $CCl_3O_2^{\bullet}$. This process is catalyzed by Cytochrome P450 2E1 which is located in the endoplasmatic reticulum of hepatocytes.

To proof that in all different CCl_4 treated groups has developed the same amount of bioactivated radicals, protein expression levels of Cyp2E1 were measured. For this purpose microsomes were isolated from livers of CCl_4 treated animals. Proteins were isolated from microsome preparations and immuno blotting against Cyp2E1 was carried out.

24 hours after the CCl_4 treatment was detected an induction of Cyp2E1, whereas in mock treated mice almost no enzyme expression was detectable. Equal loading of protein was controlled with ponceau stainings (Fig. 4.5.1).
This experiment indicates that the different extent of CCl_4 induced liver damage is not due to different Cyp2E1 protein expression levels.

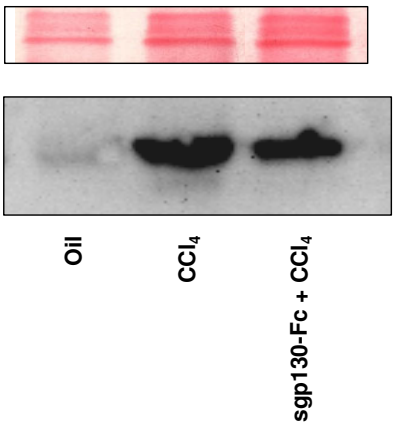

Figure 4.5.1: Expression of Cytochrome P450 2E1 (Cyp2E1). C57Bl/6N mice were treated with CCl_4 after previous injection of sgp130Fc or mock treatment. Microsomes were prepared from livers 24 hours after liver damage and immuno blotting analysis for Cyp2E1 was carried out. Equal protein amounts were controlled with Ponceau staining.

4.6 Inflammatory response: Quantification of IL-6 level

IL-6 is considered to be a main mediator of inflammatory responses. IL-6 levels were measured within the sera or liver protein lysates of CCl_4 treated mice at different time points after liver injury.
6 hours post CCl_4 injection, a 2-fold increase of IL-6 in the sera of sgp130Fc pretreated mice was detected (2,000 pg/ml) compared to CCl_4 only treated mice (ca 1,000 pg/ml) and to Hyper-IL-6 pretreated mice (ca 800 pg/ml) ($P< 0.0001$).
24 hours after CCl_4 induced liver damage, IL-6 serum levels were significantly elevated in sgp130Fc pretreated mice (ca 3,000 pg/ml) compared to CCl_4 only treated (2,000 pg/ml) and Hyper-IL-6 pretreated animals (2,000 pg/ml) ($P< 0.0001$) (Fig. 4.6.1A).
Within protein lysates of liver tissue, elevated IL-6 levels in sgp130Fc pretreated mice were detected 6 hours after CCl_4 treatment compared to CCl_4 only ($P< 0.05$) and Hyper-IL-6 pretreated mice ($P< 0.0001$).

24 and 48 hours after CCl_4-induced liver damage IL-6 levels increased in liver homogenates compared to mock control. There was no significant difference between the groups detectable (Fig. 4.6.1B).

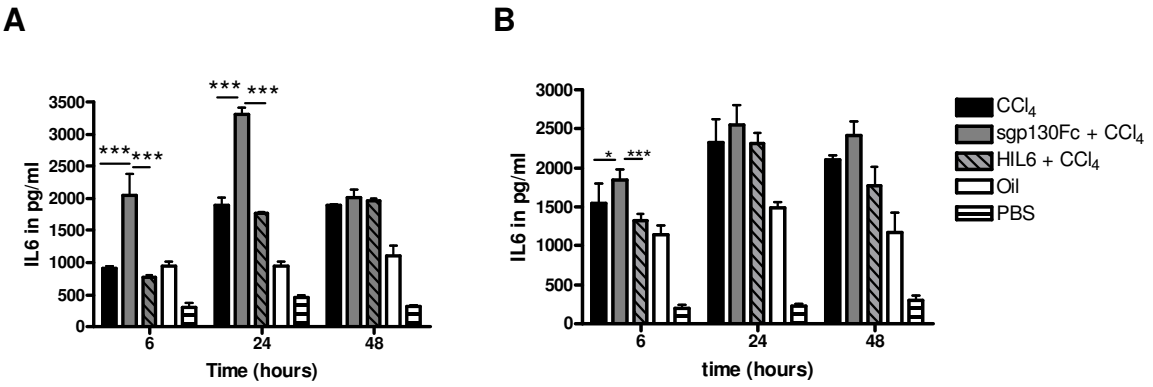

Figure 4.6.1: IL-6 expression after CCl_4 induced damage. (A) IL-6 was measured in serum at the indicated time points. IL-6 levels increased after CCl_4 treatment. The rise is significantly higher in sgp130Fc pretreated mice 6 hours and 24 hours after treatment. (B) IL-6 was measured in liver lysates in pg/ml per µg lysate at the indicated time points. IL-6 lysate levels increased after CCl_4 treatment. The increase is significantly higher in sgp130Fc pretreated mice 6 hours after CCl_4 treatment. Unpaired student`s t test: * P< 0.05; ***P< 0.0001.

4.7 STAT 3 phosphorylation

IL-6 stimulation via the membrane-bound or via the soluble IL-6 Receptor leads to activation and dimerization of two gp130 molecules and therewith to activation of the STAT3 signaling cascade.

After 0, 2, 4 and 6 hours liver extracts of CCl_4 only and sgp130Fc pretreated mice were prepared and immuno blotting analysis for P-STAT3, STAT3, and β-actin was carried out. 0 hours after the intoxication no STAT3 phosphorylation was visible. 2 hours after CCl_4 induced liver damage a beginning STAT3 phosphorylation could be detected, which is peaking in intensity 4 hours after the intoxication and declining 6 hours after the liver damage. The STAT3 phosphorylation in sgp130Fc pretreated mice is diminished compared to CCl_4 only treated mice (Fig. 4.7.1).

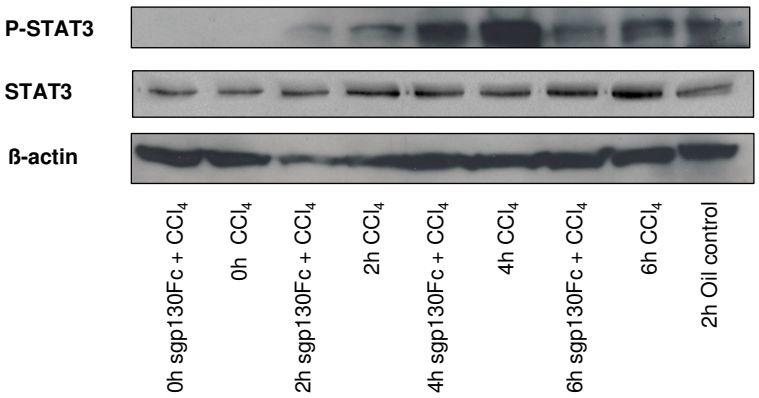

Figure 4.7.1: Expression of P-STAT3. C57Bl/6N mice were treated with CCl_4 after previous injection of sgp130Fc or mock treatment. Lysates were prepared from livers 0, 2, 4 and 6 hours after CCl_4 and immuno blotting analysis for P-STAT3, STAT3 and ß-actin was carried out.

4.8 Acute phase response after CCl_4 treatment

IL-6 promotes inflammatory events through the expansion and activation of T-cells, differentiation of B-cells and the induction of acute-phase substances by hepatocytes. Furthermore IL-6 is produced in large amounts by endothelial cells in response to proinflammatory signals including TNF-α and hypoxia.

Due to the proinflammatory properties of IL-6 and the detection of large amounts of IL-6 in the sera and liver lysates after CCl_4 induced damage, the acute phase response in this liver damage model was analyzed.

Serum amyloid A (SAA) proteins are a family of apolipoproteins associated with high-density lipoprotein (HDL) in plasma. Different isoforms of SAA (mainly SAA1, SAA2 and SAA3) are expressed in response to inflammatory stimuli. These proteins are produced predominantly by hepatocytes and are induced by the proinflammatory cytokines IL-1, IL-6, and TNF-α e.g. following exposure to lipopolysaccharide (LPS).

An additional acute phase response protein is haptoglobin, which is predominantly expressed by hepatocytes and is, like the SAAs, IL-6 dependent.

After RNA extraction and reverse transcription, TaqMan-based “gene expression assays” for SAA1, SAA3, Haptoglobin and β2-microglobulin were performed on an ABI-Prism/7000 Sequence Detection System. Primers for SAA1 are localized around exon 3-4 boundary, primers for SAA3 are localized around exon 2-3 boundary, primers for haptoglobin are localized around exon 4-5 boundary, and primers for ß2-microglobulin are localized around exon 1-2 boundary. All data were analyzed in

duplicates and mRNA expression levels were normalized to ß2-microglobulin as expression control. The expression level of only CCl_4 treated mice was set to 1. All other values were given as fold control of expression.

Surprisingly, 6 hours after the CCl_4 induced liver damage, mRNA levels of SAA1, SAA3 and haptoglobin were increased in sgp130Fc pretreated mice in comparison to CCl_4 only treated mice. SAA1 and SAA3 levels were 6 fold increased when compared to CCl_4 only treated mice, haptoglobin was 2 fold increased in sgp130 pretreated mice (Fig. 4.8.1).

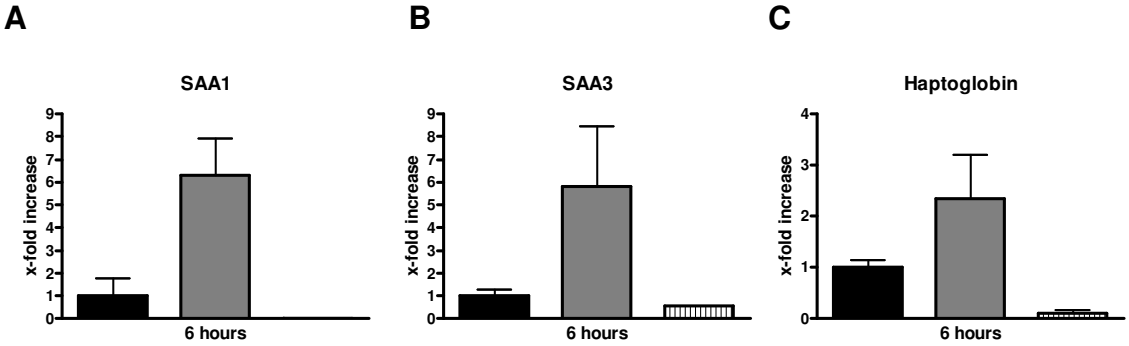

Figure 4.8.1: RealTime PCR analysis of acute phase response. mRNA of the acute phase response genes SAA1 (A), SAA3 (B) and Haptoglobin (C) were measured in liver tissue 6 hours after treatment with CCl_4 after previous injection with PBS (black bars), sgp130Fc (grey bars) and PBS control animals (striped bars). mRNA expression levels were normalized to ß2-microglobulin as expression control. Expression level of only CCl_4 treated C57Bl/6 mice was set to 1. All other values are given as fold control of expression.

In an additional experimental data set 10-12 weeks old male C57/Bl6N mice were injected with 3 ml CCl_4 per kg body weight, pretreated with 250 µg sgp130Fc i.p. (18 hours before intoxication), injected with 250 µg sgp130Fc alone i.p. (18 hours before intoxication) or injected with 1 µg IL-6 i.p. (2 hours before intoxication). 6 hours after CCl_4 treatment were the mice sacrificed.

After RNA extraction and reverse transcription, TaqMan-based “gene expression assays” for SAA1 and β2-microglobulin were performed on an ABI-Prism/7000 Sequence Detection System. All data were analyzed in duplicates and mRNA expression levels were normalized to ß2-microglobulin as expression control. The expression level of only sgp130Fc treated C57Bl/6 mice was set to 1.

6 hours after CCl_4 injection, SAA1 mRNA levels of sgp130Fc + CCl_4 treated mice were increased 10 fold, mRNA levels of CCl_4 only treated mice 1.5 fold and mRNA levels of IL-6 treated mice were increased 3 fold compared to sgp130Fc only treated animals (Fig. 4.8.2).

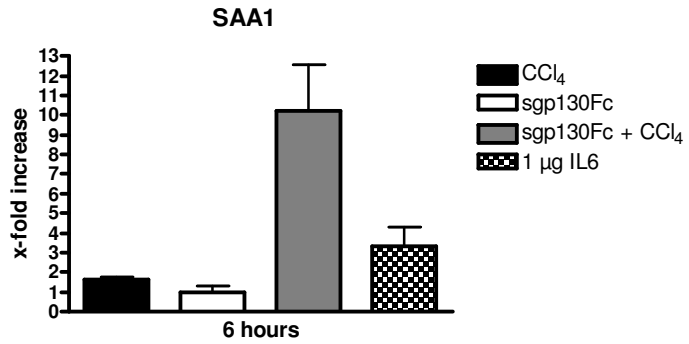

Figure 4.8.2: RealTime PCR analysis of SAA1. SAA1 was measured in liver tissue 6 hours after CCl_4, with pretreatment with sgp130Fc, with sgp130Fc alone, or with 1 µg IL-6 (all treatments i.p.). mRNA expression levels were normalized to ß2-microglobulin as expression control. The expression level of only sgp130Fc treated C57Bl/6 mice was set to 1. All other values are given as fold control of expression.

To determine the onset of acute phase gene expression, different time points were analyzed.

After RNA extraction and reverse transcription, TaqMan-based "gene expression assays" for SAA1, SAA3 and β2-microglobulin were performed on an ABI-Prism/7000 Sequence Detection System. All data were analyzed in duplicates and mRNA expression levels were normalized to ß2-microglobulin as expression control. The expression level of solvent control treated C57Bl/6 mice was set to 1.

4 hours after CCl_4 induced liver damage SAA1 mRNA levels were elvated in CCl_4 only and sgp130Fc pretreated mice to around 10 fold compared to mock control animals. 6 hours after the intoxication SAA1 mRNA levels peaked in sgp130Fc pretreated mice to a 40 fold increase compared to mock treated mice, whereas SAA1 mRNA levels of CCl_4 only treated mice remained at levels about 10 fold increase (Fig. 4.8.3A).

SAA3 mRNA levels were increased 4 hours after CCl_4 induced liver damage. CCl_4 only treated mice developed levels of around 8 fold increase, while sgp130Fc pretreated mice displayed levels of about 20 fold increase compared to mock treated mice. 6 hours after the intoxication SAA3 mRNA levels were declining (Fig. 4.8.3B).

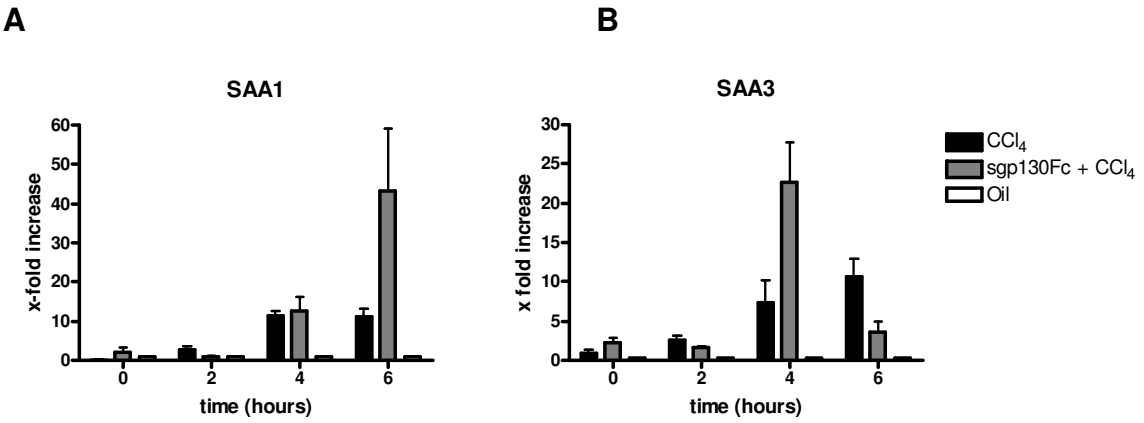

Figure 4.8.3: RealTime PCR analysis of acute phase response genes. The acute phase response genes SAA1 (A) and SAA3 (B) were measured at the indicated time points. mRNA expression levels were normalized to ß2-microglobulin as expression control. The expression level of mock treated C57Bl/6 mice was set to 1. All other values are given as fold control of expression.

4.9 Impact of IL-6 Transsignaling on glycogen content within the liver

Glycogen was stained within liver sections using Periodic Acidic Schiff (PAS) staining. After 24h, livers were almost empty of glycogen, whereas livers of mock treated mice contained usual amounts of glycogen. 48h after CCl_4 treatment, glycogen was reestablished in CCl_4 only treated and Hyper-IL-6 pretreated animals, whereas livers of sgp130Fc pretreated mice still lacked glycogen (Fig. 4.9.1). These findings indicate that IL-6 Transsignaling has an influence on the glycogen metabolism or the kinetic of glycogen synthesis after CCl_4 induced liver damage.

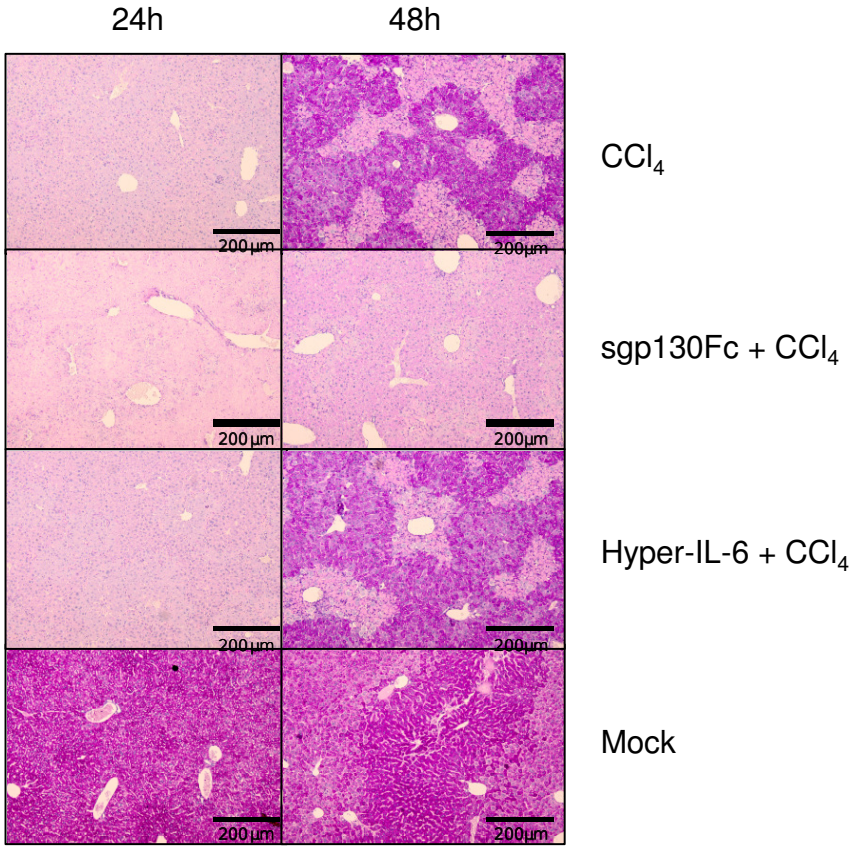

Figure 4.9.1: Glycogen staining of liver sections after CCl_4 injection. PAS stainings of liver sections showed a regular glycogen restoration 48 hours after CCl_4 injection in CCl_4 treated and Hyper-IL-6 pretreated mice, when compared to sgp130Fc pretreated animals, whereas livers of sgp130Fc pretreated mice still lacked glycogen.

After 6 and 48 hours liver extracts of CCl_4 only, Hyper-IL-6 pretreated, and sgp130Fc pretreated mice were prepared and immuno blotting analysis for P-GSK-3ß and β-actin was carried out.

6 hours after CCl_4 induced liver damage, an increase of P-GSK-3ß was detectable, which declined 48 hours after CCl_4 injection. Hyper-IL-6 treated animals showed the same tendencies, whereas sgp130Fc pretreated mice displayed a sustained GSK-3ß phosphorylation even 48 hours after the damage (Fig. 4.9.3).

There is evidence that 48 hours after the CCl_4 intoxication, the glycogen synthase is still active in sgp130Fc pretreated mice, whereas in CCl_4 only or Hyper-IL-6 pretreated mice the glycogen synthase is inactive (Fig. 4.9.2).

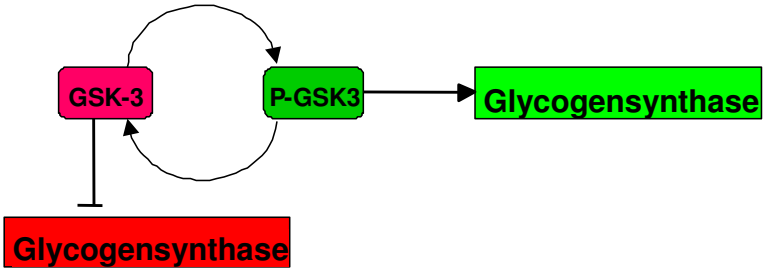

Figure 4.9.2: Schematic illustration of glycogensynthase. The glycogensynthase is activated (green) when GSK-3 is inactivated by phosphorylation. When GSK-3 is dephosphorylated, the Glycogensynthase is inhibited (red). GSK-3: Glycogen-synthase-kinase-3, P-GSK-3: Phosphorylated Glycogen-synthase-kinase-3

After RNA extraction and reverse transcription, TaqMan-based "gene expression assays" for GSK-3ß and β2-microglobulin were performed on an ABI-Prism/7000 Sequence Detection System. Primers for GSK-3ß are localized around exon 8-9 boundary and primers for ß2-microglobulin are localized around exon 1-2 boundary. All data were analyzed in duplicates and mRNA expression levels were normalized to ß2-microglobulin as expression control.

6, 24 and 48 hours after CCl_4 induced liver damage, mRNA expression levels of CCl_4 only and sgp130Fc pretreated mice achieved comparable amounts of GSK-3ß (Fig. 4.9.4).

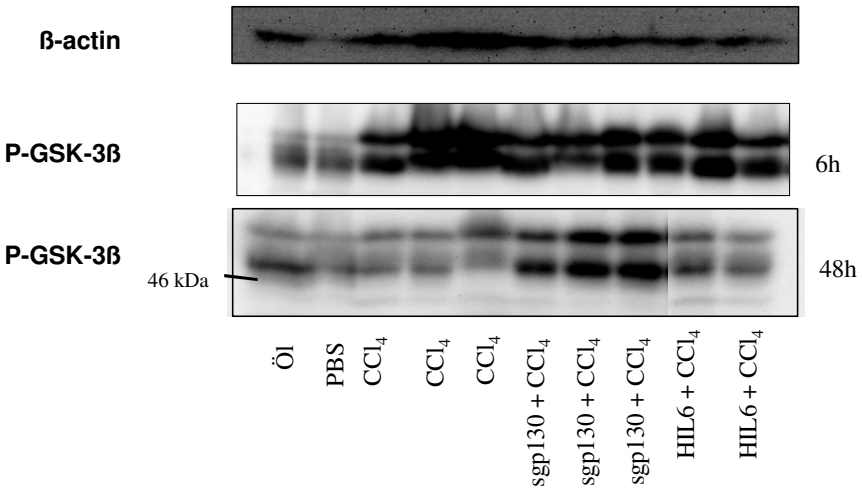

Figure 4.9.3: Phosphorylation state of GSK-3ß. C57Bl/6N mice were treated with CCl_4 after previous injection of sgp130Fc or mock treatment. Lysates were prepared from livers 6 and 48 hours after liver damage and immuno blotting analysis for P-GSK-3ß and ß-actin was carried out. 6 hours after CCl_4 intoxication, a pronounced GSK-3ß-phosphorylation was visible. 48 hours after the liver damage, GSK-3ß phosphorylation is still detectable in sgp130Fc pretreated mice, but not in CCl_4 only and Hyper-IL-6 pretreated animals.

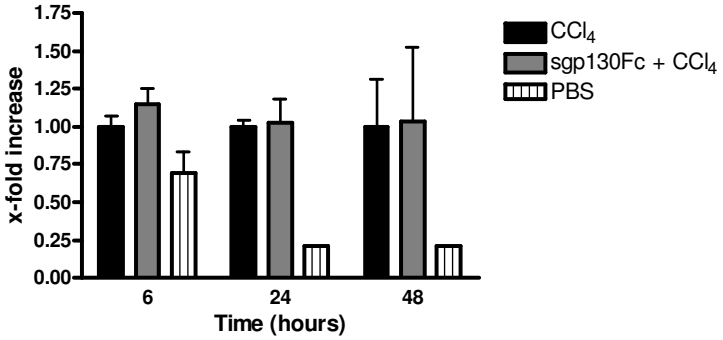

Figure 4.9.4: RealTime PCR analysis of GSK-3ß. Glycogen synthase kinase 3 (GSK-3ß) was measured in liver tissue at the indicated time points. mRNA expression levels were normalized to ß2-microglobulin as expression control. The expression level of solvent treated C57Bl/6 mice was set to 1. All other values are given as fold control of expression in solvent control animals. GSK-3ß gene expression of CCl_4 only and sgp130Fc pretreated mice reached comparable amounts.

4.10 Quantification of liver regeneration via BrdU-incorporation

Liver regeneration was quantified via BrdU stainings. Two hours prior to sacrificing, mice were injected with BrdU. Positive cells were visualized immunhistochemically and representative pictures and quantification were carried out.

48 hours after CCl_4 induced liver damage, a diminished number of BrdU positive hepatocytes were detected in liver sections of sgp130Fc pretreated mice. In comparison, in liver sections of CCl_4 only and Hyper-IL-6 pretreated animals were detected higher numbers of BrdU positive hepatocytes (Fig. 4.10.1A).

Quantification of given pictures offered significantly reduced percentage of BrdU positive cells in sgp130Fc pretreated mice of around 15 %, in comparison to about 20 % positive cells in CCl_4 only ($P < 0.0001$) and Hyper-IL-6 pretreated mice ($P < 0.005$) (Fig. 4.10.1B).

We concluded that regeneration depends in parts on signaling via IL-6/sIL-6R, since a blockade of this pathway led to a reduction of proliferating cells.

A

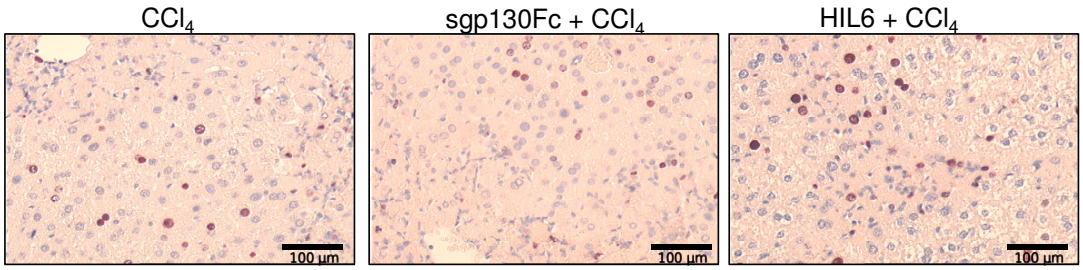

B

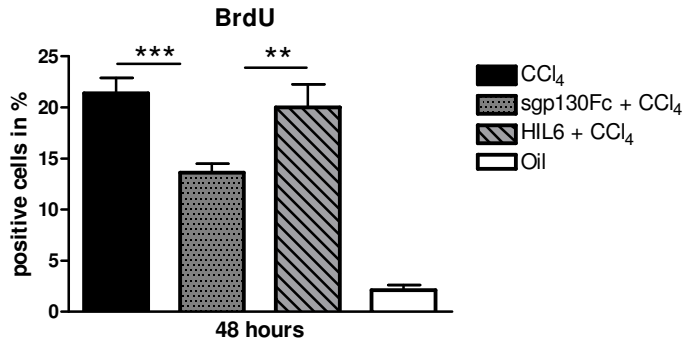

Figure 4.10.1: Bromodeoxyuridine (BrdU) staining and quantification. (A) BrdU staining of liver sections 48 hours after treatment with CCl_4 in 20 fold magnification. Two hours prior to sacrificing, mice were injected with 10 µg/µl BrdU i.p. Positive cells were visualized immunhistochemically. (B) Quantification of liver sections of sgp130Fc pretreated mice showed significantly less BrdU positive cells compared to CCl_4 only and Hyper-IL-6 pretreated mice. Unpaired student`s t test: ** $P< 0.005$; ***$P< 0.0001$.

4.11 Impact of neutrophils on the severity of CCl_4-induced liver damage

It is known that in case of tissue damage or inflammation, neutrophils are infiltrating into the tissue. To determine the role of neutrophils after CCl_4 treatment, we depleted neutrophils in CCl_4 and sgp130Fc pretreated mice and investigated the impact of this neutrophil depletion on the severity of liver damage.

Therefore C57/Bl6N mice were injected with 100 µg of a purified rat anti-mouse Ly6G/Ly6C monoclonal antibody 18 hours before CCl_4 injection and sacrificed 24 hours later. Depletion was controlled by staining of neutrophils on paraffin tissue sections.

Measuring ALT levels revealed that depletion of neutrophils reduced the liver damage in both groups:

C57Bl/6 mice developed 24 hours after CCl_4 treatment ALT serum levels of around 7,500 U/L. When these animals were pretreated with the neutrophil depleting antibody, ALT levels were significantly reduced to about 2,500 U/L ($P< 0.0001$).

C57/Bl6 mice, in which IL-6 Transsignaling is blocked, developed 24 hours after CCl_4 treatment ALT serum levels of around 15,000 U/L, which is significantly higher than in mice with intact IL-6 Transsignaling ($P< 0.0001$). When these animals were pretreated with the neutrophil depleting antibody, ALT levels were significantly reduced to about 10,000 U/L ($P< 0.0001$) (Fig. 4.11.1A). Neutropenia led in both groups to an ALT reduction of around 5,000 U/L.

The presence of sgp130Fc was demonstrated by sgp130 Elisa (Fig. 4.11.1B).

These findings demonstrate that neutrophil depletion reduces the amount of liver damage, even when IL-6 Transsignaling is blocked. Neutrophils are therefore in this model no explanation for the observed higher damage in the sgp130Fc treatment group, which is also shown in blood flow cytometry analysis (Fig. 4.11.2).

A

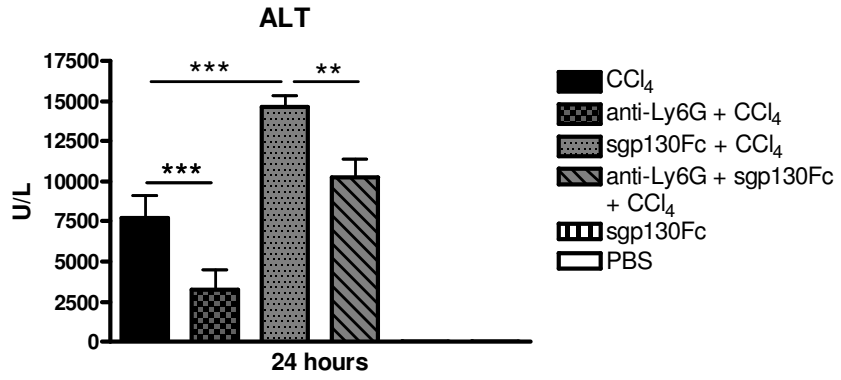

B

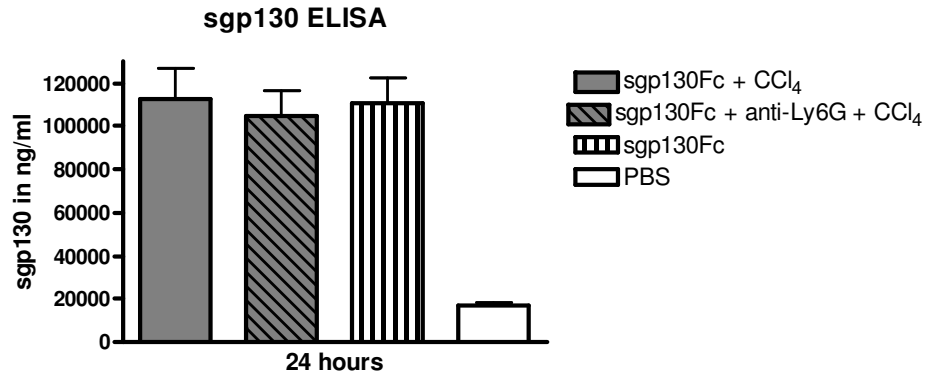

Figure 4.11.1: Measurement of ALT serum levels in neutrophil depleted mice. (A) C57Bl/6N mice were treated with CCl_4 after previous injection of sgp130Fc or mock treatment. Both groups were either pretreated with the neutrophil depleting antibody anti-mouse Ly6G/Ly6C 18 hours before CCl_4 or received no depleting antibody. Mice were sacrificed 24 hours after the CCl_4 treatment and ALT serum levels were measured. (B) Serum sgp130Fc levels were measured via ELISA 24 hours after CCl_4 intoxication. Unpaired student`s t test: ** P< 0.005; ***P< 0.0001.

C57/Bl6N mice were treated with CCl_4 after previous injection of sgp130Fc or mock treatment. After 0, 2 and 4 hours blood samples were taken and blood flow cytometry analysis was performed using a FITC Ly6G and a PE CD11b antibody. Quantitative analysis revealed increasing numbers of neutrophils 4 hours after CCl_4 in both groups (Fig. 4.11.2A).

In a second experiment sgp130 transgenic and C57/Bl6 mice were treated with 3 ml/kg body weight CCl_4. After 6, 24 and 48 hours blood samples were obtained and flow cytometry analysis was performed. Quantitative analysis showed a peak of neutrophils 24 hours after the damage in both groups with no differences between the groups (Fig. 4.11.2B).

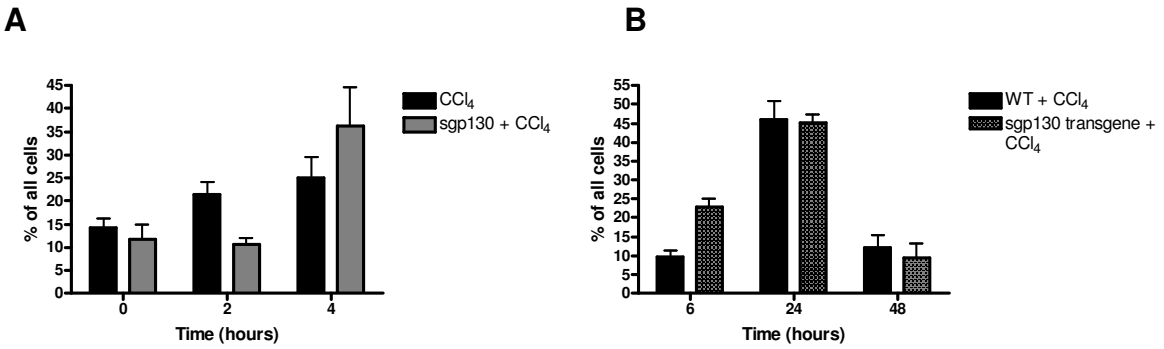

Figure 4.11.2: Quantitative blood flow cytometry analysis of neutrophils. (A) C57Bl/6N mice were treated with CCl_4 after previous injection of sgp130Fc or mock treatment. Quantitative blood flow cytometry analysis of neutrophils in percent at the indicated timepoints after CCl_4 induced liver damage was carried out. (B) C57Bl/6N and sgp130 transgenic mice were treated with CCl_4. Quantitative blood flow cytometry analysis of neutrophils in percent at the indicated timepoints after CCl_4 induced liver damage was performed.

5 Discussion

5.1 CCl_4 induced liver damage

In the present work I could show that liver damage and regeneration in response to acute CCl_4 liver damage was strongly influenced by IL-6 Transsignaling. sgp130 is a natural, specific inhibitor of IL-6 Transsignaling (63) and we have developed a sgp130Fc fusion protein to block IL-6 Transsignaling without influencing classical IL-6 signaling (100).

Acute liver damage was induced with a single i.p. injection of 3 ml/kg body weight CCl_4 in various mouse groups. Either IL-6 Transsignaling was blocked with a single i.p. injection of sgp130Fc, or IL-6 Transsignaling was accelerated with a single i.p. injection of Hyper-IL-6. For the control group, mice which received no pretreatment were used. Thus, the control group mice developed a normal induction of IL-6 Transsignaling response to CCl_4 induced liver damage.

The extent of liver damage between the various groups was analyzed at different timepoints, starting with early timepoints at 2 to 6 hours and proceeding with 24 and 48 hours. A number of different parametes indicative of liver damage were quantified.

It can be concluded that IL-6 Transsignaling has an positive effect on the extent of induced liver damage, the amount of oxidative stress, IL-6 levels, the induction of acute phase response and finally on liver glycogen content and regeneration.

5.2 Impact of blocked IL-6 Transsignaling on lipid peroxidation

CCl_4 is metabolized by the P450 mixed function oxygenase system of the endoplasmatic reticulum to the free radical, $CCl_3^{\bullet}$ (83, 101). The major cytochrome isoenzyme to execute biotransformation of CCl_4 is Cyp2E1, but Cyp2B1 and Cyp2B2 are also capable of attacking CCl_4 (102, 103). The resulting $CCl_3^{\bullet}$ radical is able to bind covalently to the active site or to the heme group of Cyp2E1, thereby causing suicide inactivation of Cyp2E1 (104-107). The $CCl_3^{\bullet}$ radical reacts with various biologically important substances such as aminoacids, nucleotides, fatty acids, proteins, nucleic acids, and lipids. In the presence of oxygen, the $CCl_3^{\bullet}$ radical is converted to the trichloromethyl peroxy radical, $CCl_3O_2^{\bullet}$. This radical is more reactive than the $CCl_3^{\bullet}$ radical, and is abstracting a hydrogen from polyunsaturated fatty acids, thereby initiating the process of lipid peroxidation (108-112). The abstraction of a

hydrogen from fatty acids initiates a complex series of reactions that terminate in the complete disintegration of the polyunsaturated fatty acids by compromising membrane functions and by covalent binding of reactive intermediates.

Oxidative stress is commonly quantified via the amount of lipid peroxidation in liver tissue, using thiobarbituric acid reactive substances (TBARS) as a marker. Katz et al showed that IL-6 deficient mice exhibit higher lipid peroxidation after CCl_4 treatment than C57/Bl6 control mice (93), allocating IL-6 a crucial role in this process.

Donato et al. reported that an increase of IL-6 in endothelial cells led to enhanced activity of NADPH oxidase and therewith to increased amounts of reactive oxygen species. Due to the endothelial dysfunction, this results finally in atherosclerosis (113).

In the present work I could show significantly increased lipid peroxidation 4 and 6 hours after CCl_4 treatment when IL-6 Transsignaling was blocked with sgp130Fc, compared to control mice (Fig. 4.4.1). These differences in lipid peroxidation appeared to be independent of the metabolized amount of radicals, as protein expression levels of Cyp2E1 are comparable in sgp130Fc pretreated and control mice (Fig. 4.5.1). Nevertheless it is not possible at the moment to monitor the extent of detoxifying activities, which are occuring after CCl_4-induced acute liver damage.

Other parameters for oxidative stress or common cell damage are uric acid and potassium in blood serum. Apart from the fact that uric acid is the final oxidation product of purine metabolism and is excreted in urine, uric acid plays a protective role in defending organs and tissue from oxidative damage by attenuating oxidation of plasma lipids, lipoproteins, and unsaturated fatty acids. A critical role for uric acid in antioxident defense and lipid peroxidation has been identified in human blood plasma (96-99).

Potassium plays a crucial role in maintenance of membrane potential. The intracellular concentration is up to 40 times higher than the extracellular concentration. Therefore serum potassium could be used as a marker for general cell damage.

A specific upregulation in uric acid and potassium, sera levels was found in mice with blocked IL-6 Transsignaling 24 and 48 hours after the CCl_4-induced liver damage (Fig. 4.3.5). This indicates that there is increased oxidative stress present in the absence of intact Transsignaling. These results imply that IL-6 Transsignaling protects cells from oxidative stress.

Furthermore, varios parameters of liver damage were quantified. Serum ALT and AST levels were found to be significantly higher when IL-6 Transsignaling was blocked 24 and 48 hours after CCl_4 induced liver damage (Fig. 4.3.1). This enhanced liver damage was also visible morphologically in Hematoxylin/Eosin stainings showing massive necrotic areas. DAPI stainings show more intact nuclei in livers of mice with intact IL-6 Transsignaling (Fig. 4.3.3 and Fig. 4.3.4).
These data indicate that the extent of liver damage is significantly controlled by IL-6 Transsignaling, which could be the consequence of reduced reactive oxygen species and free radicals.

5.3 Impact of IL-6 Transsignaling on IL-6 induction

TNFα is a proinflammatory cytokine with pleiotrophic effects and multiple roles in host defense. TNFα has a pivotal role in liver pathophysiology, because it can either induce hepatocyte cell death or hepatocyte proliferation and liver regeneration. TNFα is produced mainly by macrophages but also by a broad variety of other cell types including lymphoid cells, mast cells, endothelial cells, fibroblasts and neuronal cells (114). TNFα is primarily produced as a type II transmembrane protein but may be released in soluble trimeric form via proteolytic cleavage by the metalloprotease TNF-converting enzyme (TACE) (114). In response to LPS and other bacterial products, large amounts of TNFα are generated. TNFα exerts its biological functions via interactions with two different membrane receptors, TNF-R1 and TNF-R2. TNFα can induce apoptosis via the intracellular death domain of TNF-R1, but it can also initiate signaling pathways leading to the activation of the transcription factor nuclear factor-κB (NF-κB), and therefore via MAPK cascades and JNK to a prevention of apoptosis and to proliferation.
TNFα signaling is required for normal liver regeneration. Mice lacking the TNF-R1 subunit display abnormal and delayed regeneration after partial hepatectomy (115). Lack of TNF signaling can be overcome by a single injection of recombinant IL-6, suggesting that TNF functions mostly to release IL-6.
In the initiation phase of liver regeneration, TNFα and IL-6 are responsible for priming of quiescent hepatocytes. This results in an induction of hepatocytes to become sensitive to growth factors and competent for replication. During proliferation phase,

hepatocytes enter into the cell cycle's G1-phase and are stimulated by complete mitogens including hepatocyte growth factor (HGF), transforming growth factor-α (TGFα) and epidermal growth factor (EGF).

The fact that IL-6 is of importance in the response to liver damage has already been described (70). IL-6 levels increase after liver injury induced by partial hepatectomy or chemical induced liver damage, and liver regeneration is markedly reduced in IL-6 deficient mice. After partial hepatectomy, IL-6 deficient mice exhibit reduced regeneration rates and an impaired STAT3 activation (70).

The important role of IL-6 has also been examined in the CCl_4 liver damage model. Many of the molecular events are not mediated by hepatocytes, but by two types of nonparenchymal liver cells, e.g. Kupffer cells and stellate cells. Kupffer cells, the resident macrophages of liver, are activated by CCl_4 and release thereon TNFα, nitric oxide, TGFβ, and IL-1, IL-6 and IL-10 (82). Stellate cells, while quiescent, are fat-storing cells, but after activation of CCl_4 display a typical acute phase response (116), release TGFα, nitric oxide and begin to overproduce type-1 collagen, which could result in liver fibrosis.

Early after CCl_4 treatment, IL-6 expression increases. The source of IL-6 are mainly mesenchymal cells of the peritoneum induced by inflammatory cytokines like IL-1α, IL-1β, and TNFα (117). The increased IL-6 response is blunted in TNFαRI knockout mice (118). The consequences of this early IL-6 production are not fully understood. In the present work I could show that a modulation of the IL-6 Transsignaling pathway with sgp130Fc has an increasing effect on the amount of IL-6 production at early time points after the injury.

In several experiments I demonstrated that IL-6 serum levels increased 6 to 24 hours after CCl_4 induced liver damage (Fig. 4.5.1). This increase was significantly higher in sgp130Fc pretreated animals. This data show that IL-6 Transsignaling is involved in the regulation of IL-6 production at early time points after CCl_4 induced liver damage.

Focusing on the degree of liver damage induced by CCl_4, it already has been shown that IL-6 and IL-6 signal pathways are involved in this process. Studies by Katz et. al. report that mortality rates are dose dependent and higher in IL-6 deficient mice (93). The role of IL-6 in modulating toxin-induced liver injury is still unclear. Following acute carbon tetrachloride treatment, IL-$6^{-/-}$ mice develop increased hepatocellular injury and defective regeneration as well as reduced hepatocyte DNA synthetic and mitotic responses (92). In contrast, chronical carbon tetrachloride treated IL-$6^{-/-}$ mice showed

reduced liver damage scores, lower aminotransferase levels and diminished apoptosis (94).

IL-6 promotes inflammatory events through the induction of acute-phase proteins. Because of the proinflammatory properties of IL-6 and the production of large amounts of IL-6 in the sera and liver lysates after CCl_4 induced damage, the acute phase response in this liver damage mouse model was analyzed.

Different isoforms of SAA (mainly SAA1, SAA2 and SAA3), as well as haptoglobin and fibrinogen are expressed in response to inflammatory stimuli. These proteins are produced predominantly by hepatocytes and are induced by the proinflammatory cytokines IL-1, IL-6 and TNF-α under acute inflammatory conditions.

6 hours after CCl_4 induced liver damage, mRNA levels of SAA1, SAA3 and haptoglobin increased in sgp130Fc pretreated mice in comparison to CCl_4 only treated mice. SAA1 and SAA3 increased 6 fold when compared with CCl_4 only treated mice, haptoglobin increased 2 fold in sgp130 pretreated mice (Fig. 4.8.1).

Blockade of IL-6 Transsignaling by sgp130Fc seemed to have an enhancing effect on the amount of induced acute phase response to CCl_4. The IL-6 level in the sera of these mice, as well as in liver lysate, were elevated when IL-6 Transsignaling was blocked. This enhanced IL-6 response could be the source of the elevated acute phase response, although the levels of phosphorylated STAT3 was diminished in liver lysates of sgp130Fc treated mice (Fig. 4.7.1).

5.4 The role of neutrophils

Investigating possible explanations for these observations I focused on the impact of infiltrating neutrophils within the liver. It has been described that neutrophils have damaging effects in CCl_4 induced liver damage. In previous studies Ohta et al (119) claim that CCl_4 induced liver damage can be reduced by neutrophil depletion. In further studies it has been shown that the infiltration of neutrophils is controlled by IL-6 Transsignaling. In an air-pouch model of acute inflammation, Rabe et al demonstrated that fewer neutrophils infiltrate to the site of inflammation when the IL-6 Transsignal pathway is blocked (64). Nechemia-ArbelyIn et al displayed in a $HgCl_2$-induced acute kidney injury (AKI) model a critical role for IL-6 in recruiting neutrophils. IL-$6^{-/-}$ mice were resistant to $HgCl_2$-induced AKI compared to wild-type mice. The accumulation of peritubular neutrophils was lower in IL-$6^{-/-}$ mice than in

wild-type mice, and neutrophil depletion before $HgCl_2$ administration in wild-type mice significantly reduced AKI. Stimulation of IL-6 Transsignaling with Hyper-IL-6 activated STAT3 in renal tubular epithelium and prevented AKI, allocating IL-6 simultaneously an inflammatory response function and, through a mechanism of Transsignaling, a protective function for the kidney from further injury (120).

In the model of CCl_4 induced liver damage I could show that when neutrophils were depleted before CCl_4 treatment, liver damage was reduced, becoming evident in decreased ALT serum level (Fig. 4.11.1 A). However, in the sgp130Fc pretreated mice, ALT levels were still higher than in CCl_4 only treated animals. The amount of reduction in ALT levels due to the depletion of neutrophils was almost the same in mice with intact and blocked IL-6 Transsignaling (ca. 5000 U/L, Fig. 4.11.1 A).

Moreover, flow cytometric analysis of blood samples were performed using a FITC Ly6G and a PE CD11b antibody. Quantitative analysis revealed increasing numbers of neutrophils in the blood 4 hours after CCl_4 induced liver damage, peaking 24 hours after setting the damage. When IL-6 Transsignaling was blocked by sgp130Fc no major differences were observed in comparison to mice with intact IL-6 Transsignaling (Fig. 4.8.2 and 4.8.3).

I therefore hypothesize that the effect of IL-6 Transsignaling on the extent of CCl_4 induced liver damage is not dependent on neutrophils.

5.5 Consequences to glycogen content and liver regeneration

Closely related to induced liver damage is the subsequent induction of liver regeneration. Liver has an enormous potential to regenerate after injury, and the regeneration is clearly dependent on IL-6 signaling pathways.

It has already been established that CCl_4 affects hepatocellular levels of Ca^{2+} by compromising the ability of hepatocytes to maintain Ca^{2+} levels (121). Hepatocellular Ca^{2+} is sequestered into the three main compartments: cytosol (low Ca^{2+}), endoplasmatic reticulum and mitochondria (both higher Ca^{2+}). The loss of Ca^{2+} levels in ER and mitochondria therefore lead to a breakdown of the ATPase ion pumping systems (122, 123).

CCl_4 exposure activates phosphorylases, among others the glycogenphosphorylase, and causes glycogen depletion in the liver (124-126). Constant ATP levels could therefore prevent mortality caused by high dose of CCl_4.

I could show via PAS staining that the glycogen content within the liver varies between the different treated groups: at early time points, 24 hours after CCl_4 injection, all glycogen was consumed in the liver. Within two days glycogen storages filled up in C57Bl/6 mice. However, when IL-6 Transsignaling was blocked this process was significantly impaired or slowed down (Fig. 4.9.1). The reasons for this phenomenon are not yet understood. Glycogen synthase kinase 3 (GSK-3) is a kinase, that mediates the addition of phosphate molecules on certain serine and threonine amino acids of glycogen synthase, which results in an inhibition of glycogen synthase.

6 hours after CCl_4 induced liver damage a strong phosphorylation of GSK-3ß was detectable in all CCl_4 treated groups, which means an induction of glycogen synthase via inhibition of GSK-3ß. However 48 hours after the intoxication, GSK-3ß phosphorylation was still visible in mice with blocked IL-6 Transsignaling via sgp130Fc, whereas in CCl_4 only and Hyper-IL-6 pretreated mice, very minor GSK-3ß phosphorylation was detectable (Fig. 4.9.2).

Usually gp130 signaling leads to recruitment of phospoinositid-3-kinase (PI3K), which activates via phosphoinositoltriphosphat (PIP3) the phosphokinase B (PKB). PKB then phosphorylates the constitutively active glycogen-synthase-kinase-3 (GSK-3) and therewith inactivates it. In consequence, glycogen-synthase takes place (Fig. 5.1).

A blockade of IL-6 Transsignaling via sgp130Fc should lead to a reduction in gp130 signaling, and therefore to less glycogen synthase due to less P-GSK-3. In fact I observed lower glycogen content in PAS stained livers of sgp130Fc pretreated mice 48 hours after the liver damage in comparison to CCl_4 only treated mice (Fig. 4.9.1). On the other hand, immuno blot analysis revealed a higher GSK-3 phosphorylation in livers of sgp130Fc pretreated mice 48 hours after the liver damage, when compared to CCl_4 only treated animals (Fig. 4.9.2).

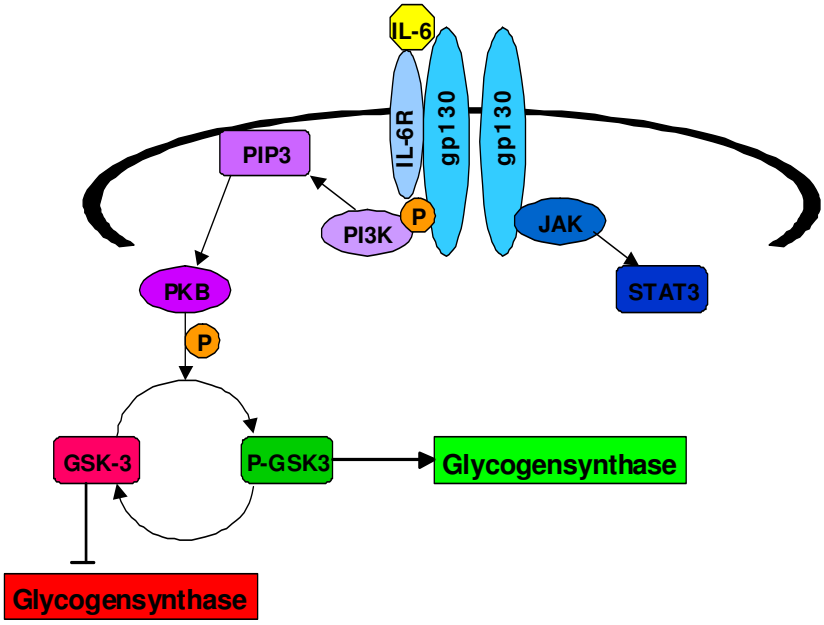

Figure 5.1: Simplified illustration of gp130 signaling. PI3K is recruited and activating PKB. PKB phosphorylates and therewith inactivates GSK-3. As a consequence of this inactivation, glycogensynthase takes place (green). When GSK-3 is dephosphorylated, the Glycogensynthase is inhibited (red). PI3K = phospoinositid-3-kinase, PIP3 = phosphoinositoltriphosphat, PKB = phosphokinase B and GSK-3 = glycogen-synthase-kinase-3.

Sgp130Fc pretreated mice seem to require the glycogen synthase for a longer period of time to restore their glycogen stocks after CCl_4 induced liver damage. This can be the consequence of more extensive damage, becoming evident in a reduced number of working ATPase, or that the IL-6 Transsignaling pathway is essential for glycogen metabolism.

Interestingly, Drucker et al. obtained in a D-Gal induced damage model different results. In sgp130 transgenic mice glycogen consumption was inhibited after injection of D-Gal, when compared to WT mice, indicating that the sIL-6R is needed for the stimulation of glycogen consumption (127).

I could further show that in C57Bl/6 mice, proliferation, quantified by BrdU incorporation, increased 48 hours after CCl_4 injection compared to sgp130Fc pretreated mice. In mice with blocked IL-6 Transsignaling was less energy available, in the form of less glycogen within the liver. This finding could be one explanation for an impaired liver regeneration in sgp130Fc pretreated animals.

5.6 Clinical perspectives of sgp130Fc

It is already known that IL-6 is involved in a number of chronic inflammation diseases. In 1997 a group in Japan began with the development of the humanized IL-6R antibody *Tocilizumab*, which is meanwhile applied in clinical trials to treat a number of chronic inflammatory diseases like rheumatoid arthritis (RA), juvenile idiopathic arthritis (JIA), multicentric Castleman disease (MCD), and lupus nephritis. Since 2009 is *Tocilizumab* approved in Europe and since 2010 in USA for the treatment against RA.

Treatment with *Tocilizumab* alleviated chronic inflammatory symptoms, e.g. improvements in erythrocyte sedimentation rate (ESR), C-reactive protein (CRP), fibrinogen and serum amyloid A (SAA) levels (128-132).

Recently it has been demonstated that patients treated with *Tocilizumab* develop significantly increased serum levels of total cholestorol (TC), high-density lipoprotein (HDL), low-density lipoprotein (LDL), apolipoprotein A-1 (Apo A-1) and apolipoprotein A-2 (Apo A-2), as well as gained body weight after 3 months of treatment. Similarly, the serum levels of triglyceride (TG) and apolipoprotein B (Apo B) tended to increase, but were not significant (129, 133).

In this regard, it should be noted that the mean serum LDL levels rise beyond 140 mg/dl in *Tocilizumab*-treated patients, which can be an independent risk factor for cardiovascular events. These findings could be important, even though the serum levels of both HDL and LDL increased at the same time, and accordingly the atherogenic indices do not increase. Further analysis are therefore indispensable to determine the risk of elevated LDL levels during long-term use of *Tocilizumab*.

While *Tocilizumab* blocks classical IL-6 signaling and IL-6 Transsignaling, sgp130Fc just affects IL-6 Transsignaling without interfering with classical IL-6 signaling. This could be a critical advantage of sgp130Fc in the treatment of chronic inflammatory diseases. Humanized sgp130Fc is at the moment in preclinical trials. The occuring side effects, especially concerning cardiovascular and atherosclerotic aspects, still have to be analyzed in detail.

5.7 Outlook

Taken together, these data demonstrate the protective effect of IL-6 Transsignaling on liver damage and regeneration in an acute CCl_4-induced liver damage model. A

specific blockade of IL-6 Transsignaling led to increased IL-6 levels, enhanced liver damage and increased acute phase response. Reasons for these findings are still not fully understood, but they emphasize the importance of the endogenous IL-6 Transsignaling pathway in CCl_4 induced liver damage. Based on these results it should be taken into consideration that blocking IL-6 signaling pathways could be used as a treatment option in different inflammatory pathological states. In this work I showed that consequences of a blockade of IL-6 Transsignaling has very diverse effects on liver damage and regeneration in context of an acute CCl_4 induced liver damage. In further experiments these findings should be compared with blocking both IL-6 pathways (IL-6 classical and IL-6 Transsignaling) by treatment with a neutralizing IL-6 antibody. The direct comparison of either blocking IL-6 Transsignaling by sgp130Fc, or blocking classical and IL-6 Transsignaling by an IL-6-antibody would be of great interest and a promising aim for the future.

6 Summary

The liver has the unique capability to regenerate its mass after damage and injury. Nevertheless liver failure is still a serious medical problem and enhancing the regenerative potential of the liver could be an effective and promising therapy.
Interleukin-6 is known to play an important role in mediating pro-mitotic and pro-survival activities within the regenerative process.
It already has been shown that IL-6 Transsignaling plays a crucial role in liver regeneration using the example of the effect of Hyper-IL-6 in accelerating liver regeneration following partial hepatectomy.
Carbontetrachloride (CCl_4) can be used to mimic drug induced hepatoxicity. Through the metabolization by cytochrome P450 dependent monooxygenase, the reactive $CCl_3^{\bullet}$ and $CCL_3O_2^{\bullet}$ radicals are formed which can covalently bind to proteins, lipids and nucleic acids and this could lead to lipidperoxidation and liver damage.
The aim of the present study was to investigate the impact of IL-6 Transsignaling on liver damage and regeneration in this CCl_4 induced liver damage mouse model.
Therefore mice were treated with substances either blocking IL-6 Transsignaling (soluble gp130Fc) or accelerating IL-6 Transsignaling (Hyper-IL-6). Afterwards the mice were treated intraperitoneally with a single dose of CCl_4, leading to acute liver damage.
Mice in which IL-6 Transsignaling was blocked displayed higher liver damage, becoming evident in enhanced lipid peroxidation 4 to 6 hours after CCl_4 treatment. Subsequently ALT and AST serum levels were strongly increased from 24 to 48 hours after CCl_4 treatment, with significantly higher levels in sgp130Fc pretreated mice. Moreover, uric acid and potassium serum level were elevated in mice with blocked IL-6 Transsignaling 48 hours after CCl_4 injection.
IL-6 serum level were elevated at early time points in mice pretreated with sgp130Fc compared to CCl_4 only treated mice. As a consequence, acute phase genes like SAA1, SAA3 and haptoglobin were upregulated 6 hours after CCl_4, although STAT-3 phosphorylation was diminished. When IL-6 Transsignaling was blocked by sgp130Fc, mRNA levels of SAA1 and SAA3 increased 6 fold, mRNA levels of haptoglobin increased 2 fold compared to CCl_4 only treated animals.
In addition, glycogen storage was altered after blockage of IL-6 Transsignaling. 24 hours after the damage all glycogen within the liver was consumed. While glycogen

storages were filled up in livers of mice with normal or accelerated IL-6 Transsignaling, this process was significantly impaired when IL-6 Transsignaling was blocked. Animals pretreated with sgp130Fc showed lower BrdU incorporation, indicating a lower proliferation index.

Overall, these data indicate a critical role of IL-6 Transsignaling in a CCl_4 induced liver damage mouse model.

7 Zusammenfassung

Die Leber besitzt die einzigartige Fähigkeit sich nach Schädigung oder Verletzung zu regenerieren. Dennoch stellt Leberversagen immer noch ein ernsthaftes medizinisches Problem dar, und eine Verbesserung des regenerativen Potenzials der Leber könnte eine effektive und vielversprechende Therapiemethode sein.
Interleukin-6 ist für seine wichtige Rolle bei der Vermittlung von pro-mitotischen und überlebensfördernden Signalen innerhalb des regenerativen Prozesses bekannt.
Es wurde schon mehrfach gezeigt, dass IL-6 Transsignaling eine entscheidende Rolle während der Leberregeneration spielt, welches sich am Beispiel von Hyper-IL-6 verdeutlichen läßt. Hyper-IL-6 hat nach partieller Hepatektomie einen beschleunigenden Effekt auf die Leberregeneration.
Kohlenstofftetrachlorid (CCl_4) kann als Modell für medikamentös induzierten Leberschaden verwendet werden. Durch die Cytochrom P4502E1 abhängigen Monooxygenasen wird CCl_4 zu den Radikalen $CCl_3^{\bullet}$ and $CCL_3O_2^{\bullet}$ umgesetzt. Die Radikale binden kovalent an Proteine, Lipide und Nukleinsäuren, was letztendlich zu Lipidperoxidation und Leberschädigung führt.
Ziel der vorliegenden Arbeit war es, den Einfluss von IL-6 Transsignaling auf das Ausmaß von CCl_4 induzierten Leberschaden und die Regenerationsfähigkeit zu bestimmen.
Zu diesem Zweck wurden Mäuse mit unterschiedlichen Substanzen behandelt, die sich entweder blockierend (sgp130Fc) oder stimulierend (Hyper-IL-6) auf das IL-6 Transsignaling auswirken. Anschließend wurden die Mäuse einmalig intraperitoneal mit einer akuten Leberschaden auslösenden CCl_4 Dosis behandelt.
Mäuse, in denen IL-6 Transsignaling blockiert war, entwickelten einen höheren Leberschaden, der in erhöhter Lipidperoxidation 4 und 6 Stunden nach CCl_4 Behandlung sichtbar wurde. Zusätzlich waren die ALT und AST Serumlevel nach 24 und 48 Stunden stark erhöht, insbesondere in Mäusen, die zuvor mit sgp130Fc behandelt wurden. Außerdem waren, ebenfalls nach 48 Stunden, höhere Harnsäure- und Kaliumwerte im Serum von Mäusen mit blockierten IL-6 Transsignaling detektierbar.
Zu frühen Zeitpunkten waren die IL-6 Serumwerte erhöht, insbesondere in Mäusen, die mit sgp130Fc vorbehandelt worden sind. Als Konsequenz darauf wurden einige

Akut Phase Gene, wie SAA1, SAA3 und Haptoglobin, 6 Stunden nach CCl_4 Behandlung hochreguliert, obwohl die STAT3 Phosphorylierung vermindert war.
In Tieren mit blockiertem IL-6 Transsignaling waren die SAA1 und SAA3 Werte 6 Mal, und die Haptoglobin Werte doppelt so hoch, verglichen mit Tieren, die ausschließlich mit CCl_4 behandelt wurden.
Zusätzlich dazu war die Glycogenspeicherung verändert: 24 Stunden nach dem Schaden war der gesamte Glycogenspeicher der Leber bei allen Tieren verbraucht. Während sich in Mäusen mit intakten oder stimulierten IL-6 Transsignaling die Glycogenspeicher nach 48 Stunden bereits wieder gefüllt hatten, war der Prozess in Mäusen mit blockierten IL-6 Transsignaling deutlich vermindert. Diese Tiere zeigten ebenfalls eine geringere BrdU-Aufnahme, was auf eine geringere Proliferationsrate hindeutet.
Insgesamt weisen diese Daten dem IL-6 Transsignaling eine wichtige Rolle im CCl_4 induzierten Leberschadenmodell zu.

8 References

1. Hirano, T., K. Yasukawa, H. Harada, T. Taga, Y. Watanabe, T. Matsuda, S. Kashiwamura, K. Nakajima, K. Koyama, A. Iwamatsu, S. Tsunasawa, F. Sakiyama, H. Matsui, Y. Takahara, T. Taniguchi, and T. Kishimoto. 1986. Complementary DNA for a novel human interleukin (BSF-2) that induces B lymphocytes to produce immunoglobulin. *Nature* 324:73-76.
2. Muraguchi, A., T. Hirano, B. Tang, T. Matsuda, Y. Horii, K. Nakajima, and T. Kishimoto. 1988. The essential role of B cell stimulatory factor 2 (BSF-2/IL-6) for the terminal differentiation of B cells. *J. Exp. Med.* 167:332-344.
3. Kishimoto, T., S. Akira, M. Narazaki, and T. Taga. 1995. Interleukin-6 family of cytokines and gp130. *Blood* 86:1243-1254.
4. Kallen, K.-J. 2002. The role of transsignalling via the agonistic soluble IL-6 receptor in human diseases. *Biochem Biophys Acta* 1592:323-343.
5. Gadient, R. A., and P. H. Patterson. 1999. Leukemia inhibitory factor, Interleukin 6, and other cytokines using the GP130 transducing receptor: roles in inflammation and injury. *Stem cells (Dayton, Ohio)* 17:127-137.
6. Jones, S. A., S. Horiuchi, N. Topley, N. Yamamoto, and G. M. Fuller. 2001. The soluble interleukin 6 receptor: mechanisms of production and implications in disease. *FASEB J* 15:43-58.
7. Shalaby, M. R., A. Waage, and T. Espevik. 1989. Cytokine regulation of interleukin 6 production by human endothelial cells. *Cell Immunol* 121:372-382.
8. Yan, S. F., I. Tritto, D. Pinsky, H. Liao, J. Huang, G. Fuller, J. Brett, L. May, and D. Stern. 1995. Induction of interleukin 6 (IL-6) by hypoxia in vascular cells. Central role of the binding site for nuclear factor-IL-6. *J Biol Chem* 270:11463-11471.
9. Gauldie, J., C. Richards, D. Harnish, P. Lansdorp, and H. Baumann. 1987. Interferon beta 2/B-cell stimulatory factor type 2 shares identity with monocyte-derived hepatocyte-stimulating factor and regulates the major acute phase protein response in liver cells. *Proc Natl Acad Sci USA* 84:7251-7255.
10. Okada, M., M. Kitahara, S. Kishimoto, T. Matsuda, T. Hirano, and T. Kishimoto. 1988. IL-6/BSF-2 functions as a killer helper factor in the in vitro induction of cytotoxic T cells. *J. Immunol.* 141:1543-1549.
11. Nicola, N. A., D. Metcalf, M. Matsumoto, and G. R. Johnson. 1983. Purification of a factor inducing differentiation in murine myelomonocytic leukemia cells. Identification as granulocyte colony-stimulating factor. *J Biol Chem* 258:9017-9023.
12. Chen, Q., D. T. Fisher, K. A. Clancy, J. M. Gauguet, W. C. Wang, E. Unger, S. Rose-John, U. H. von Andrian, H. Baumann, and S. S. Evans. 2006. Fever-range thermal stress promotes lymphocyte trafficking across high endothelial venules via an interleukin 6 trans-signaling mechanism. *Nat Immunol* 7:1299-1308.
13. Kopf, M., H. Baumann, G. Freer, M. Freudenberg, M. Lamers, T. Kishimoto, R. Zinkernagel, H. Bluethmann, and G. Kohler. 1994. Impaired immune and acute-phase responses in interleukin-6-deficient mice. *Nature* 368:339-342.
14. Alonzi, T., E. Fattori, D. Lazzaro, P. Costa, L. Probert, G. Kollias, F. De Benedetti, V. Poli, and G. Ciliberto. 1998. Interleukin 6 is required for the development of collagen-induced arthritis. *J Exp Med* 187:461-468.

15. Okuda, Y., S. Sakoda, C. C. Bernard, H. Fujimura, Y. Saeki, T. Kishimoto, and T. Yanagihara. 1998. IL-6-deficient mice are resistant to the induction of experimental autoimmune encephalomyelitis provoked by myelin oligodendrocyte glycoprotein. *Int Immunol* 10:703-708.
16. Heinrich, P. C., I. Behrmann, S. Haan, H. M. Hermanns, G. Muller-Newen, and F. Schaper. 2003. Principles of interleukin (IL)-6-type cytokine signalling and its regulation. *Biochem J* 374:1-20.
17. Hirano, T., T. Matsuda, and K. Nakajima. 1994. Signal transduction through gp130 that is shared among the receptors for the interleukin 6 related cytokine subfamily. *Stem Cells Dayt* 12:262-277.
18. Giese, B., C. Roderburg, M. Sommerauer, S. B. Wortmann, S. Metz, P. C. Heinrich, and G. Muller-Newen. 2005. Dimerization of the cytokine receptors gp130 and LIFR analysed in single cells. *J Cell Sci* 118:5129-5140.
19. Taga, T., and T. Kishimoto. 1997. gp130 and the Interleukin-6 Family of Cytokines. *Annu Rev Immunol* 15:797-819.
20. Elson, G. C., E. Lelievre, C. Guillet, S. Chevalier, H. Plun-Favreau, J. Froger, I. Suard, A. B. de Coignac, Y. Delneste, J. Y. Bonnefoy, J. F. Gauchat, and H. Gascan. 2000. CLF associates with CLC to form a functional heteromeric ligand for the CNTF receptor complex. *Nat. Neurosci.* 3:867-872.
21. Guschin, D., N. Rogers, J. Briscoe, B. Witthuhn, D. Watling, F. Horn, S. Pellegrini, K. Yasukawa, P. Heinrich, G. R. Stark, J. N. Ihle, and I. A. Kerr. 1995. A major role for the protein tyrosine kinase JAK1 in the JAK/STAT signal transduction pathway in response to interleukin-6. *EMBO J* 14:1421-1429.
22. Gerhartz, C., B. Heesel, J. Sasse, U. Hemmann, C. Landgraf, J. Schneider Mergener, F. Horn, P. C. Heinrich, and L. Graeve. 1996. Differential activation of acute phase response factor/STAT3 and STAT1 via the cytoplasmic domain of the interleukin 6 signal transducer gp130. I. Definition of a novel phosphotyrosine motif mediating STAT1 activation. *J. Biol. Chem.* 271:12991-12998.
23. Heinrich, P. C., I. Behrmann, G. Muller Newen, F. Schaper, and L. Graeve. 1998. Interleukin-6-type cytokine signalling through the gp130/Jak/STAT pathway. *Biochem J* 334:297-314.
24. Zhong, Z., Z. Wen, and J. E. J. Darnell. 1994. Stat3: a STAT family member activated by tyrosine phosphorylation in response to epidermal growth factor and interleukin-6. *Science* 264:95-98.
25. Wegenka, U. M., J. Buschmann, C. Lütticken, P. C. Heinrich, and F. Horn. 1993. Acute-phase response factor, a nuclear factor binding to acute-phase response elements, is rapidly activated by interleukin-6 at the posttranslational level. *Mol Cell Biol* 13:276-288.
26. Schumann, R. R., C. J. Kirschning, A. Unbehaun, H. P. Aberle, H. P. Knope, N. Lamping, R. J. Ulevitch, and F. Herrmann. 1996. The lipopolysaccharide-binding protein is a secretory class 1 acute-phase protein whose gene is transcriptionally activated by APRF/STAT/3 and other cytokine-inducible nuclear proteins. *Mol Cell Biol* 16:3490-3503.
27. Hill, C. S., and R. Treisman. 1995. Differential activation of c-fos promoter elements by serum, lysophosphatidic acid, G proteins and polypeptide growth factors. *Embo J* 14:5037-5047.
28. Coffer, P., C. Lutticken, A. van Puijenbroek, M. Klop-de Jonge, F. Horn, and W. Kruijer. 1995. Transcriptional regulation of the junB promoter: analysis of STAT-mediated signal transduction. *Oncogene* 10:985-994.

29. Chung, C. D., J. Liao, B. Liu, X. Rao, P. Jay, P. Berta, and K. Shuai. 1997. Specific inhibition of Stat3 signal transduction by PIAS3. *Science* 278:1803-1805.
30. Endo, T. A., M. Masuhara, M. Yokouchi, R. Suzuki, H. Sakamoto, K. Mitsui, A. Matsumoto, S. Tanimura, M. Ohtsubo, H. Misawa, T. Miyazaki, N. Leonor, T. Taniguchi, T. Fujita, Y. Kanakura, S. Komiya, and A. Yoshimura. 1997. A new protein containing an SH2 domain that inhibits JAK kinases. *Nature* 387:921-924.
31. Starr, R., T. A. Willsonm, E. M. Viney, L. J. Murray, J. R. Rayner, B. J. Jenkins, T. J. Gonda, W. S. Alexander, D. Metcalf, N. A. Nicola, and D. J. Hilton. 1997. A family of cytokine-inducible inhibitors of signalling. *Nature* 387:917-921.
32. Naka, T., M. Narazaki, M. Hirata, T. Matsumoto, S. Minamoto, A. Aono, N. Nishimoto, T. Kajita, T. Taga, K. Yoshizaki, S. Akira, and T. Kishimoto. 1997. Structure and function of a new STAT-induced STAT inhibitor. *Nature* 387:924-929.
33. Stahl, N., T. J. Farruggella, T. G. Boulton, Z. Zhong, J. E. Darnell, Jr., and G. D. Yancopoulos. 1995. Choice of STATs and other substrates specified by modular tyrosine-based motifs in cytokine receptors. *Science* 267:1349-1353.
34. Oberg, H. H., D. Wesch, S. Grussel, S. Rose-John, and D. Kabelitz. 2006. Differential expression of CD126 and CD130 mediates different STAT-3 phosphorylation in CD4+CD25- and CD25high regulatory T cells. *Int Immunol* 18:555-563.
35. Müllberg, J., H. Schooltink, T. Stoyan, P. C. Heinrich, and S. Rose-John. 1992. Protein kinase C activity is rate limiting for shedding of the interleukin-6 receptor. *Biochem Biophys Res Commun* 189:794-800.
36. Lust, J. A., K. A. Donovan, M. P. Kline, P. R. Greipp, R. A. Kyle, and N. J. Maihle. 1992. Isolation of an mRNA encoding a soluble form of the human interleukin-6 receptor. *Cytokine* 4:96-100.
37. Jones, S., and S. Rose-John. 2002. The role of soluble receptors in cytokine biology: The agonistic properties of the sIL-6R/IL-6 complex. *Biochim. Biophys. Acta.* 1592:251-264.
38. Rose-John, S., and P. C. Heinrich. 1994. Soluble receptors for cytokines and growth factors: generation and biological function. *Biochem J* 300:281-290.
39. Rose-John, S., and M. F. Neurath. 2004. IL-6 trans-signaling: the heat is on. *Immunity* 20:2-4.
40. Jones, S. A., D. Novick, S. Horiuchi, N. Yamamoto, A. J. Szalai, and G. M. Fuller. 1999. C-reactive protein: a physiological activator of interleukin 6 receptor shedding. *J Exp Med* 189:599-604.
41. Walev, I., P. Vollmer, M. Palmer, S. Bhakdi, and S. Rose-John. 1996. Pore-forming toxins trigger shedding of receptors for interleukin 6 and lipopolysaccharide. *Proc Natl Acad Sci USA* 93:7882-7887.
42. Matthews, V., B. Schuster, S. Schütze, K.-J. Kallen, and S. Rose-John. 2003. Cholesterol depletion of the plasma membrane triggers shedding of the human interleukin-6 receptor by TACE and independently of PKC. *J Biol Chem* 278:38829-38839.
43. Chalaris, A., B. Rabe, K. Paliga, H. Lange, T. Laskay, C. A. Fielding, S. A. Jones, S. Rose-John, and J. Scheller. 2007. Apoptosis is a natural stimulus of IL6R shedding and contributes to the proinflammatory trans-signaling function of neutrophils. *Blood* 110:1748-1755.

44. Honda, M., S. Yamamoto, M. Cheng, K. Yasukawa, H. Suzuki, T. Saito, Y. Osugi, T. Tokunaga, and T. Kishimoto. 1992. Human soluble IL-6 receptor: its detection and enhanced release by HIV infection. *J Immunol* 148:2175-2180.
45. Hurst, S. M., T. S. Wilkinson, R. M. McLoughlin, S. Jones, S. Horiuchi, N. Yamamoto, S. Rose-John, G. M. Fuller, N. Topley, and S. A. Jones. 2001. Control of leukocyte infiltration during inflammation: IL-6 and its soluble receptor orchestrate a temporal switch in the pattern of leukocyte recruitment. *Immunity* 14:705-714.
46. Richards, P. J., M. A. Nowell, S. Horiuchi, R. M. McLoughlin, C. A. Fielding, S. Grau, N. Yamamoto, M. Ehrmann, S. Rose-John, A. S. Williams, N. Topley, and S. A. Jones. 2006. Functional characterization of a soluble gp130 isoform and its therapeutic capacity in an experimental model of inflammatory arthritis. *Arthritis Rheum* 54:1662-1672.
47. McLoughlin, R. M., B. J. Jenkins, D. Grail, A. S. Williams, C. A. Fielding, C. R. Parker, M. Ernst, N. Topley, and S. A. Jones. 2005. IL-6 trans-signaling via STAT3 directs T cell infiltration in acute inflammation. *Proc Natl Acad Sci U S A* 102:9589-9594.
48. Romano, M., M. Sironi, C. Toniatti, N. Polentarutti, P. Fruscella, P. Ghezzi, R. Faggioni, W. Luini, V. van Hinsbergh, S. Sozzani, F. Bussolino, V. Poli, G. Ciliberto, and A. Mantovani. 1997. Role of IL-6 and its soluble receptor in induction of chemokines and leukocyte recruitment. *Immunity* 6:315-325.
49. Tamura, T., N. Udagawa, N. Takahashi, C. Miyaura, S. Tanaka, Y. Yamada, Y. Koishihara, Y. Ohsugi, K. Kumaki, T. Taga, T. Kishimoto, and T. Suda. 1993. Soluble interleukin-6 receptor triggers osteoclast formation by interleukin 6. *Proc Natl Acad Sci USA* 90:11924-11928.
50. Klouche, M., S. Bhakdi, M. Hemmes, and S. Rose-John. 1999. Novel Path of activation of primary human smooth muscle cells: upregulation of gp130 creates an autocrine activation loop by IL-6 and its soluble receptor. *J Immunol* 163:4583-4589.
51. Atreya, R., J. Mudter, S. Finotto, J. Müllberg, T. Jostock, S. Wirtz, M. Schütz, B. Bartsch, M. Holtmann, C. Becker, D. Strand, J. Czaja, J. F. Schlaak, H. A. Lehr, F. Autschbach, G. Schürmann, N. Nishimoto, K. Yoshizaki, H. Ito, T. Kishimoto, P. R. Galle, S. Rose-John, and M. F. Neurath. 2000. Blockade of IL-6 transsignaling abrogates established experimental colitis in mice by suppression of the antiapoptotic resistance of lamina propria T cells. *Nat Med* 6:583-588.
52. Becker, C., M. C. Fantini, C. Schramm, H. A. Lehr, S. Wirtz, A. Nikolaev, J. Burg, S. Strand, R. Kiesslich, S. Huber, H. Ito, N. Nishimoto, K. Yoshizaki, T. Kishimoto, P. R. Galle, M. Blessing, S. Rose-John, and M. F. Neurath. 2004. TGF-beta suppresses tumor progression in colon cancer by inhibition of IL-6 trans-signaling. *Immunity* 21:491-501.
53. Rose-John, S., J. Scheller, G. Elson, and S. A. Jones. 2006. Interleukin-6 biology is coordinated by membrane-bound and soluble receptors: role in inflammation and cancer. *J Leukoc Biol* 80:227-236.
54. Dinarello, C. A. 1998. Interleukin-1, interleukin-1 receptors and interleukin-1 receptor antagonist. *Int Rev Immunol* 16:457-499.
55. Wajant, H., F. Henkler, and P. Scheurich. 2001. The TNF-receptor-associated factor family: scaffold molecules for cytokine receptors, kinases and their regulators. *Cell Signal* 13:389-400.
56. Gessner, A., and M. Rollinghoff. 2000. Biologic functions and signaling of the interleukin-4 receptor complexes. *Immunobiology* 201:285-307.

57. Müllberg, J., T. Geib, T. Jostock, S. H. Hoischen, P. Vollmer, N. Voltz, D. Heinz, P. R. Galle, M. Klouche, and S. Rose-John. 2000. IL-6-Receptor Independent Stimulation of Human gp130 by Viral IL-6. *J Immunol* 164:4672-4677.
58. Fischer, M., J. Goldschmitt, C. Peschel, K. J. Kallen, J. P. J. Brakenhoff, A. Wollmer, J. Grötzinger, and S. Rose-John. 1997. A designer cytokine with high activity on human hematopoietic progenitor cells. *Nat Biotechnol* 15:142-145.
59. Peters, M., G. Blinn, F. Solem, M. Fischer, K.-H. Meyer zum Büschenfelde, and S. Rose-John. 1998. In Vivo and in vitro Activity of the gp130 Stimulating Designer Cytokine Hyper-IL-6. *J Immunol* 161:3575-3581.
60. Galun, E., E. Zeira, D. Shouval, O. Pappo, M. Peters, and S. Rose-John. 2000. Liver regeneration induced by a designed hIL-6/shIL-6R fusion protein reverses severe hepatocellular injury. *FASEB J* 14:1979-1987.
61. Peters, M., G. Blinn, T. Jostock, P. Schirmacher, K. H. Meyer zum Büschenfelde, P. R. Galle, and S. Rose-John. 2000. Combined Interleukin-6 and soluble Interleukin-6 receptor accelerates murine liver regeneration. *Gastroenterol* 119:1663-1671.
62. Montero-Julian, F. A. 2001. The soluble IL-6 receptors: serum levels and biological function. *Cell Mol Biol* 47:583-597.
63. Jostock, T., J. Müllberg, S. Özbek, R. Atreya, G. Blinn, N. Voltz, M. Fischer, M. F. Neurath, and S. Rose-John. 2001. Soluble gp130 is the natural inhibitor of soluble IL-6R transsignaling responses. *Eur J Biochem* 268:160-167.
64. Rabe, B., A. Chalaris, U. May, G. H. Waetzig, D. Seegert, A. S. Williams, S. A. Jones, S. Rose-John, and J. Scheller. 2008. Transgenic blockade of interleukin 6 transsignaling abrogates inflammation. *Blood* 111:1021-1028.
65. Ali, A., K. P. Hoeflich, and J. R. Woodgett. 2001. Glycogen synthase kinase-3: properties, functions, and regulation. *Chem Rev* 101:2527-2540.
66. Woodgett, J. R. 1994. Regulation and functions of the glycogen synthase kinase-3 subfamily. *Semin Cancer Biol* 5:269-275.
67. Guengerich, F. P. 2008. Cytochrome p450 and chemical toxicology. *Chem Res Toxicol* 21:70-83.
68. Peters, M., K. H. Meyer zum Buschenfelde, and S. Rose-John. 1996. The function of the soluble IL-6 receptor in vivo. *Immunology letters* 54:177-184.
69. Sekiyama, K. D., M. Yoshiba, and A. W. Thomson. 1994. Circulating proinflammatory cytokines (IL-1 beta, TNF-alpha, and IL-6) and IL-1 receptor antagonist (IL-1Ra) in fulminant hepatic failure and acute hepatitis. *Clin Exp Immunol* 98:71-77.
70. Cressman, D. E., L. E. Greenbaum, R. A. DeAngelis, G. Ciliberto, E. E. Furth, V. Poli, and R. Taub. 1996. Liver failure and defective hepatocyte regeneration in interleukin-6-deficient mice. *Science* 274:1379-1383.
71. Higgins, G. M., Anderson, R.M. 1931. Experimental pathology of the liver. I. Restoration of the liver of the white rat following partial surgical removal. *Arch. Pathol.*:186-202.
72. Taub, R. 2004. Liver regeneration: from myth to mechanism. *Nat Rev Mol Cell Biol* 5:836-847.
73. Yamada, Y., E. M. Webber, I. Kirillova, J. J. Peschon, and N. Fausto. 1998. Analysis of liver regeneration in mice lacking type 1 or type 2 tumor necrosis factor receptor: requirement for type 1 but not type 2 receptor. *Hepatology (Baltimore, Md* 28:959-970.
74. Fausto, N. 2000. Liver regeneration. *J Hepatol* 32:19-31.

75. Trautwein, C., T. Rakemann, M. Niehof, S. Rose-John, and M. P. Manns. 1996. Acute-phase response factor, increased binding, and target gene transcription during liver regeneration. *Gastroenterology* 110:1854-1862.
76. Blindenbacher, A., X. Wang, I. Langer, R. Savino, L. Terracciano, and M. H. Heim. 2003. Interleukin 6 is important for survival after partial hepatectomy in mice. *Hepatology (Baltimore, Md* 38:674-682.
77. Wuestefeld, T., C. Klein, K. L. Streetz, U. Betz, J. Lauber, J. Buer, M. P. Manns, W. Muller, and C. Trautwein. 2003. Interleukin-6/glycoprotein 130-dependent pathways are protective during liver regeneration. *J Biol Chem* 278:11281-11288.
78. Hecht, N., O. Pappo, D. Shouval, S. Rose-John, E. Galun, and J. H. Axelrod. 2001. Hyper-IL-6 gene therapy reverses fulminant hepatic failure. *Mol. Therap.* 3:683-687.
79. Maezono, K., K. Mawatari, K. Kajiwara, A. Shinkai, and T. Maki. 1996. Effect of alanine on D-galactosamine-induced acute liver failure in rats. *Hepatology (Baltimore, Md* 24:1211-1216.
80. Tiegs, G., J. Hentschel, and A. Wendel. 1992. A T cell-dependent experimental liver injury in mice inducible by concanavalin A. *The Journal of clinical investigation* 90:196-203.
81. Drucker, C., J. Gewiese, S. Malchow, J. Scheller, and S. Rose-John. 2009. Impact of interleukin-6 classic- and trans-signaling on liver damage and regeneration. *J Autoimmun*.
82. Weber, L. W., M. Boll, and A. Stampfl. 2003. Hepatotoxicity and mechanism of action of haloalkanes: carbon tetrachloride as a toxicological model. *Crit Rev Toxicol.* 33:105-136.
83. Recknagel, R. O., E. A. Glende, Jr., J. A. Dolak, and R. L. Waller. 1989. Mechanisms of carbon tetrachloride toxicity. *Pharmacol Ther.* 43:139-154.
84. Gutteridge, J. M., and B. Halliwell. 1990. The measurement and mechanism of lipid peroxidation in biological systems. *Trends in biochemical sciences* 15:129-135.
85. Simeonova, P. P., R. M. Gallucci, T. Hulderman, R. Wilson, C. Kommineni, M. Rao, and M. I. Luster. 2001. The role of tumor necrosis factor-alpha in liver toxicity, inflammation, and fibrosis induced by carbon tetrachloride. *Toxicology and applied pharmacology* 177:112-120.
86. Armendariz-Borunda, J., J. M. Seyer, A. E. Postlethwaite, and A. H. Kang. 1991. Kupffer cells from carbon tetrachloride-injured rat livers produce chemotactic factors for fibroblasts and monocytes: the role of tumor necrosis factor-alpha. *Hepatology.* 14:895-900.
87. Czaja, M. J., K. C. Flanders, L. Biempica, C. Klein, M. A. Zern, and F. R. Weiner. 1989. Expression of tumor necrosis factor-alpha and transforming growth factor-beta 1 in acute liver injury. *Growth factors (Chur, Switzerland)* 1:219-226.
88. Czaja, M. J., J. Xu, and E. Alt. 1995. Prevention of carbon tetrachloride-induced rat liver injury by soluble tumor necrosis factor receptor. *Gastroenterology* 108:1849-1854.
89. Edwards, M. J., B. J. Keller, F. C. Kauffman, and R. G. Thurman. 1993. The involvement of Kupffer cells in carbon tetrachloride toxicity. *Toxicol Appl Pharmacol.* 119:275-279.
90. Louis, H., J. L. Van Laethem, W. Wu, E. Quertinmont, C. Degraef, K. Van den Berg, A. Demols, M. Goldman, O. Le Moine, A. Geerts, and J. Deviere. 1998. Interleukin-10 controls neutrophilic infiltration, hepatocyte proliferation, and

liver fibrosis induced by carbon tetrachloride in mice. *Hepatology.* 28:1607-1615.

91. Muriel, P., N. Alba, V. M. Perez-Alvarez, M. Shibayama, and V. K. Tsutsumi. 2001. Kupffer cells inhibition prevents hepatic lipid peroxidation and damage induced by carbon tetrachloride. *Comp Biochem Physiol C Toxicol Pharmacol* 130:219-226.
92. Kovalovich, K., R. A. DeAngelis, W. Li, E. E. Furth, G. Ciliberto, and R. Taub. 2000. Increased toxin-induced liver injury and fibrosis in interleukin-6-deficient mice. *Hepatology (Baltimore, Md* 31:149-159.
93. Katz, A., J. Chebath, J. Friedman, and M. Revel. 1998. Increased sensitivity of IL-6-deficient mice to carbon tetrachloride hepatotoxicity and protection with an IL-6 receptor-IL-6 chimera. *Cytokines, cellular & molecular therapy* 4:221-227.
94. Rio, A., M. A. Gassull, X. Aldeguer, I. Ojanguren, E. Cabre, and E. Fernandez. 2008. Reduced liver injury in the interleukin-6 knockout mice by chronic carbon tetrachloride administration. *European journal of clinical investigation* 38:306-316.
95. van Dam, M., J. Müllberg, H. Schooltink, T. Stoyan, J. P. Brakenhoff, L. Graeve, P. C. Heinrich, and S. Rose-John. 1993. Structure-function analysis of interleukin-6 utilizing human/murine chimeric molecules. Involvement of two separate domains in receptor binding. *The Journal of biological chemistry* 268:15285-15290.
96. Ames, B. N., R. Cathcart, E. Schwiers, and P. Hochstein. 1981. Uric acid provides an antioxidant defense in humans against oxidant- and radical-caused aging and cancer: a hypothesis. *Proceedings of the National Academy of Sciences of the United States of America* 78:6858-6862.
97. Frei, B., R. Stocker, and B. N. Ames. 1988. Antioxidant defenses and lipid peroxidation in human blood plasma. *Proc Natl Acad Sci U S A.* 85:9748-9752.
98. Hasegawa, T., and M. Kuroda. 1989. [A new role of uric acid as an antioxidant in human plasma]. *Rinsho byori* 37:1020-1027.
99. Wayner, D. D., G. W. Burton, K. U. Ingold, L. R. Barclay, and S. J. Locke. 1987. The relative contributions of vitamin E, urate, ascorbate and proteins to the total peroxyl radical-trapping antioxidant activity of human blood plasma. *Biochimica et biophysica acta* 924:408-419.
100. Rose-John, S., G. H. Waetzig, J. Scheller, J. Grotzinger, and D. Seegert. 2007. The IL-6/sIL-6R complex as a novel target for therapeutic approaches. *Expert opinion on therapeutic targets* 11:613-624.
101. Slater, T. F. 1984. Free-radical mechanisms in tissue injury. *Biochem J* 222:1-15.
102. Gruebele, A., K. Zawaski, D. Kaplan, and R. F. Novak. 1996. Cytochrome P4502E1- and cytochrome P4502B1/2B2-catalyzed carbon tetrachloride metabolism: effects on signal transduction as demonstrated by altered immediate-early (c-Fos and c-Jun) gene expression and nuclear AP-1 and NF-kappa B transcription factor levels. *Drug metabolism and disposition: the biological fate of chemicals* 24:15-22.
103. Raucy, J. L., J. C. Kraner, and J. M. Lasker. 1993. Bioactivation of halogenated hydrocarbons by cytochrome P4502E1. *Critical reviews in toxicology* 23:1-20.
104. Fernandez, G., M. C. Villarruel, E. G. de Toranzo, and J. A. Castro. 1982. Covalent binding of carbon tetrachloride metabolites to the heme moiety of

cytochrome P-450 and its degradation products. *Research communications in chemical pathology and pharmacology* 35:283-290.
105. Fujii, K. 1997. Preventive effect of isoflurane on destruction of cytochrome P450 during reductive dehalogenation of carbon tetrachloride in guinea-pig liver microsomes. *Drug metabolism and drug interactions* 14:99-107.
106. Manno, M., F. De Matteis, and L. J. King. 1988. The mechanism of the suicidal, reductive inactivation of microsomal cytochrome P-450 by carbon tetrachloride. *Biochemical pharmacology* 37:1981-1990.
107. Manno, M., R. Ferrara, S. Cazzaro, P. Rigotti, and E. Ancona. 1992. Suicidal inactivation of human cytochrome P-450 by carbon tetrachloride and halothane in vitro. *Pharmacology & toxicology* 70:13-18.
108. Cheeseman, K. H., E. F. Albano, A. Tomasi, and T. F. Slater. 1985. Biochemical studies on the metabolic activation of halogenated alkanes. *Environmental health perspectives* 64:85-101.
109. Comporti, M. 1985. Lipid peroxidation and cellular damage in toxic liver injury. *Laboratory investigation; a journal of technical methods and pathology* 53:599-623.
110. Forni, L. G., J. E. Packer, T. F. Slater, and R. L. Willson. 1983. Reaction of the trichloromethyl and halothane-derived peroxy radicals with unsaturated fatty acids: a pulse radiolysis study. *Chemico-biological interactions* 45:171-177.
111. Mico, B. A., and L. R. Pohl. 1983. Reductive oxygenation of carbon tetrachloride: trichloromethylperoxyl radical as a possible intermediate in the conversion of carbon tetrachloride to electrophilic chlorine. *Archives of biochemistry and biophysics* 225:596-609.
112. Tribble, D. L., T. Y. Aw, and D. P. Jones. 1987. The pathophysiological significance of lipid peroxidation in oxidative cell injury. *Hepatology.* 7:377-386.
113. Donato, A. J., G. L. Pierce, L. A. Lesniewski, and D. R. Seals. 2009. Role of NFkappaB in age-related vascular endothelial dysfunction in humans. *Aging* 1:678-680.
114. Wajant, H., K. Pfizenmaier, and P. Scheurich. 2003. Tumor necrosis factor signaling. *Cell Death Differ.* 10:45-65.
115. Yamada, Y., I. Kirillova, J. J. Peschon, and N. Fausto. 1997. Initiation of liver growth by tumor necrosis factor: deficient liver regeneration in mice lacking type I tumor necrosis factor receptor. *Proceedings of the National Academy of Sciences of the United States of America* 94:1441-1446.
116. Nieto, N., J. A. Dominguez-Rosales, L. Fontana, A. Salazar, J. Armendariz-Borunda, P. Greenwel, and M. Rojkind. 2001. Rat hepatic stellate cells contribute to the acute-phase response with increased expression of alpha1(I) and alpha1(IV) collagens, tissue inhibitor of metalloproteinase-1, and matrix-metalloproteinase-2 messenger RNAs. *Hepatology (Baltimore, Md* 33:597-607.
117. Yamaji, K., K. Ohnishi, R. Zuinen, Y. Ochiai, T. Chikuma, and H. Hojo. 2008. Interleukin-6 production by peritoneal mesothelial cells and its regulation by inflammatory factors in rats administered carbon tetrachloride intraperitoneally. *Toxicology and applied pharmacology* 226:38-45.
118. Yamada, Y., and N. Fausto. 1998. Deficient liver regeneration after carbon tetrachloride injury in mice lacking type 1 but not type 2 tumor necrosis factor receptor. *The American journal of pathology* 152:1577-1589.
119. Ohta, Y., Y. Imai, T. Matsura, A. Kitagawa, and K. Yamada. 2006. Preventive effect of neutropenia on carbon tetrachloride-induced hepatotoxicity in rats. *J Appl Toxicol* 26:178-186.

120. Nechemia-Arbely, Y., D. Barkan, G. Pizov, A. Shriki, S. Rose-John, E. Galun, and J. H. Axelrod. 2008. IL-6/IL-6R axis plays a critical role in acute kidney injury. *J Am Soc Nephrol* 19:1106-1115.
121. Thiers, R. E., E. S. Reynolds, and B. L. Vallee. 1960. The effect of carbon tetrachloride poisoning on subcellular metal distribution in rat liver. *The Journal of biological chemistry* 235:2130-2133.
122. Morel, P., C. Tallineau, R. Pontcharraud, A. Piriou, and F. Huguet. 1998. Effects of 4-hydroxynonenal, a lipid peroxidation product, on dopamine transport and Na+/K+ ATPase in rat striatal synaptosomes. *Neurochemistry international* 33:531-540.
123. Parola, M., E. Albano, R. Autelli, G. Barrera, M. E. Biocca, L. Paradisi, and M. U. Dianzani. 1990. Inhibition of the high affinity Ca2(+)-ATPase activity in rat liver plasma membranes following carbon tetrachloride intoxication. *Chemico-biological interactions* 73:103-119.
124. Albano, E., R. Carini, M. Parola, G. Bellomo, L. Goria-Gatti, G. Poli, and M. U. Dianzani. 1989. Effects of carbon tetrachloride on calcium homeostasis. A critical reconsideration. *Biochemical pharmacology* 38:2719-2725.
125. Kodavanti, P. R., U. P. Kodavanti, and H. M. Mehendale. 1991. Carbon tetrachloride-induced alterations of hepatic calmodulin and free calcium levels in rats pretreated with chlordecone. *Hepatology (Baltimore, Md* 13:230-238.
126. Long, R. M., and L. Moore. 1986. Elevated cytosolic calcium in rat hepatocytes exposed to carbon tetrachloride. *The Journal of pharmacology and experimental therapeutics* 238:186-191.
127. Drucker, C., B. Rabe, A. Chalaris, E. Schulz, J. Scheller, and S. Rose-John. 2009. Interleukin-6 Trans-Signaling Regulates Glycogen Consumption After d-Galactosamine-Induced Liver Damage. *J Interferon Cytokine Res*.
128. Beck, J. T., S. M. Hsu, J. Wijdenes, R. Bataille, B. Klein, D. Vesole, K. Hayden, S. Jagannath, and B. Barlogie. 1994. Brief report: alleviation of systemic manifestations of Castleman's disease by monoclonal anti-interleukin-6 antibody. *N Engl J Med* 330:602-605.
129. Genovese, M. C., J. D. McKay, E. L. Nasonov, E. F. Mysler, N. A. da Silva, E. Alecock, T. Woodworth, and J. J. Gomez-Reino. 2008. Interleukin-6 receptor inhibition with tocilizumab reduces disease activity in rheumatoid arthritis with inadequate response to disease-modifying antirheumatic drugs: the tocilizumab in combination with traditional disease-modifying antirheumatic drug therapy study. *Arthritis Rheum* 58:2968-2980.
130. Nishimoto, N., Y. Kanakura, K. Aozasa, T. Johkoh, M. Nakamura, S. Nakano, N. Nakano, Y. Ikeda, T. Sasaki, K. Nishioka, M. Hara, H. Taguchi, Y. Kimura, Y. Kato, H. Asaoku, S. Kumagai, F. Kodama, H. Nakahara, K. Hagihara, K. Yoshizaki, and T. Kishimoto. 2005. Humanized anti-interleukin-6 receptor antibody treatment of multicentric Castleman disease. *Blood* 106:2627-2632.
131. Nishimoto, N., M. Sasai, Y. Shima, M. Nakagawa, T. Matsumoto, T. Shirai, T. Kishimoto, and K. Yoshizaki. 2000. Improvement in Castleman's disease by humanized anti-interleukin-6 receptor antibody therapy. *Blood* 95:56-61.
132. Storage, S. S., H. Agrawal, and D. E. Furst. 2010. Description of the efficacy and safety of three new biologics in the treatment of rheumatoid arthritis. *The Korean journal of internal medicine* 25:1-17.
133. Kawashiri, S. Y., A. Kawakami, S. Yamasaki, T. Imazato, N. Iwamoto, K. Fujikawa, T. Aramaki, M. Tamai, H. Nakamura, H. Ida, T. Origuchi, Y. Ueki, and K. Eguchi. 2009. Effects of the anti-interleukin-6 receptor antibody,

tocilizumab, on serum lipid levels in patients with rheumatoid arthritis. *Rheumatology international*.

9 Appendix

9.1 Abbreviations

A	Adenine
ADAM	A Disintegrin And Metalloprotease
AEC	3-Amino-9-Ethylcarbazol
Ag	Antigen
Akt	Proteinkinase B
AKI	Acute kidney injury
ALT	Alanine Aminotransferase
APC	Allophycocyanin
APP	Acute Phase Protein
APS	Ammonium Persulfate
AST	Aspartate Aminotransferase
ATP	Adenosine 5'-Triphosphate
BCA	Bicinchoninic Acid
bp	Base Pairs
BrdU	5-Bromo-2-Deoxyuridine
BSA	Bovine Serum Albumin
C	Cytosine
CBM	Cytokine Binding Module
CCl_4	Carbontetrachloride
cDNA	Complementary DNA
CLC	Cardiotrophin-Like Cytokine
CNTF	Ciliary Neutrotrophic Factor
CNTFR	Ciliary Neutrotrophic Factor Receptor
ConA	Concanavalin A
CRP	C-Reactive Protein
CT-1	Cardiothrophin-1
CYP	Cytochrome
DAPI	4,6-Diamino-2-Phenylindole Dihydrochloride

dATP	Deoxy Adenosine Triphosphate
D-Gal	D-Galactosamine
dl	Deciliter
DMSO	Dimethylsulfoxide
DNA	Deoxyribonucleic Acid
dNTP	2`-Desoxyribonucleotide-5´-Triphosphate
DTT	Dithithreitol
EAE	Experimental Autoimmune Encephalomyelitis
ECL	Electrochemiluminescence
EDTA	Ethylenediaminetetraacetic Acid
EGF	Epidermal Growth Factor
ELISA	Enzyme Linked Immunosorbent Assay
ER	Endoplasmatic Reticulum
Erk	Extracellular Signal Regulated Kinase
EtOH	Ethanol
FACS	Fluorescence Activated Cell Sorter
Fc	Fragment Crystallizable
Fig	Figure
FITC	Fluorescein isothiocyanate
G	Guanosine
gp130	Glycoprotein 130
Grb2	Growth Factor Receptor Bound Protein 2
GSK-3	Glycogen Synthase Kinase 3
h	Hour
HB-EGF	Heparin Binding-Epidermal Growth Factor
HDL	High Density Lipoprotein
HE	Hematoxylin/ Eosin
HGF	Hepatocyte Growth Factor
hIL-6	human IL-6
HRP	Horseradish Peroxidase

IB	Immunoblotting
IFN α,γ	Interferon α,γ
Ig-domain	Immunoglobulin-Domain
IL	Interleukin
IL-6R	Interleukin-6 Receptor
i.p.	Intraperitoneal Injection
IVC	Individually Ventilated Cages
JAK	Janus Kinase
kb	Kilobase Pairs
kDa	Kilodalton
kg	Kilogram
L	Liter
LB	Lysogeny Broth
LIF	Leukaemia Inhibitory Factor
LIFR	Leukaemia Inhibitory Factor Receptor
LPS	Lipopolysaccharide
mAB	Monoclonal Antibody
MAPK	Mitogen-Activated Protein Kinase
MDA	Malondialdehyde
min	Minute
mg	Milligram
ml	Milliliter
mRNA	Messenger RNA
µg	Microgram
µl	Microliter
NADPH	Nicotinamide Adenine Dinucleotide Phosphate
NFκB	nuclear factor of activated B-cells
ng	Nanogram
nm	Nanometer

NP	Neuropoietin
OD	Optic Density
OSM	Oncostatin M
PARP	Poly ADP ribose polymerase
PAS	Periodic Acidic Schiff
PBS	Phosphate Buffered Saline
PCR	Polymerase Chain Reaction
PE	Phytoerythrin
Pfu	*Pyrococcus Furiosus*
pg	Picogram
PGSK-3	Phosphorylated Glycogen Synthase Kinase-3
PI3K	Phosphoinositid-3-Kinase
PIAS	Protein Inhibitors of Activated STAT
PIP3	Phospho-Inositol-Phospate-3
PKB	Protein Kinase B
PKC	Protein Kinase C
PMA	Phorbol 12-Myristate 13-Acetate
POD	Peroxidase
p-STAT3	Phospho-STAT3
p value	Probability
PVDF	Polyvinylidene Fluoride
RA	Rheumatoid Arthritis
RNA	Ribonucleic Acid
ROS	Reactive Oxygen Species
rpm	Rounds Per Minute
RT	Room Temperature
RT-PCR	Reverse Transcriptase PCR
SAA	Serum Amyloid A
SCNTFR	Soluble Ciliary Neutrotrophic Factor Receptor
SD	Standard Deviation

SDS	Sodium Dodecyl Sulfate
SDS-PAGE	SDS-Polyacrylamide Gel Electrophoresis
sgp130	Soluble gp130
SH2-domain	Src Homology-2 Domain
SHP-2	Src homology protein 2 tyrosine phosphatase-2
sIL-6R	soluble IL-6R
SOCS	Suppressors Of Cytokine Signalling
S-phase	Synthesis Phase
STAT	Signal Transducers and Activators of Transcription
T	Thymine
TACE	Tumor Necrosis Factor-Alpha Converting Enzyme (ADAM17)
Taq	*Thermus Aquaticus*
TBA	Thiobarbituric Acid
TBARS	Thiobarbituric Acid Reactive Substances
TBE	Tris Borate EDTA
TBS	Tris Buffered Saline
TEMED	N,N,N',N'-Tetramethylethylenediamine
TGF	Transforming Growth Factor
TMP	1,1,3,3-Tetramethoxypropane
TNF	Tumor Necrosis Factor
TNFR1	Tumor Necrosis Factor Receptor 1
TNFR2	Tumor Necrosis Factor Receptor 1
U	Units
UV	Ultraviolette
V	Volt
v/v	Volume per Volume
vIL-6	Viral interleukin-6
w/v	Weight per Volume
WT	Wildtype

9.2 Accession numbers

ß2-microglobulin	Mm00437762_m1
GSK-3ß	Mm00444911_m1
Haptoglobin	Mm00516884_m1
SAA1	Mm00656927_m1
SAA3	Mm00441203_m1

9.3 Publications

Impact of interleukin-6 classic- and trans-signaling on liver damage and regeneration.

Drucker C, Gewiese J, Malchow S, Scheller J, Rose-John S.

J Autoimmun. 2010 Feb;34(1):29-37. Epub 2009 Aug 29.

ADAM17-mediated shedding of the IL6R induces cleavage of the membrane stub by gamma-secretase.

Chalaris A, Gewiese J, Paliga K, Fleig L, Schneede A, Krieger K, Rose-John S, Scheller J.

Biochim Biophys Acta. 2010 Feb;1803(2):234-245. Epub 2009 Dec 21.

Submitted:

Essential Role of Neutrophil Mobilization in Concanavalin A-Induced Hepatitis is Based on Classic IL-6 Signaling but not IL-6 Trans-Signaling

Sven Malchow, Wolfgang Thaiss, Nathalie Jänner, Jessica Gewiese, Christoph Garbers, Kosuke Yamamoto, Stefan Rose-John* and Jürgen Scheller*

Role of IL-6 trans-signaling in CCl_4 induced liver damage

Jessica Gewiese, Claudia Drucker, Jürgen Scheller, Sven Malchow, Stefan Rose-John

9.4 Curriculum vitae

Lebenslauf

Persönliche Daten

Name	**Jessica Gewiese**
Email:	jazge@web.de
Geburtsdatum	20.02.1982
Geburtsort	Kiel
Familienstand	ledig

Studium

04/07-06/10	Promotion (rer.nat.) im Biochemischen Institut der Universität Kiel, Medizinische Fakultät Arbeitsthema: Physiological consequences of Blokade of IL-6 Transsignaling *in vivo*
07/06-03/07	Anfertigung einer Diplomarbeit im Biochemischen Institut der Universität Kiel- AG Rose-John (Beurteilung “sehr gut“)
06/06	Erfolgreiche mündliche Diplomprüfung (Notendurchschnitt: 1,0)
10/02-03/07	Studium der Biologie an der CAU in Kiel Abschluss Diplom Hauptfach: Mikrobiologie Nebenfächer: Zellbiologie und Biochemie

Auslandsaufenthalte

06/05-09/05	Studiumsbezogenes Praktikum im L`Institut Pasteur in Paris, Thema: *Plasmodium falciparum* (Malariaerreger)

Schulbildung

08/92-06/01	Gymnasium Altenholz
08/88-06/92	Grundschule Altenholz

Kenntnisse

Sprachen

Englisch (gut)
Französisch (befriedigend)
Spanisch (Grundkenntnisse)
Dänisch (Grundkenntnisse)

9.5 Acknowledgment

Danksagung

Sehr herzlich bedanken möchte ich mich bei Herrn Professor Rose-John, der mich während meiner Zeit in seinem Institut fachlich wie auch persönlich sehr unterstützt und gefördert hat. Außerdem möchte ich Ihm für seinen zügig vorgenommenen Korrekturen danken.

Besonderer Dank gilt auch Frau Dr. Claudia Drucker für die Betreuung dieser Promotion und die interessanten wie auch unterhaltsamen Diskussionen.

Besonders möchte ich mich auch bei Herrn Professor Schulz für die Übernahme des Zweitgutachtens dieser externen Promotion bedanken.

Bei meinen Laborkollegen Antje Schütt, Nina Adam, Athena Chalaris, Sven Malchow, Jan Suthaus, Christoph Garbers, Marija Stevanovic, Katja Möller und Doreen Floß möchte ich mich für die freundschaftliche und lustige Zusammenarbeit im Labor bedanken, ohne die manches sicherlich wesentlich schwerer zu ertragen gewesen wäre.

Bei Nico Schneider und Nadja Timm möchte ich mich für die Hilfe im Labor und im Tierstall bedanken.

Vielen, vielen, vielen Dank Tom für Deine Unterstützung und Liebe in allen Lebenslagen.

Mama, Papa, Christian. Vielen Dank für Alles.

9.6 Eidesstattliche Erklärung

Hiermit versichere ich, Jessica Gewiese, an Eides statt, dass ich die vorliegende Arbeit selbstständig und nur mit Hilfe der angegebenen Hilfsmittel und Quellen unter Anleitung meiner akademischen Lehrer angefertigt habe.

Diese Dissertation wurde bisher an keiner anderen Fakultät vorgelegt.

Ich erkläre, kein anderes Promotionsverfahren ohne Erfolg beendet zu haben, und dass keine Aberkennung eines bereits erworbenen Doktorgrades vorliegt.

Ich erkläre, dass die Arbeit unter Einhaltung der Regeln guter wissenschaftlicher Praxis der Deutschen Forschungsgemeindschaft entstanden ist.

Kiel, den 18.05.20010
Jessica Gewiese